



**GEOLOGICAL SURVEY OF CANADA**

**OPEN FILE 5663**

---

**Late Quaternary geological history of the SW Grand Banks  
Slope and Rise off Green Bank and Whale Bank: implications  
for geohazard assessment**

---

S. Ledger-Piercey, D.J.W. Piper

2007



Natural Resources  
Canada

Ressources naturelles  
Canada

**Canada**

**GEOLOGICAL SURVEY OF CANADA**

**OPEN FILE 5663**

**Late Quaternary geological history of the  
SW Grand Banks Slope and Rise off  
Green Bank and Whale Bank:  
implications for geohazard assessment**

S. Ledger-Piercey, D. J.W. Piper

**2007**

©Her Majesty the Queen in Right of Canada 2007  
Available from  
Geological Survey of Canada  
601 Booth Street  
Ottawa, Ontario K1A 0E8

**Ledger-Piercey, S., Piper, D.J.W.**

**2007:** Late Quaternary geological history of the SW Grand Banks Slope and Rise off Green Bank and Whale Bank: implications for geohazard assessment, Geological Survey of Canada, Open File 5663, ??p.

Open files are products that have not gone through the GSC formal publication process.

**Preface:**

This Open File is one of a series reporting on geohazards on the continental slope off southeastern Canada. It provides an interpretation of the late Quaternary geology of part of the Laurentian sub-basin based on high-resolution seismic profiles and cores. Based on this, a summary of the geohazards is provided.

**Acknowledgments:**

We thank the officers, crew and scientific staff of Hudson cruises 2002-046 and 2003-033. Calvin Campbell assisted with Arc-GIS, Kate Jarrett managed core splitting and processing, Kieran McDonald assisted with drafting. Review by Mark Deptuck improved this report. Work funded by GSC projects X-36 and the Canada Program for Energy Research and Development (PERD, project 532211).

**Authors' addresses:**

Shannon Ledger-Piercey and David J.W. Piper  
Geological Survey of Canada (Atlantic), Bedford Institute of Oceanography, P.O. Box 1006,  
Dartmouth, Nova Scotia, B2Y 4A2, Canada  
[dpiper@nrcan.gc.ca](mailto:dpiper@nrcan.gc.ca)

**Abstract**

A reconnaissance survey of late Quaternary stratigraphy and geohazards has been carried out on the deep continental margin seaward of Green Bank, Haddock Channel and Whale Bank, based on sparse Hunttec sparker lines and seven new piston cores. The area is crossed by the large Haddock valley seaward of Haddock Channel. To the southeast, Whale Slope is relatively undissected, but the slope seaward of Green Bank is dissected by tributaries of Haddock and Halibut valleys.

Five regional reflections were correlated throughout much of the study area in Hunttec sparker profiles. The distribution of major mass-transport deposits, evacuation surfaces and headscarps was mapped. Most piston cores penetrated to between Heinrich layer 1 and the last glacial maximum and recovered principally mud. Cores adjacent to Haddock Valley contained abundant thin sand beds of late Pleistocene age. Cores were correlated with adjacent long core records on St Pierre Slope and at the Narwhal well site. Extrapolation of ages from cores suggests that the recurrence interval of regional failures is several tens of thousands of years. More frequent local failures are found at the foot of active fault scarps.

## **Introduction**

The SW Grand Banks Rise off Green Bank and Haddock Channel (Fig. 1) is remarkable for the shallow salt tectonics in the area (interpreted from confidential industry multichannel seismic profiles) and the presence of a bottom-simulating reflection indicative of the presence of gas hydrates. In the Pleistocene, the region received sediment from glacial ice and associated meltwater plumes, principally from ice streams through Laurentian Channel, Halibut Channel, Haddock Channel and South Whale basin (Shaw et al. 2006), but also ice on the outer banks such as St Pierre Bank (Bonifay and Piper, 1988) and Whale Bank (Pass et al. 2000).

Study of the Late Quaternary history of the area thus has the potential to answer several questions concerning the regional geological framework and the nature of geohazards on the southeastern Canadian deep-water margin. These include in particular:

- changes in sedimentation rates between the continental slope and continental rise and the flux of sediment in the Labrador current
- the timing of seabed sediment failures and their relationship to active salt tectonics

## **Methods**

Piston cores and Hunttec DTS sparker sub-bottom profiler data were collected on the 2002-046 and 2003-033 Geological Survey of Canada cruises on CCGS Hudson (Figs. 1b, 2). A total of seven piston cores were studied from the main study area, plus two cores (073, 074) in similar water depths on lower St Pierre Slope (see also McCall, 2006). Each unsplit core was run through a Geotek multi-sensor track device to measure bulk density, P-wave velocity and magnetic susceptibility at a resolution of 1 cm. Discrete P-wave velocity and shear strength measurements were taken at 10 cm intervals where possible on split cores. Colour was measured using a Minolta Spectrophotometer at 5 cm intervals on the split core face. Measurements are expressed in terms of the L, a and b values (ASTM E308-85 and E1164-02). Further details of core lab procedures are provided by Tripsanas et al. (2007). Radiocarbon dates are expressed throughout the paper in radiocarbon years with a -0.4 ka reservoir correction applied.

The Hunttec DTS 1 kJ sparker system was towed about 100 m below the sea surface and paper copies of the profiles were interpreted. The centre frequency for the Hunttec sparker is about 1.5 kHz and spans from 0.5-2.5 kHz. The maximum vertical resolution is, therefore, about 0.20 m. More than 1000 line-km of Hunttec DTS seismic-reflection profiles are available. Seismic correlation has been carried out by defining key reflections at a type section (Fig. 3) and then correlating them where possible by tracing individual reflections.

Such correlation was possible in areas of smooth sea floor, but was commonly difficult in areas where fault scarps, mass-transport deposits, evacuation of failed sediment and major valleys complicate the stratigraphy. Therefore, where necessary, tentative “jump” correlations were made on the basis of sub-bottom thickness and reflector character.

Small, active, high-angle faults can be readily recognised in high-resolution seismic reflection profiles from offsets in sub-seabed reflectors, with displacement increasing with depth (fault A in Fig. 4). Larger faults are more difficult to define with certainty, because they are characterized by steep slopes that return hyperbolic diffractions (fault B in Fig. 4; faults Band C in Fig. 5). Evidence of recent movement on such faults may be provided by changes in dip and sediment thickness (fault C in Fig. 4; fault A in Fig. 5), whereas inactive faults show only a drape of sediment (fault D in Fig. 4). Faults can only be correlated between profiles where the line spacing is less than a few kilometres.

Previous bathymetric data are extremely sparse in > 500 m water depth in the region. A new bathymetric map (Fig. 2) has been prepared by contouring bathymetric picks at 5 minute intervals from 12 kHz echosounder records from the two Hudson cruises. Depths are based on  $v = 1463$  m/s and no further corrections have been applied.

## **Bathymetry**

The study area is part of the SW Grand Banks Rise, which slopes gradually to the south west (Fig. 1b). This part of the Rise is deeply incised by a south-trending submarine valley (“Halibut valley”) originating from Halibut Channel. A second major valley (“Haddock valley”) crossing the western portion of the study area originates at the seaward limit of Haddock Channel. A smaller valley (“Green valley”) is present to the north west. In the eastern part of the study area there are many depressions related to active fault scarps. Only where closely spaced survey lines are available can the continuity of such depressions be established. For example, in the far east of the study area is a 60-m-deep fault-bound depression (Fig. 5) that runs approximately north to south.

After the completion of this study, multibeam bathymetry of the study area became available (Mosher and Piper, 2007). This data is shown as an underlay in Figure 2, but has not been analysed in detail.

## **Piston cores**

Piston cores are described in numeric order. Cores 73 and 74 are from lower St Pierre Slope and provide a stratigraphic tie to the better known stratigraphy of Laurentian Fan (Skene and Piper 2003) and St Pierre Slope (Piper et al. 2005; McCall 2006). Piston core

locations on seismic profiles are shown in Appendix B and summary down-core descriptions are shown in Figures 6-9. Detailed down-core logs are presented in Appendix 4.

### ***Piston core 2002046-73***

Core 73 was taken on the flank of a low ridge in 2595 m of water. In Hunttec sparker profiles (Fig. B1), sediment on the ridge appears well stratified. Downslope from core 73, reflections at 2-5 ms appear to be absent, suggesting that there is an unconformity present in the upper part of core 74.

The piston core is 12.61 m long (Fig. 6). The liner was broken and the core is disturbed from 0.20-1.83 m. There is flow in at the base of the core at 11.87–12.29 m. The core is predominantly grey brown and red brown mud, massive with intermittent sandy blebs, granules, and at 2.2 m red and brown clay clasts. Below 4.7 m the sediment is laminated. Interbedded grey green and brown mud with local disseminated sand and sandy lenses are found below 6.12m. A detrital-carbonate-rich bed, identified as H1 (cf. Piper and Skene 1998) is present at 3.67–3.86 m. It consists of pale brown to tan mud with ice rafted detritus, showing peaks in bulk density, magnetic susceptibility, and p-wave velocity.

The trigger weight core is short, but suggests that at most a few decimeters of sediment are missing at the top of the piston core. This is confirmed by core-seismic correlation, which shows that reflector G (green), corresponding to H1, is at about 4 m sub-bottom.

### ***Piston core 2002046-74***

Core 74 was taken on a gentle terrace in 2672 m of water, deeper, but on the same valley side as core 73. As noted above, in the Hunttec sparker profile there appears to be a shallow unconformity with 1-3 m of sediment missing (Fig. B1). Downslope, a near surface mass-transport deposit is visible. Reflectors are parallel stratified to 12 ms subbottom, where the acoustic response is less coherent.

The piston core measures 12.76 m in length (Fig. 6). The edges of the core were damaged in the upper 1 m during core splitting. The core contains a few layers of olive grey and red mud. The olive grey mud is mostly massive with local worm burrows, and at 11.26–12.61 m there are some sandy laminations and a 16 cm brown mud bed. The red brown mud is massive to faintly laminated with some black mottling and laminations of brown and olive grey muds.

The trigger weight core is 2 m long and correlation with the piston core suggests that 0.2 – 0.4 m is missing from the top of the piston core. In the piston core there is an abrupt

increase in bulk density at 3.1–3.2 m that is interpreted as an unconformity. Correlation of core 74 with core 73 using “a” values confirms that a 3–4 m thick section of core 73, including H1, is absent in core 74 (Fig. 6). Red-brown intervals in core 74 are 1.5 times thicker than the corresponding interval in core 73.

#### ***Piston core 2002046-75***

Core 75 was taken on a low ridge in 2163 m of water, close to the type section of the seismic stratigraphy (Fig. 3). In Hunttec sparker profiles, sediment on the ridge appears well stratified (Fig. B2). At approximately 2 m the seismic profile is acoustically incoherent. At 6 to 7 ms reflectors are of high amplitude.

The piston core is 12.9 m in length and consists mostly of olive grey to grey mud with some grey brown intervals (Fig. 7). There is a Heinrich layer (H1) with ice rafted detritus at 5.91–6.00 m, correlating to a peak in bulk density, magnetic susceptibility, and P wave velocity. Four red brown intervals are found between 10.09–11.43 m. They measure 3–13 cm in thickness and correlate to increased “a” values. There is intermittent gas cracking starting at 8.1 m.

No trigger-weight core was recovered, but the correlation of the G (green) reflector to H1 suggests that little sediment is missing at the top of the piston core.

#### ***Piston core 2002046-76***

Core 76 was taken in a shallow valley between two low ridges in 2163 m of water. In Hunttec sparker profiles, sediment in the valley appears relatively transparent to 6 ms (Fig. B3). Below this, the sediment is well stratified, with lower amplitude reflections present again below 16 ms. There is clear correlation of reflections to those on the local ridge at core site 75, with the upper transparent interval about 1 ms thicker in the valley.

The piston core is 12.53 m long and is predominantly olive grey and greenish grey mud with a few sandy laminations (Fig. 7). Abundant spicules are present at 2.23 m. There is a tan interval with many granules at 7.47–7.59 m that correlates to a peak in bulk density, and magnetic susceptibility and is identified as H1. At 8.90–9.03 m and 12.1–12.3 m there are red brown intervals that corresponds to an increase in a\* value. Occasional minor cracking was present in the first few meters and widespread cracking at 6.2 – 6.95 m. The core was accidentally frozen from 7.8 m to base.

The trigger-weight core was very short, but the correlation of the G (green) reflector to H1 suggests that little sediment is missing at the top of the piston core.

### ***Piston core 2002046-77***

Core 77 was taken on a low ridge on the lower continental slope in 988 m of water (Fig. B4). In Hunttec sparker profiles, sediment on the ridge appears stratified, but adjacent gullies contain mass-transport deposits. The uppermost 3 ms of the seismic profile is acoustically incoherent and locally has hyperbolic diffractions. The reflection at the base of this packet appears to cut down across deeper reflections on the side of the gully and is at 3 ms sub-bottom at the core site. It is interpreted as an unconformity, overlain by blocky or otherwise disturbed sediment, capped by a seafloor drape of sediment. There is no evidence for more than a metre or so of missing sediment at the unconformity. Below the unconformity, reflections appear continuous.

The piston core is undisturbed to 10.6 m, below which there is flow in (Fig. 8). Comparison of the bulk density plot between piston and trigger weight cores suggests that 45 cm of sediment may be missing from the top of the piston core. The precise position of the unconformity in the core is uncertain, but the core-seismic correlation suggests somewhere between 2.0 and 3.0 m in the piston core. An increase in shear strength at about 4.5 m appears too deep to correspond to the unconformity. An abrupt increase in background levels of P-wave velocity and bulk density at 1.8–1.95 m most likely correlates with the unconformity.

### ***Piston core 2002046-78***

Core 78 was taken on a 200-m-high ridge between Haddock valley and a northern tributary in 1865 m of water, at least 200 m above the valley floor. In Hunttec sparker profiles, sediment on the ridge appears well stratified, but with some buried failure scarps (Fig. B5). It is difficult to correlate into the regional seismic stratigraphy. A reflection at about 16 ms sub-bottom is tentatively correlated with the regional reflection G (green) at the level of H1.

The piston core is 12.5 m long (Fig. 8). Comparison of the bulk density plot between piston and trigger weight cores suggests that 30 cm of sediment may be missing from the top of the piston core, but correlation of the less precise shear strength profile suggests no missing sediment.

Visual examination of the core shows abundance of olive grey mud. Below 4.6 m are abundant thin bedded sand beds that are variably bioturbated. The most prominent bioturbation is at 5.45–5.95 m and 7.1–8.0 m. Bioturbated thin-bedded sand beds are also present at 2.0–2.6 m. Possible small mass-transport blocks are present at 8.3 – 8.4 m. A red mud clast was located at 4.39 m. Two 1 mm white clay clasts that reacted with 10% HCL



were found at 7.11 and 7.19 m at approximately the horizon of reflection G (green) and may indicate the presence of H1.

#### ***Piston core 2002046-79***

Core 79 was taken on a ridge between Green valley and Halibut valley, at least 300 m above the valley floors, in 1447 m of water. In Hunttec sparker profiles, sediment on the ridge appears poorly stratified to transparent with one strong reflector (Fig. B6). There is no reliable seismic correlation to this ridge.

The piston core is 12.45 m long (Fig. 8). The core consists mostly of dark gray and olive gray silty clay. Intervals of thin bedded, variably bioturbated, fine sand beds are found at 2.9–3.1 m, 3.3–3.5 m, 5.9–7.85 m and 10.1 m to the base of the core. Visual examination of the core revealed carbonate-rich pebble-sized clay clasts at 2.5 m.

#### ***Piston core 2002046-80***

Core 80 was taken on a low ridge at the base of a steeper slope in 2050 m of water, on the southern flank of Haddock valley. In Hunttec sparker profiles, sediment on the ridge appears well stratified (Fig. B7). Reflection G (green) is correlated to about 9 ms sub-bottom. At 11 ms sub-bottom, a high amplitude reflector overlies discontinuous irregular reflections that overlie acoustically incoherent reflections at 13 ms.

The core is 12.4 m in length and contains massive greenish grey to grey brown mud (Fig. 7). Most of the core was accidentally frozen and there was some flow in at the base starting at 12.05 m. Carbonate-rich mud of H1 is found at 634-642 cm and correlates to a peak in bulk density and magnetic susceptibility. A few thin bioturbated sand beds are present from 9.8–11.5 m. There is no clear evidence for a mass-transport deposit in the core, although the corer may have been stopped by indurated blocks in such a deposit. Visual examination of the core revealed abundant carbonate clay clasts at 4.05 m. More 1 mm sized white carbonate clay clasts were seen at 3.2 m and 4.03 m.

#### ***Piston core 2003033-7***

Core 7 was taken on a low terrace 40 m above the axis of a slope gully (Fig. B8). The upper part of the seismic section has low amplitude reflections that also fill the floor of the gully. High amplitude reflections 9 ms sub-bottom at the core site correlate with very high amplitude discontinuous reflections on the floor of the gully, indicating that the slope was an active conduit for coarse-grained sediment at that time.

The core is 11.1 m in length (Fig. 7). The upper part, to 8.05 m, consists principally of olive grey bioturbated mud. The interval from 2.2–2.45 m is siltier. The lower part of the

core consists of beds of sand and thin interbedded mud. The 0.85 m long trigger-weight core is difficult to correlate with the disturbed top of the piston core, but correlation with the seismic profile suggests that little sediment has been lost at the top of the piston core.

## **Seismic stratigraphy**

A type section was chosen at core site 75, in the southeast of the study area (Fig. 3; Hudson 2002046, 245/0356). Five seismic reflections were chosen, listed by increasing depth they are named: green, orange, brown, blue and red. None of the horizons could be correlated with confidence across Haddock valley.

The green reflection can be correlated throughout most of the study area. The thickness of the section above green is variable, from 5 to 12 ms. Locally, green immediately overlies a mass-transport deposit with a rough surface (e.g. Fig. C7) and consequently the reflection is discontinuous or poorly developed.

The orange reflection is visible over about two thirds of the study area. This horizon is commonly eroded by mass-transport deposits that can be correlated in the centre of the study area, northeast and east of Haddock valley.

The brown reflection can be traced throughout the study area. However, the amplitude of the brown reflection and adjacent reflections varies making precise correlation across valleys difficult. Such correlations were made on the basis of thickness of sediment between orange and an underlying reflector with hyperbolic diffractions to estimate the position of the brown horizon.

The blue reflection is identified in more than two-thirds of the study area. Variation in amplitude of the blue and adjacent reflectors makes precise correlation across valleys difficult. The correlations are made on the basis of stratal thickness below the brown horizon, and the presence of underlying reflectors with hyperbolic diffractions.

The red reflection is identified in about one third of the seismic profiles (e.g. Fig C6). It is a high-amplitude reflection but is commonly obscured by Huntect artifacts or disappears off the bottom of the seismic record. Where continuous correlation was not possible, correlation was made on the basis of stratal thickness on adjacent lines in similar water depth and the strength and character of underlying reflectors.

Regional variations in stratal thickness between reflections are noted. Stratal thickness between green and orange ranges from 15–29 ms, being reasonably uniform on the continental slope down to 2000 m, but then decreasing on the rise (Fig. 9). In areas where correlation is confident, stratal thickness between the blue and red reflections is quite variable, ranging from 22–64 ms (Fig. C6, C19).

## **Faults**

The recognition of faults in sparker profiles is discussed above in “Methods” (Figs. 4, 5). Numerous shallow faults were located in the study area and examples are illustrated in Appendix A. Because of the spacing of the available seismic profiles, only one large normal fault could be correlated with confidence from line to line. This fault is located in the centre of the study area and runs in an east west direction, with the hanging wall to the north (Fig. 2; Figs. A2, A4, C11).

## **Mass-transport deposits and their distribution**

Several regional horizons of widespread sediment failure and deposition of acoustically incoherent mass-transport deposits can be recognised in the sparker profiles. Characteristics of the mass-transport deposits are illustrated in Appendix C. They have acoustically incoherent internal character (Fig. C1) of varying reflectivity (Fig. C2). The upper surface is commonly irregular (Figs. C1, C2, C9). In some cases, mass-transport deposits fill pre-existing depressions (e.g. Fig. C16). The base of the acoustically incoherent unit is commonly a continuous bedding plane, but in places the base steps up or down in the stratigraphy by a few metres to a normal maximum of 10 m (Figs. C1, C2, C3). Exceptionally, a mass-transport deposit may overlie a surface above which several tens of metres of sediment have been removed by erosion (e.g. Fig. C9). Smaller mass-transport deposits may pinch out laterally, but commonly the correlative bedding plane appears to be an erosional surface (Fig. C1). In places, discrete blocks are recognised in mass-transport deposits (Fig. C9) and in deeper mass-transport deposits there are features that may be either large blocks or diapirs (Fig. C22). Elsewhere, there are abrupt changes in thickness of mass-transport deposits (Figs. C9, C21) that may indicate transformation from a very blocky flow to a more mobile debris flow.

One particular setting of small, wedge-shaped mass-transport deposits is at the base of fault scarps, where a correlative head scarp can be recognised up-slope (Figs. 5, A1, A2). Headscarps to local mass-transport deposits are also recognised on the flanks of ridges (Fig. C4).

Four mass-transport deposits and associated erosion surfaces of regional extent have been recognised and their distribution mapped (Figs. 10-12). Interval I occurs a short distance below the regional green reflection (Figs. C2, C9, C16) and is regionally the most extensive failure (Fig. 10). Interval II of mass-transport deposits and erosion surfaces is located below the brown reflection. (Figs. C1, C17). Below the blue horizon, intervals III and IV of mass transport deposits and erosional surfaces are seen (Fig 12). Interval IV is

found overlying the red reflector (Figs. C19, C20). In the central part of the study area, its upper surface appears to either have large blocks or to have been deformed into diapirs (Fig. C21). Mass-transport deposits are also recognized locally at other stratigraphic horizons, for example just below the regional red reflection (Figs. C19, C20).

## **Regional correlation of cores and their interpretation**

Regional correlation is most easily achieved with the cores from the continental rise (Fig. 13). A detrital-carbonate-rich bed at sub-bottom depths of 3-7 m corresponds to peaks in the L colour parameter, magnetic susceptibility, P wave velocity and bulk density. It is identified as Heinrich Layer 1 (H1) by comparison with dated cores both to the southwest (Piper and Gould, 2004) and on Laurentian Fan (Skene and Piper, 2003). Deeper detrital-carbonate-rich Heinrich beds are not recognised in the cores. Below H1, several red mud horizons appears to correlate between core sites 75, 76, and 80 and furthermore can be correlated to cores 73, 74 and other cores described by McCall (2006) on lower St Pierre Slope and to cores 87003-9, 10 (Fig. 1) on eastern Laurentian Fan. These red muds were likely sourced from Laurentian Channel, where major red mud discharges occurred between 14.5 C-14 ka and 18 C-14 ka (Piper et al. 2007). Cores to the southwest near the Narwhal well-site also show a distinct peak in  $a^*$  colour at 0.5 to 1.0 m below H1 and a second a similar distance above (cores 34 and 35 in Fig. 13; see also Piper et al. 2005), but which red horizons they correlate with is not clear. Core 74 is about 100 m above a valley floor and core 73 is 80 m shallower. The red-brown intervals below H1 in core 74 are readily correlated with those in core 73, but are 1.5 times thicker. This suggests that they may have been deposited from muddy turbidity currents that flowed down the valley.

Correlation between cores and seismic horizons indicates that the prominent green seismic horizon corresponds to H1 in cores 73, 75, 76, and 80 (Fig. 13). The green horizon can be correlated to approximately 4 to 4.5 m in Core 77 (Fig. 14). There is about 0.5 m missing at the top of this piston core. The  $a^*$  trace at ~3.5 m depth in the piston core (4 m sub-bottom) correlates well with the  $a^*$  trace for H1 in core 80 (Fig. 14), although no tan carbonate-rich mud is present. Seismic correlation to core 78 suggests that the H1-equivalent horizon is at a sub-bottom depth of about 14 m.

Cores on the continental slope can be correlated with reasonable confidence to a well-dated long core MD-95-2031 at the Narwhal well site (Piper and Gould, 2004) on the basis of sandy intervals and systematic variations in hematite content recorded by the spectrophotometric  $a^*$  trace (Fig. 14). An upper sandy interval in cores 78 and 79 may correlate with sands of Younger Dryas age at the Narwhal well site and similar sands are

found on St Pierre Slope (McCall 2006). The deeper sand interval starts in MD95-2026 at about 13.0 C-14 ka. Correlatable changes in the  $a^*$  trace termed A, B and C by Piper et al. (2005, their figure 5) are also recognised in some cores. Furthermore, a horizon with granule-sized clasts of carbonate-rich mudstone, apparently ice-rafted, may be correlated from core 79 to core 80 (Fig. 14).

There is no H1 carbonate-rich bed recognised in slope cores 77, 78 and 79. As noted above, on the basis of seismic correlation and the  $a^*$  trace, the equivalent horizon to H1 can be correlated from core 80, where a carbonate-rich bed is present, to core 77 (Fig. 14). Seismic correlation suggests that H1 is at about 13 m sub-bottom below the base of core 78. Granule-sized clasts of carbonate-rich mudstone, apparently ice-rafted, at 7.2 m in core 78 might correspond to those at 4 m in core 80 and at 6.2 m in MD95-2026. Cores 77, 78 and 79 have rather thin Holocene sections. They are situated on ridges, potentially winnowed by the Slope Current, and are thus similar to cores described by Piper and Gould (2004) southeast of Desbarres Canyon. Core 7 is located within a slope gully, a site that may well have trapped sediment and led to high sedimentation rates, as for example cores northwest of Desbarres Canyon (Piper and Gould, 2004).

Shallow sediment failures are recognised in cores 77 and 74 and on corresponding sparker profiles. In both cases, the failures appear to be between H1 and the youngest sandy unit, which in MD95-2029 dates from about 10 C-14 ka. In core 74, erosion removed H1, but it remains in core 77. The probable mass-transport deposit at 8.3–8.4 m in core 78 might be correlative and would suggest an age of about 13.2 C-14 ka..

## **An age model for the seismic stratigraphy**

Given the lack of age control below H1, any age model for the seismic stratigraphy is of necessity speculative. Using the age model for cores developed from correlation with MD95-2031 (Fig. 14), Holocene sedimentation rates at core 79 (1447 m) are of the order of 0.16 m/ka and from base Holocene to H1, sedimentation rates are about 1.5 m/ka. Cores in deeper water show a similar order of magnitude difference between Holocene and late Pleistocene sedimentation rates (e.g. cores 75, 76, 80), but with slightly lower overall sedimentation rates.

Elsewhere on the outer continental margin off eastern Canada, notably at Orphan Knoll (Toews and Piper, 2002) and Flemish Pass (Piper and Campbell, 2005), glacial marine isotope stages (MIS) 2-4 and 6 have high-amplitude reflections in Hunttec sparker profiles, whereas interglacial MIS 5 has low amplitude reflections. It is not clear whether this criterion can be applied to the Whale Slope, but regionally, low amplitude reflections are found at

(Figs. C4, C7, C10) or somewhat below (Figs. 3, C6, C9) the blue reflection. Extrapolation of glacial sedimentation rates would put the blue reflection in the 50-80 ka age range, around MIS 4 (Fig. 15). Thickness variations below the blue reflection are not understood, and the age of the red reflection is unclear.

## **Significance for Quaternary sedimentation**

Continental slope sedimentation in the late Quaternary elsewhere on the eastern Canadian margin appears to be principally from fallout from proglacial plumes and the Whale Slope area appears no different. The H1 carbonate layer, deposited from a plume originating from Hudson Strait, is found only in continental rise cores from >2000 m and is absent in continental slope core 77, 20 km inboard. In core 77 and the cores from the continental rise, there is a distinctive signature in the red colour ( $a^*$  trace, Figs. 13, 14) that resembles that found in Orphan Basin where it is due to discharge of meltwater with red sediment through Trinity Trough at the time of H1 (Tripsanas and Piper, in press).

On the continental rise off St Pierre Bank, thick red-brown mud is present below H1. On Laurentian Fan, this facies has been interpreted as resulting from thick, muddy turbidity currents (Skene and Piper, 2003; Curran et al. 2004), probably resulting from hyperpycnal flow from an ice margin (Hesse et al. 2004; Piper et al. 2007). The systematic thickness variations in cores 73 and 74, located on the flank of a valley down which such turbidity currents may have flowed, provide evidence for deposition from the top of a muddy turbidity current.

On the continental rise off Whale Bank, there are several thin intervals of red-brown mud below H1, with the longest record in core 80 (Fig. 13). Beds also appear a little thicker in core 80 than in 75 and 76 farther to the SE. In addition, Piper and Gould (2004) found two red intervals between H1 and H2 (Fig. 13) in cores on the continental slope near the Narwhal well and the upper interval is probably also present in core 77 (Fig. 14). Two sources are possible for these various red beds. One is from meltwater discharges through Trinity Trough (Tripsanas and Piper, in press), with red sediment transported southward and westward in the Labrador Current. The other is by southeastward transport from a Laurentian Fan source, probably by entrainment of surface or mid-water plumes by Gulf Stream eddies.

In cores from the continental slope close to major canyons (i.e. cores 7, 78 and 79), thin fine-grained sand beds are common at deeper intervals in the cores. These sand intervals are tentatively correlated with core MD95-2031 (Piper and Gould, 2004) as occurring in the Younger Dryas (between the C and B correlations in Fig. 14). If the correlation of carbonate-rich IRD is correct, there was also sand supply to core 78 and probably core 79 at around

11.9 C-14 ka. Major sand supply ended in core MD95-2031 at about 13.0 C-14 ka and is correlated to the top of the sandy interval at 8 m in core 78 and 10 m in core 79. The sand beds older than 13.0 C-14 ka are probably from turbidity currents generated at an ice margin, based on ice extents summarized by Shaw et al. (2006). Younger sand beds may be related to storm wave resuspension on continental shelf banks when eustatic sea level was at least 50 m lower. Interpretation of the beds is hampered by bioturbation.

Distribution of sediment thickness in slope cores and canyons suggests that there was some winnowing of Late Pleistocene - Holocene sediment on ridges, and the trapping of sediment in canyons (Fig. 14), as also noted to the southeast by Piper and Gould (2004). This winnowing is interpreted to be the result of storm waves and the action of the slope current.

### **Significance for geohazards**

As elsewhere on the southeastern Canadian margin, widespread sediment failures occur at discrete horizons and appear to involve retrogressive failures in multiple drainage systems (Piper et al., 2003). This pattern of failure is interpreted to result from rare large earthquakes causing widespread ground shaking (Mosher et al. 2004; Piper, 2005). If the age model summarized in Figure 15 is correct, then two major events (MTD I and II) have taken place since the blue reflection, tentatively dated at about 60 ka, implying a recurrence interval of tens of thousands of years. This recurrence interval for large events recognisable on Huntec seismic profiles is similar to the range found elsewhere on the Eastern Canadian margin (e.g. the summary in Figure 7 of Piper, 2005).

Smaller failures may be recognised from unconformities in piston cores and failures on canyon walls (e.g. Jenner et al. 2007). In the Holocene, such failures are not the result of oversteepening of canyon walls by turbidity current erosion (Mosher et al. 2004) and instead are likely also the result of smaller earthquakes. Cores 74 and 77 show a correlative unconformity dating from about 13 C-14 ka.

In areas of steep fault-controlled slopes, local failures appear more frequent than the regional large MTDs. For example, Figure A1 shows three local failure deposits in the interval between the green and the orange reflections. Nevertheless, this still implies a recurrence interval of many thousands of years for such failures.

Possible diapirs present on the upper surface of regional MTD IV suggests that this mass-transport deposit may be significantly underconsolidated. Similar diapirism has been reported from Orphan basin (Campbell 2005) and Flemish Pass (Piper and Pereira, 1992; Piper and Campbell, 2004). On the other hand, these features may be large blocks entrained in the MTD. In places on St Pierre Slope (Piper et al. 2005), buried MTDs appear to localise

decollement surfaces that may subsequently be the sites from large failures (Mosher et al., 2004). It is not clear whether this risk is also present on Whale Slope.

On the Scotian Slope, thin sand beds appear to be important as failure horizons (Campbell 2000). Such sands are abundant on the ridges adjacent to Green and Haddock valleys, but are rare on the Whale Slope (core 77).

## **Conclusions**

Sedimentation on the continental slope in the area seaward of Green Bank to Whale Bank was dominated in the late Pleistocene by plume fallout of proglacial sediment, some from local Newfoundland ice and some transported in the Labrador Current. In addition, deposition of sand beds on the inter-canyon ridges adjacent to Haddock Valley was an important process. Sedimentation rates on the upper rise (~ 2000 m) are only a little lower than on the mid slope away from sand supply. Lower on the rise, seismic-reflection profiles show that late Pleistocene sediment is thinner, probably due to sediment failure in the area.

Despite the evidence for active salt tectonics in the area, the frequency of seabed sediment failures is not unusual compared with other areas on the southeastern Canadian margin. Regional seabed failures show similar character to earthquake triggered failures elsewhere on the margin, with blocky mass transport deposits and headscarps suggesting that retrogressive failure was important. Abundant sand beds adjacent to Haddock valley may localise earthquake-triggered failures. There appear to be no unusual geohazards in this part of the continental margin.



## References

- Campbell, D.C. 2000. Relationship of sediment properties to failure horizons for a small area of the Scotian Slope. Geological Survey of Canada, Current Research, 2000-D08, 7p.
- Campbell, D.C. 2005. Major Quaternary mass transport deposits in southern Orphan Basin, offshore Newfoundland and Labrador. Geological Survey of Canada, Current Research 2005-D3, 10 p.
- Curran, K., Hill, P.S., Schell, T.M., Milligan, T.G. and Piper, D.J.W. 2004. Inferring the mass fraction of flocc deposited mud: application to fine-grained turbidites. *Sedimentology*, v. 51, p. 927-944.
- Hesse, R., Rashid, H., Khodabakhsh, S., 2004. Fine-grained sediment lofting from meltwater-generated turbidity currents during Heinrich events. *Geology* 32, 449-452.
- Mosher, D.C. and Piper, D.J.W., 2007. Analysis of multibeam seafloor imagery of the Laurentian Fan and the 1929 Grand Banks landslide area. Proceedings of the 3<sup>rd</sup> International Conference on Mass Movements and their consequences.
- Mosher, D.C., Piper, D.J.W., Campbell, D.C. and Jenner, K. 2004. Near surface geology and sediment-failure geohazards of the central Scotian Slope. *American Association of Petroleum Geologists Bulletin*, v. 88, p. 703-723.
- McCall, C.W., 2006. A geological and geophysical study of the 1929 Grand Banks slide. M.Sc. thesis, Saint Mary's University, Halifax, N.S., 229 p.
- Pass, D., Piper, D. J. W. and Campbell, D. C., 2000. Quaternary geology of the continental slope in the vicinity of the Narwhal F-99 well site; Geological Survey of Canada, Open File 3894, 27 pages
- Piper, D.J.W. 2005. Late Cenozoic evolution of the continental margin of eastern Canada. *Norwegian Journal of Geology*, v. 85, p. 305-318.
- Piper, D.J.W. and Campbell, D.C. 2004. Quaternary geology of Flemish Pass and its application to geohazard evaluation for hydrocarbon development. GAC Special Paper 43, 29-43.
- Piper, D.J.W. and Gould, K. 2004. Late Quaternary geological history of the continental slope, South Whale Basin, and implications for hydrocarbon development. Current Research 2004-D1, 13 pp.
- Piper, D.J.W. and Skene, K.I., 1998. Latest Pleistocene ice-rafting events on the Scotian Margin (eastern Canada) and their relationship to Heinrich events. *Paleoceanography*, v. 13, p. 205-214.
- Piper, D.J.W., Lawrence, T., Gould, K. and Nofall, R., 2006. Report on cores 2004-024 15 and 16, DesBarres Canyon area, SW Grand Banks. Geological Survey of Canada

- Open File 5118, 26 p.
- Piper, D.J.W., MacDonald, A.W.A., Ingram, S., Williams, G.L. and McCall, C., 2005. Late Cenozoic architecture of the St Pierre Slope. *Canadian Journal of Earth Sciences*, v. 42, p. 1987-2000.
- Piper, D.J.W., Shaw, J. and Skene, K.I. 2007. Stratigraphic and sedimentological evidence for late Wisconsinan sub-glacial outburst floods to Laurentian Fan. *Palaeogeog. Palaeoclim. Palaeoecol.* 246, 101-119.
- Shaw, J., Piper, D.J.W., Fader, G.B., King, E.L., Todd, B.J., Bell, T., Batterson, M.J., and Liverman, D.J.E., 2006. A conceptual model of the deglaciation of Atlantic Canada. *Quaternary Science Reviews*, 25, 2055-2081.
- Skene, K.I. and Piper, D.J.W., 2003. Late Quaternary stratigraphy of Laurentian Fan: a record of events off the eastern Canadian continental margin during the last deglacial period. *Quaternary International*, v. 99-100, p. 135-152.
- Toews, M.W. and Piper, D.J.W., 2002. Recurrence interval of seismically-triggered mass-transport deposition at Orphan Knoll, continental margin off Newfoundland and Labrador. *Current Research 2002-E17*, 7 p.
- Tripsanas, E.K. and Piper, D.J.W., in press. Late Quaternary stratigraphy and sedimentology of Orphan Basin: implications for meltwater dispersal in the southern Labrador Sea. *Palaeogeography, Palaeoclimatology, Palaeoecology*
- Tripsanas, E.K., Piper, D.J.W. and Jarrett, K.A., 2007. Logs of piston cores and interpreted ultra-high-resolution seismic profiles, Orphan Basin. Geological Survey of Canada, Open File 5299, 339 p.

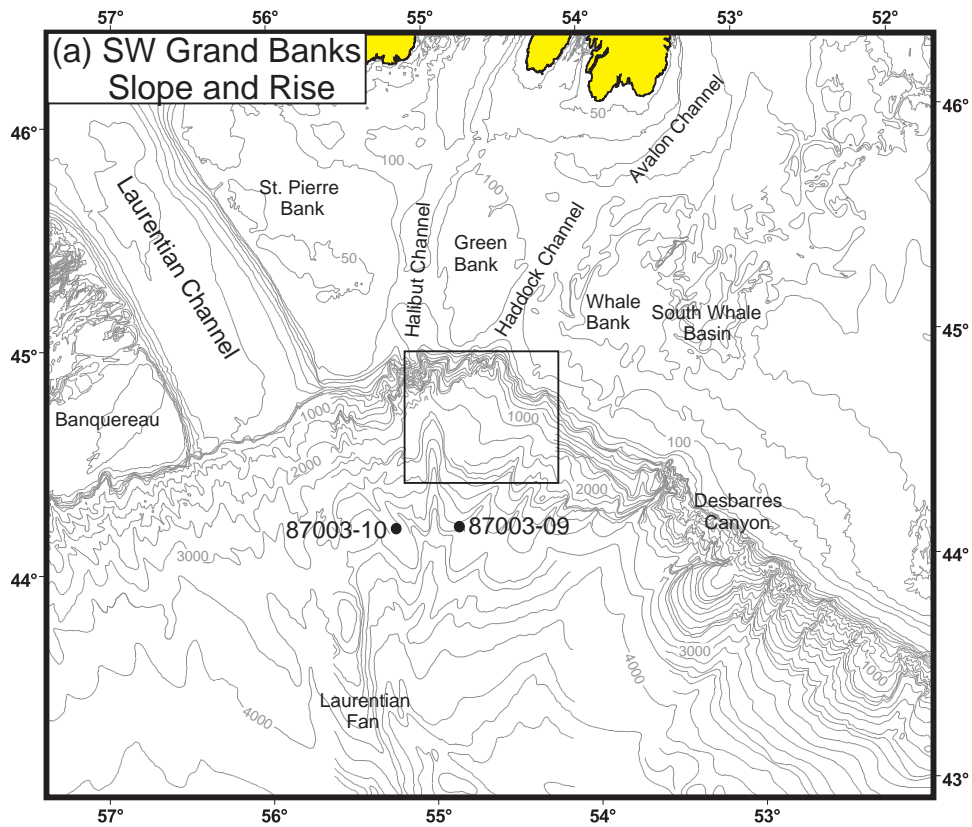


**Figure 1A.** General map of the SW Grand Banks Slope and Rise, showing location of study area.

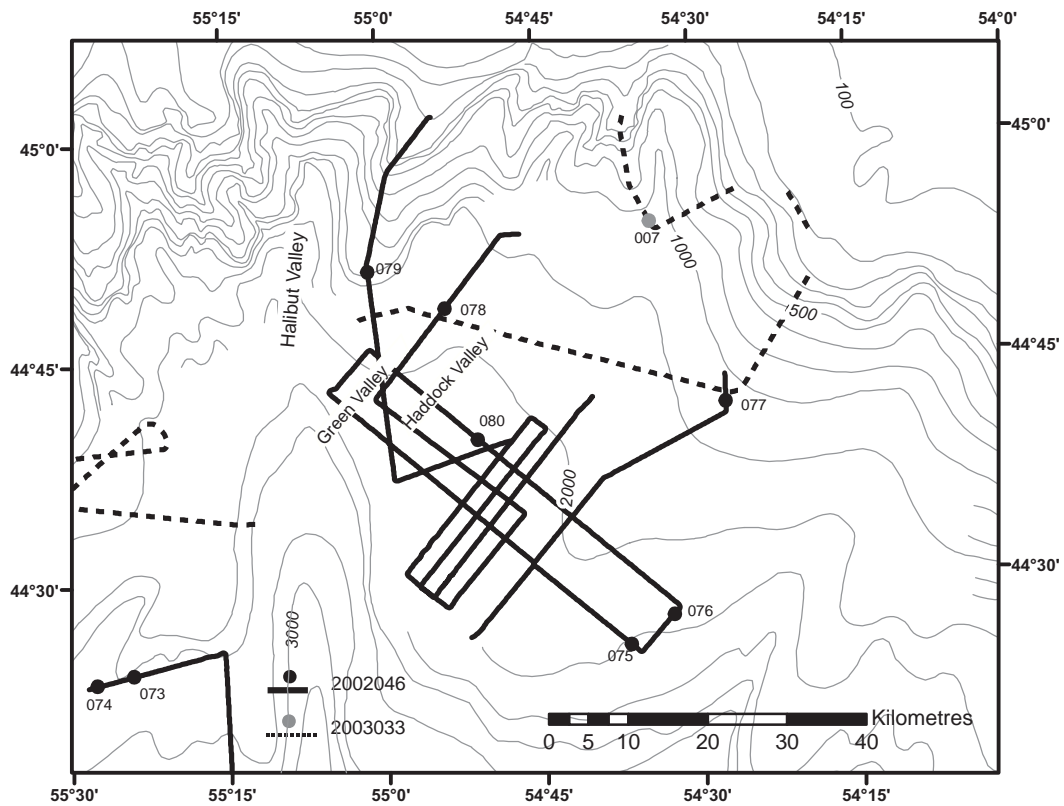


**Figure 1B.** Detail of slope off Green Bank and Haddock Channel, showing location of Hunttec sparker profiles and piston cores. Bathymetry from Canadian Hydrographic Service (Natural Resources Series 1:250 000).

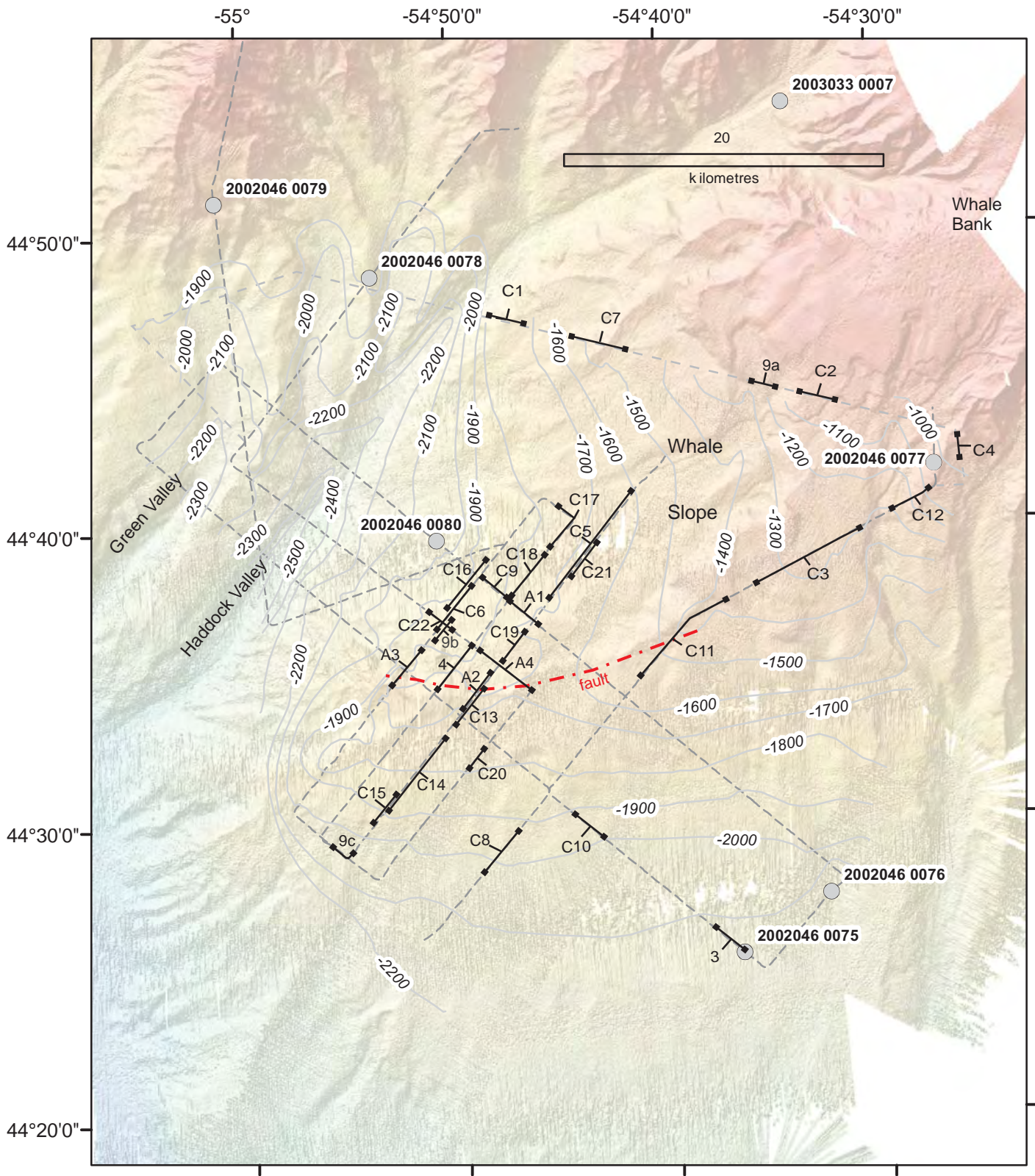


**Figure 2.** New bathymetric map of the study area, based on our new soundings. Contours in metres using  $v=1463\text{ms}^{-1}$ . Also shows location of fault and illustrated figures.

# Type Section

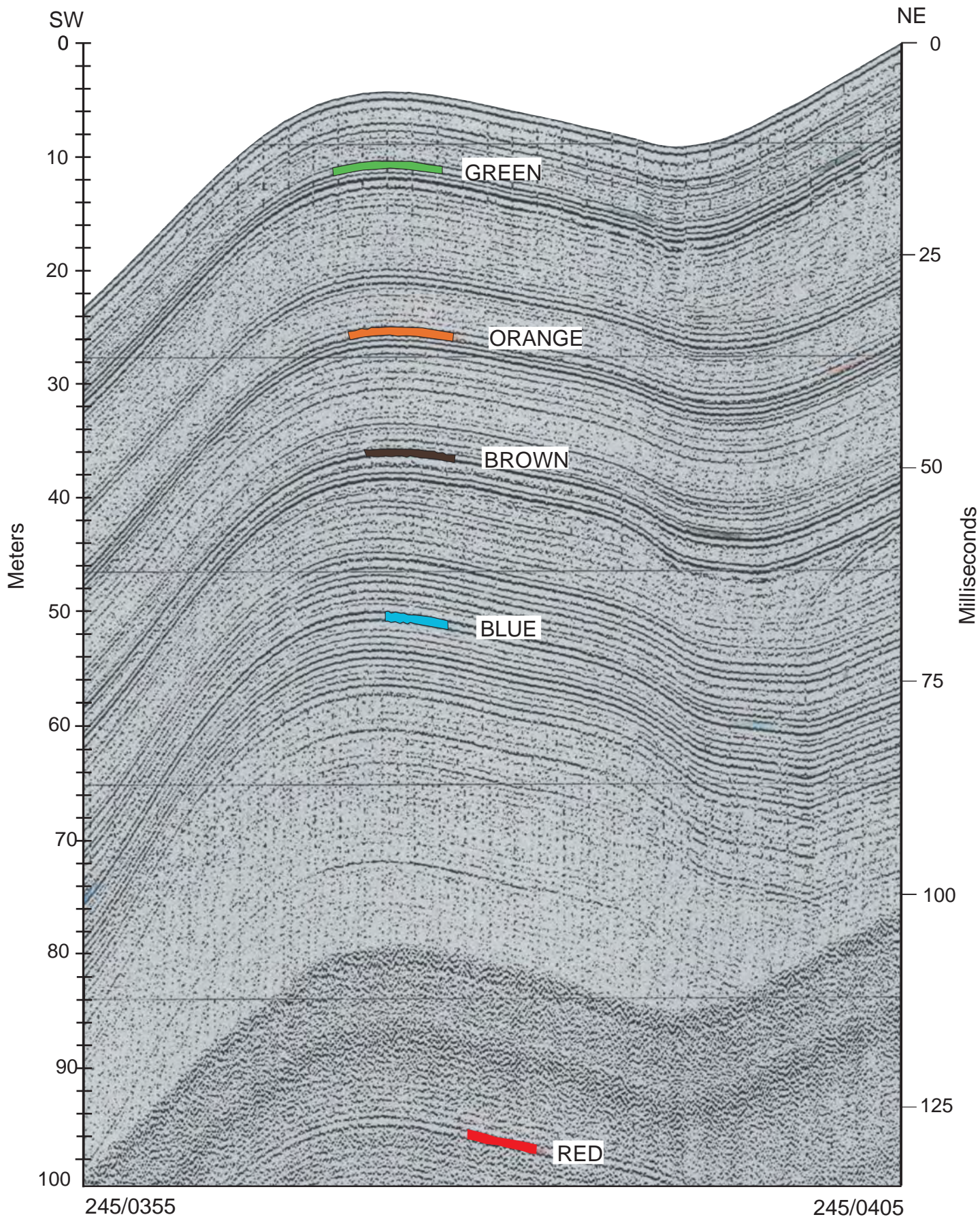


**Figure 3.** Type section of Huntec sparker seismic stratigraphy, showing reflections green, orange, brown, blue, and red.

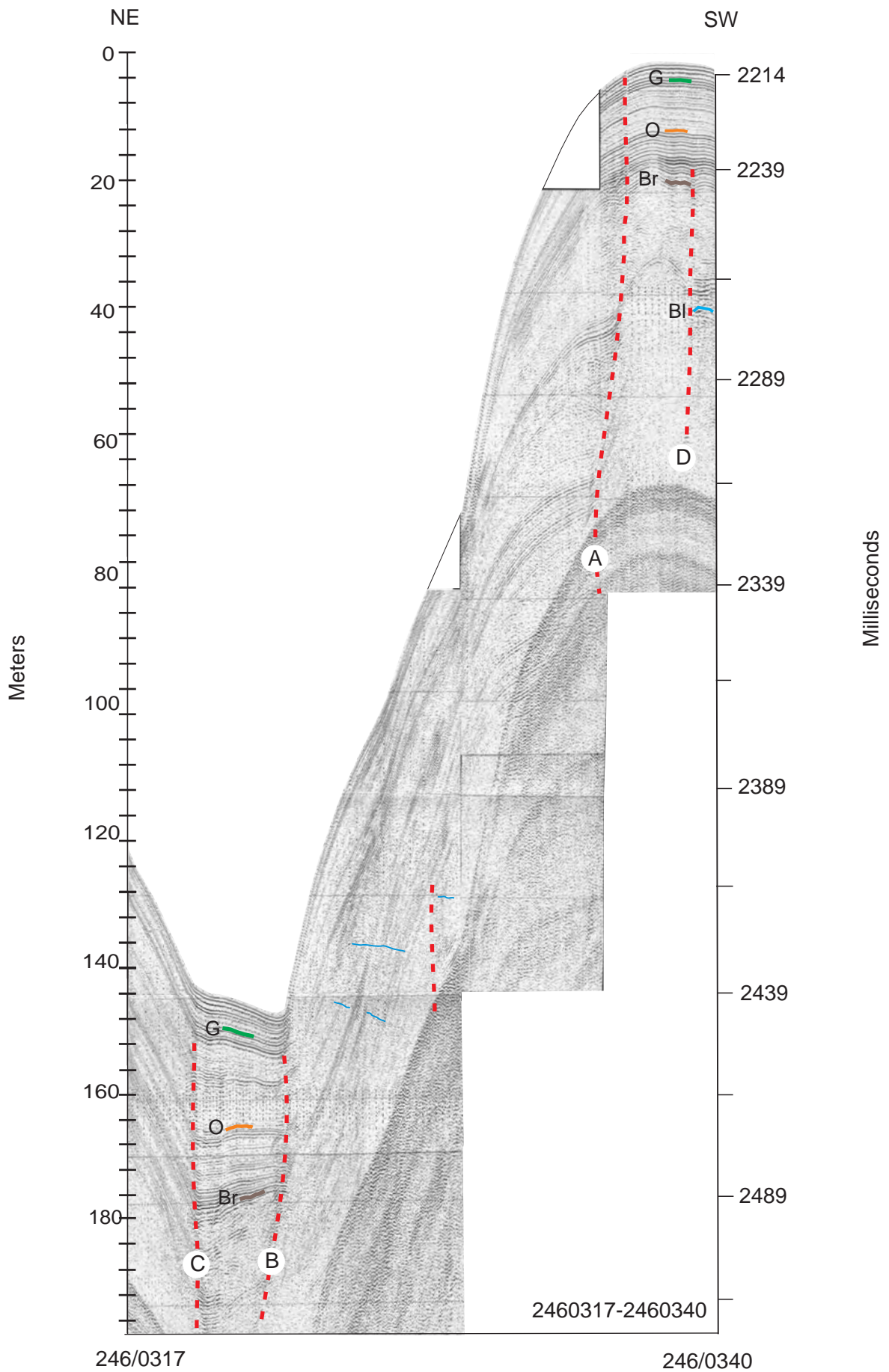


**Figure 4. Hunttec sparker profile showing the variable character of faults. For explanation, see text.**

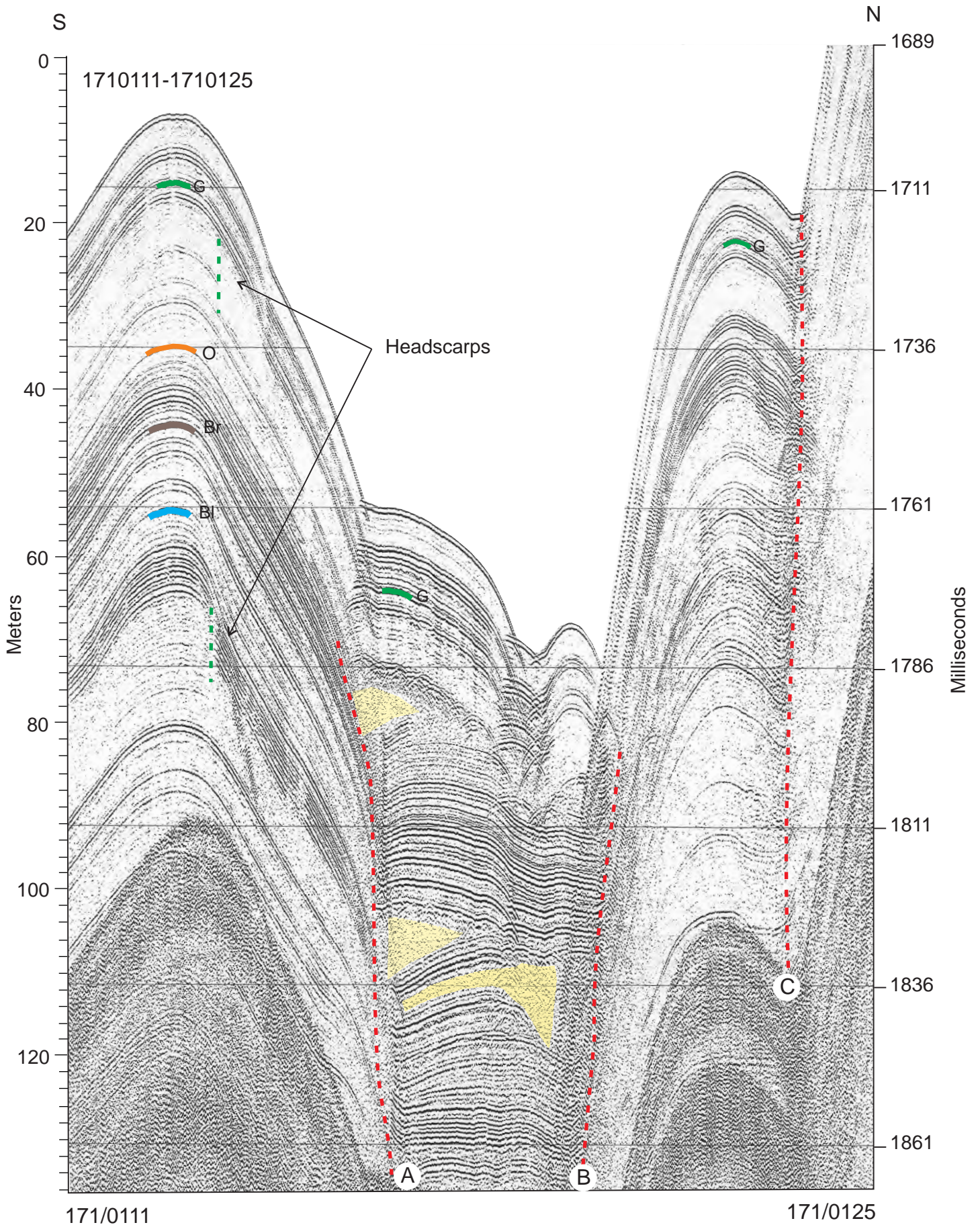


**Figure 5. Hunttec sparker profile showing fault-bound depression.**

## Core Summary Legend

### Colour Legend

Foram Ooze

Olive Grey Mud (Ogm)

Olive Grey Sandy Mud (Ogm1)

Olive Grey Mud with Ice-Rafted Detritus (Ogm2)

Brick Red Mud (Brm)

Red Brown Mud (Rbm)

Red Brown Sandy Mud (Rbm1)

Red Brown Mud with Ice-Rafted Detritus (Rbm2)

Brown Mud (Bm)

Brown Sandy Mud (Bm1)

Brown Mud with Ice-Rafted Detritus (Bm2)

Grey Mud (Gm)

Grey Sandy Mud (Gm1)

Grey Mud with Ice-Rafted Detritus (Gm2)

Tan Mud

Sand or Gravel

Debris Flow

Mudclast Conglomerate

Diamicton

Folded Mud Block

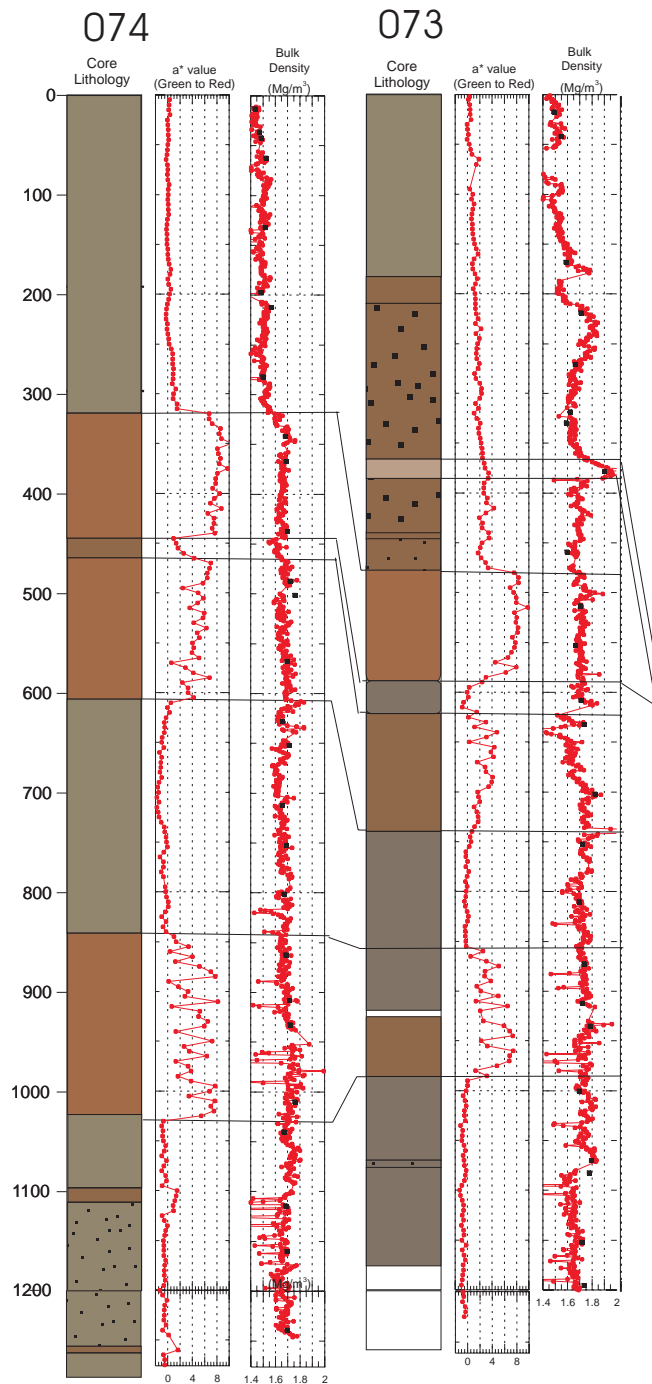


**Figure 6. Piston cores 73 and 74, lower St. Pierre Slope.**



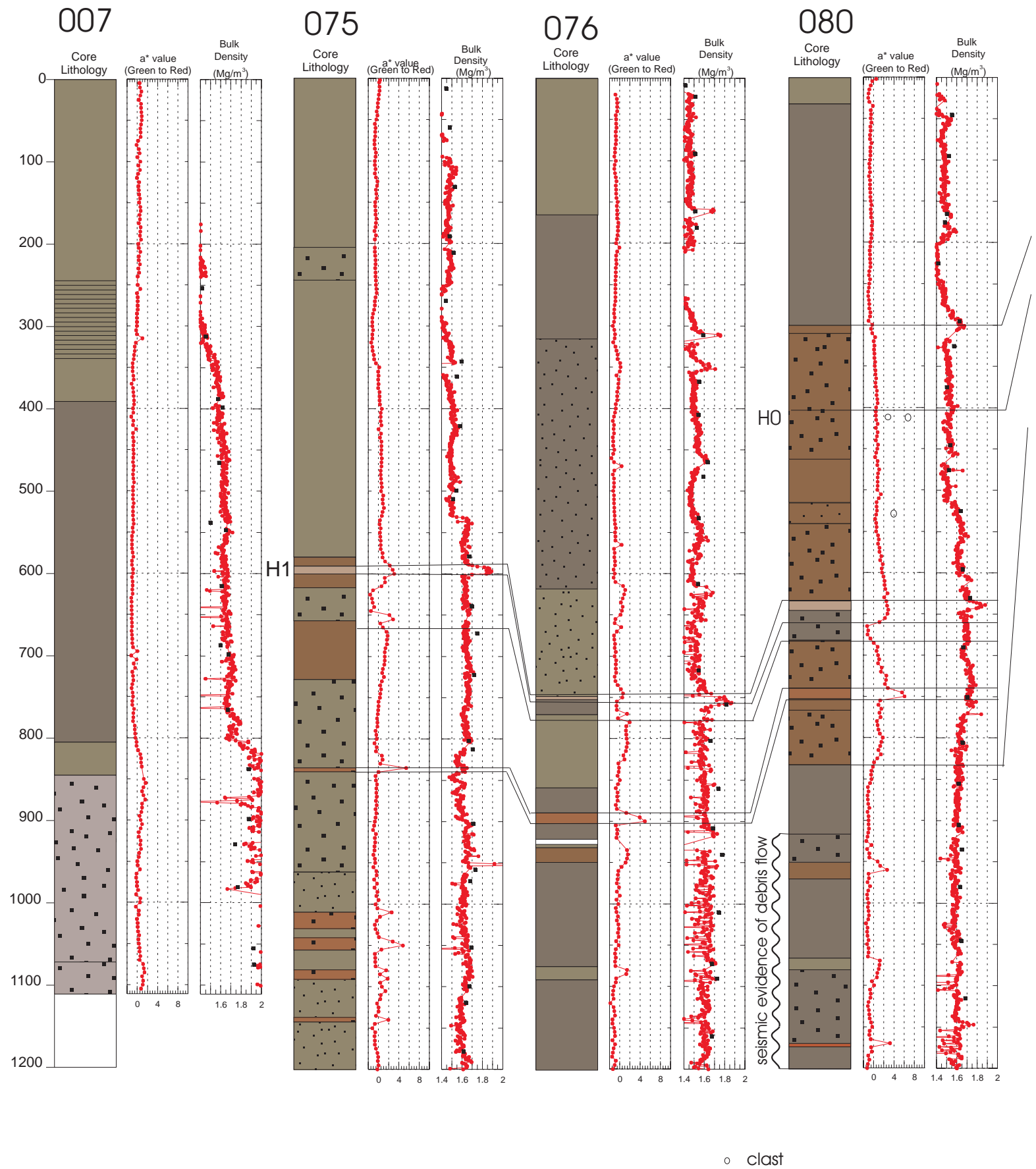


**Figure 7. Piston cores 7, 75, 76 and 80, SW Grand Banks Slope.**

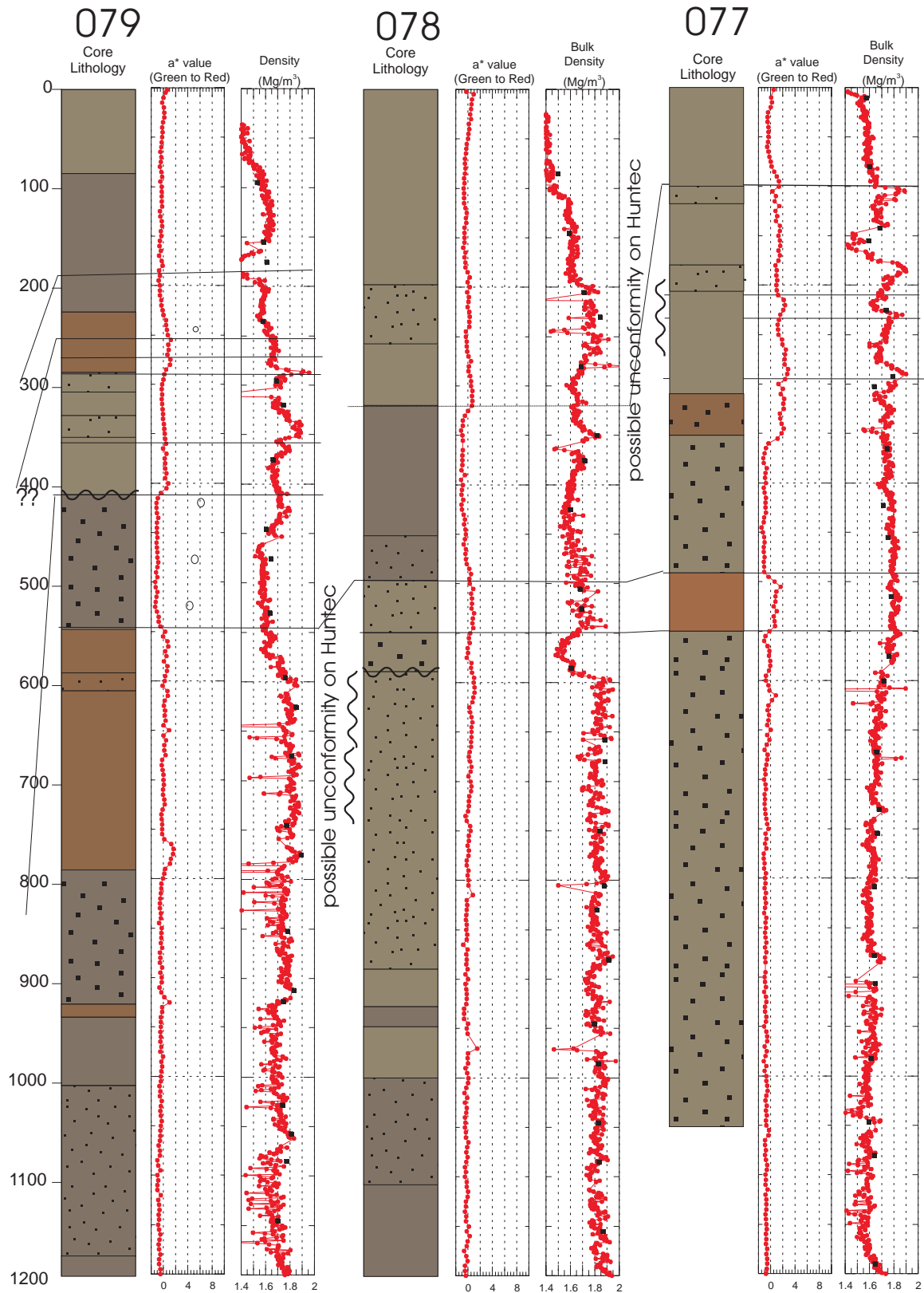


**Figure 8. Piston cores 77, 78 and 79, SW Grand Banks Rise.**

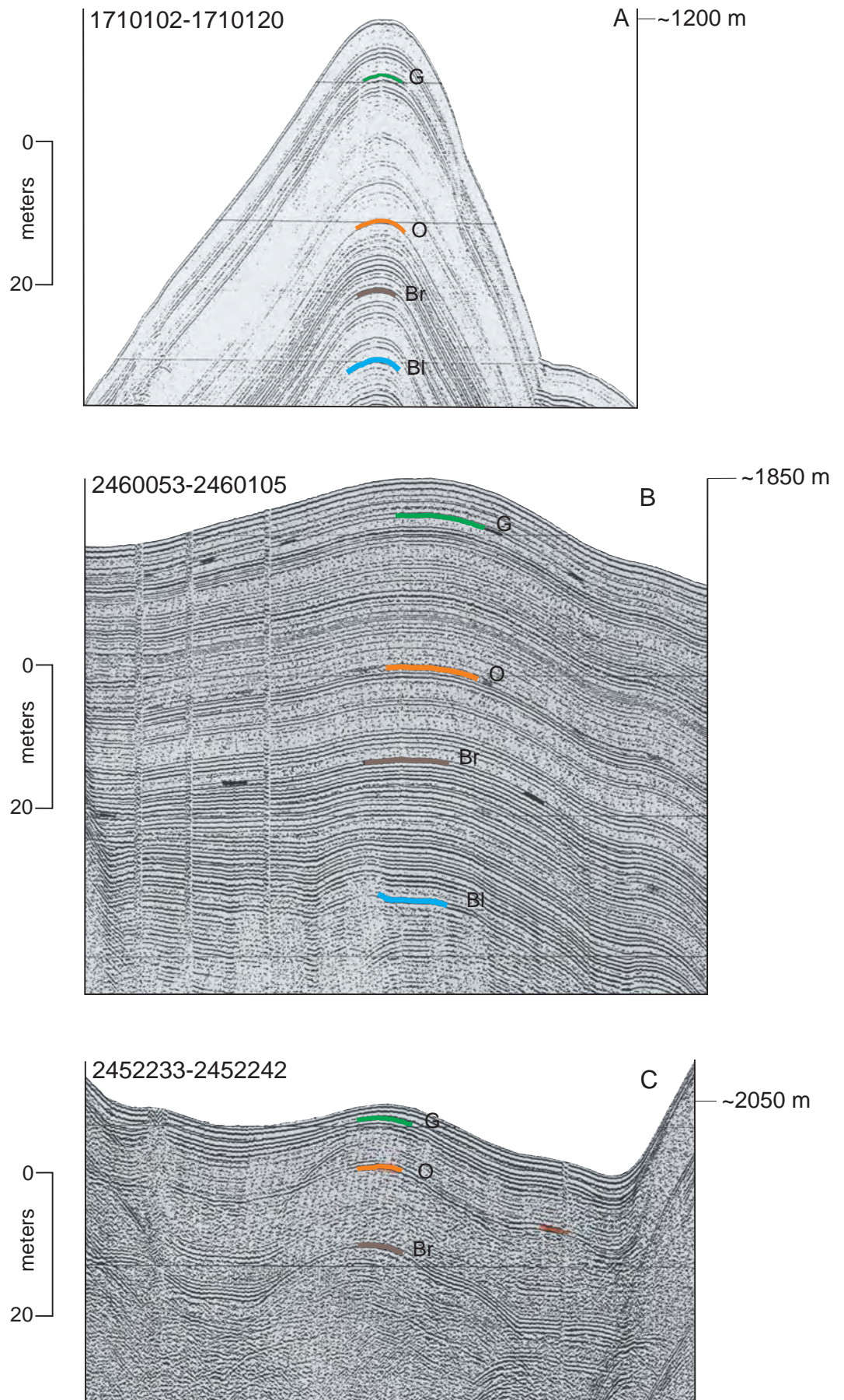


**Fig. 9:** Variation in stratal thickness between green and orange reflections

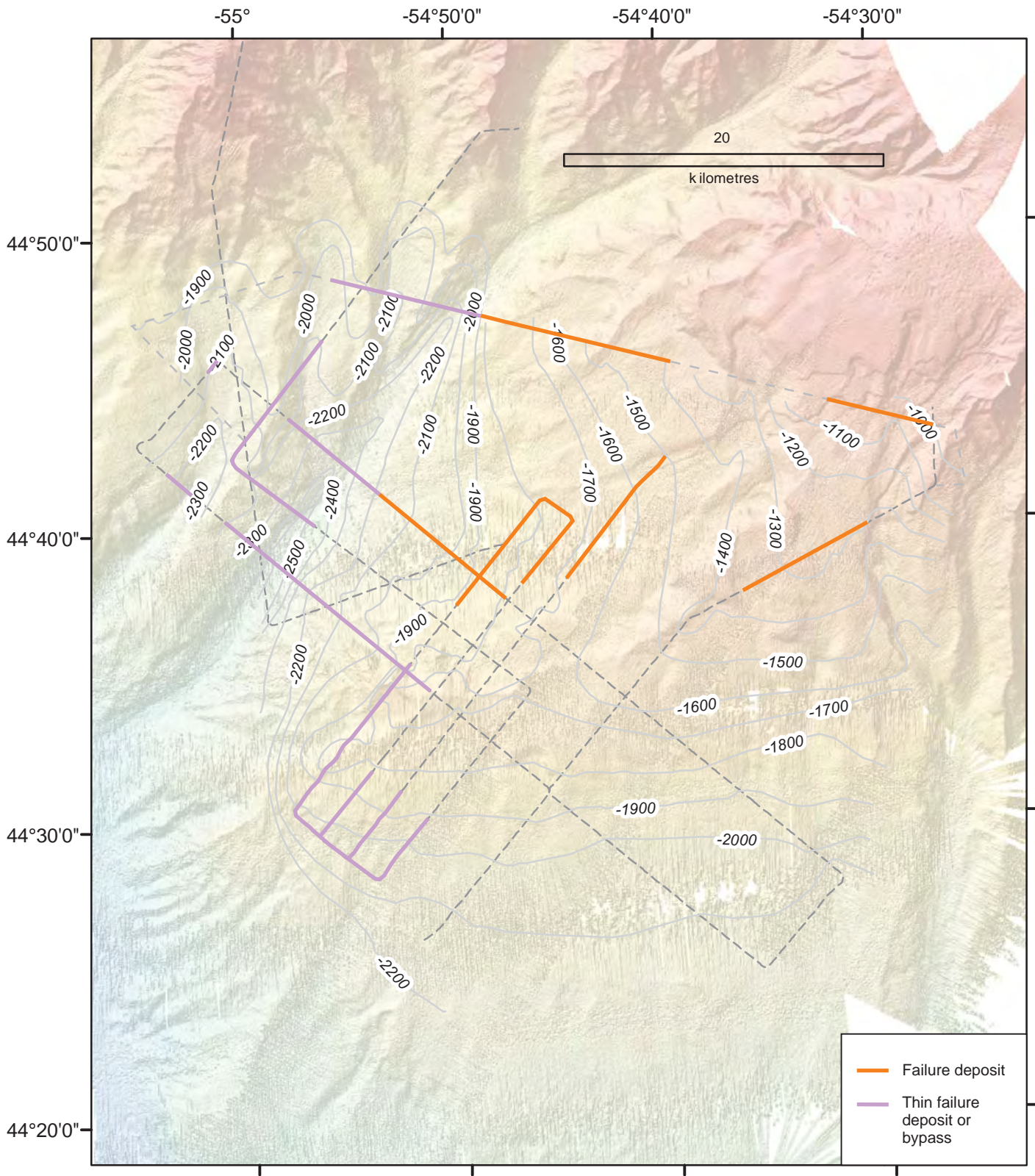


**Figure 10:** Detail of Interval I of mass-failure features

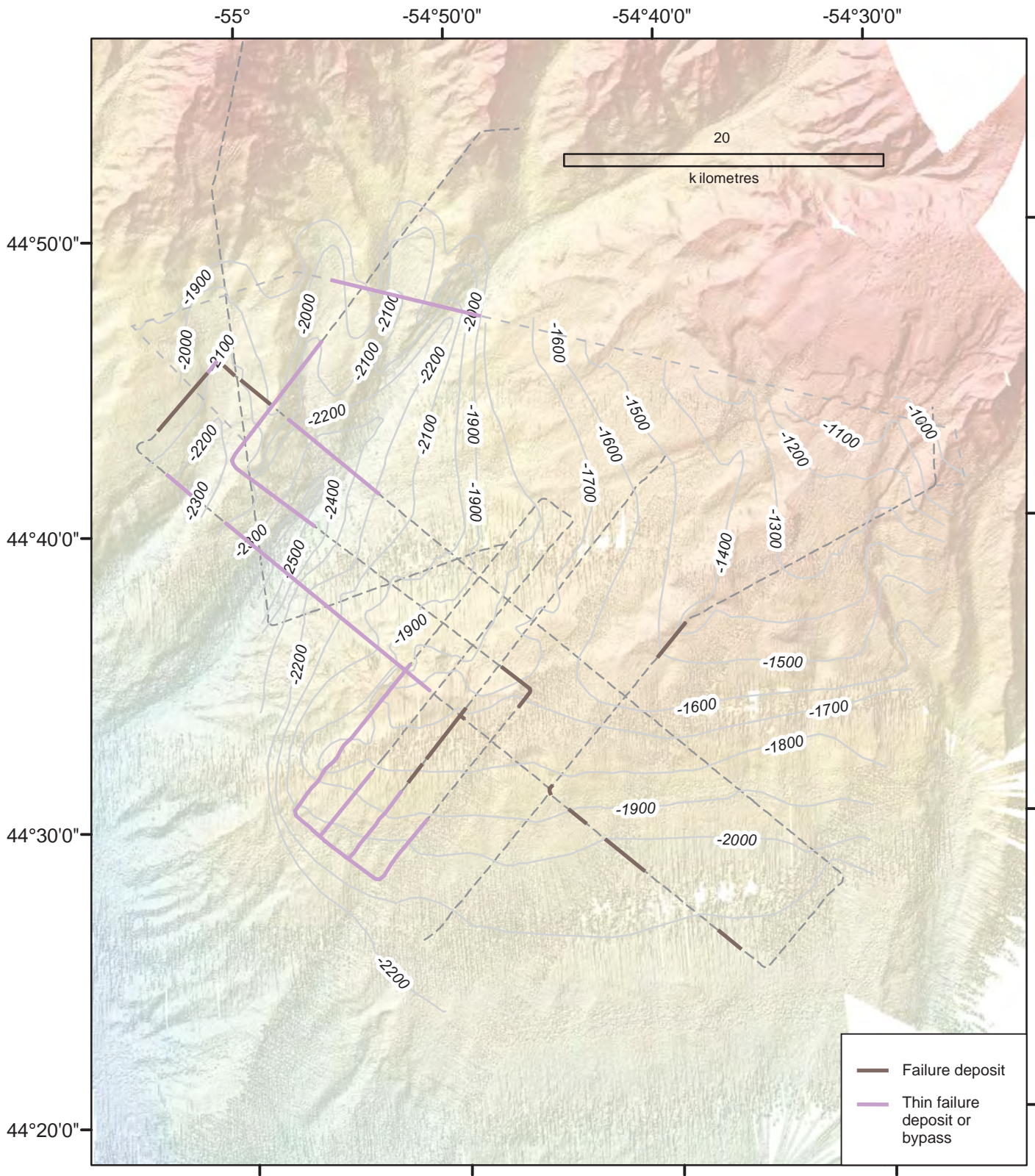


**Figure 11:** Detail of Interval II of mass-failure features

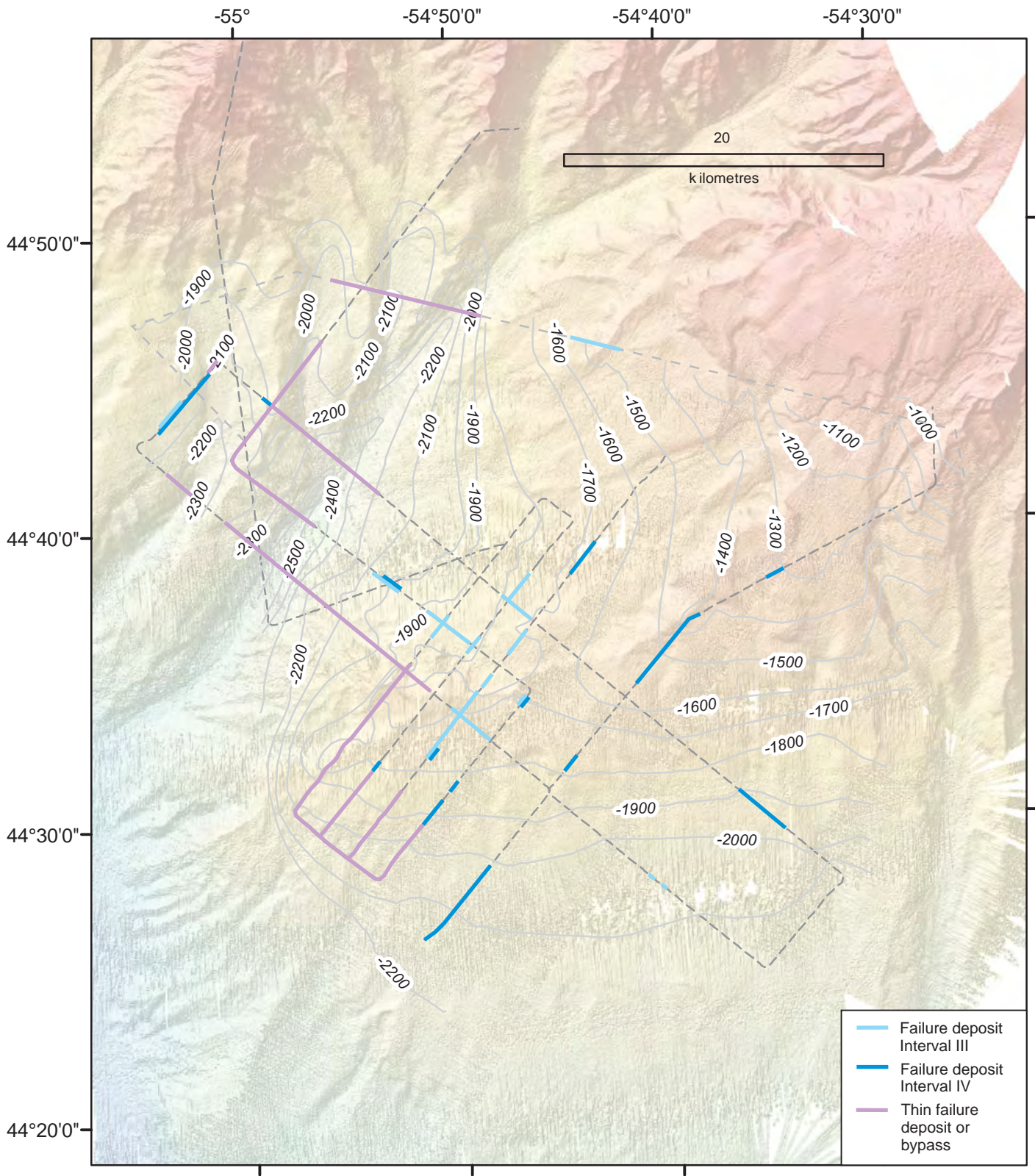


**Figure 12:** Detail of Intervals III and IV of mass-failure features

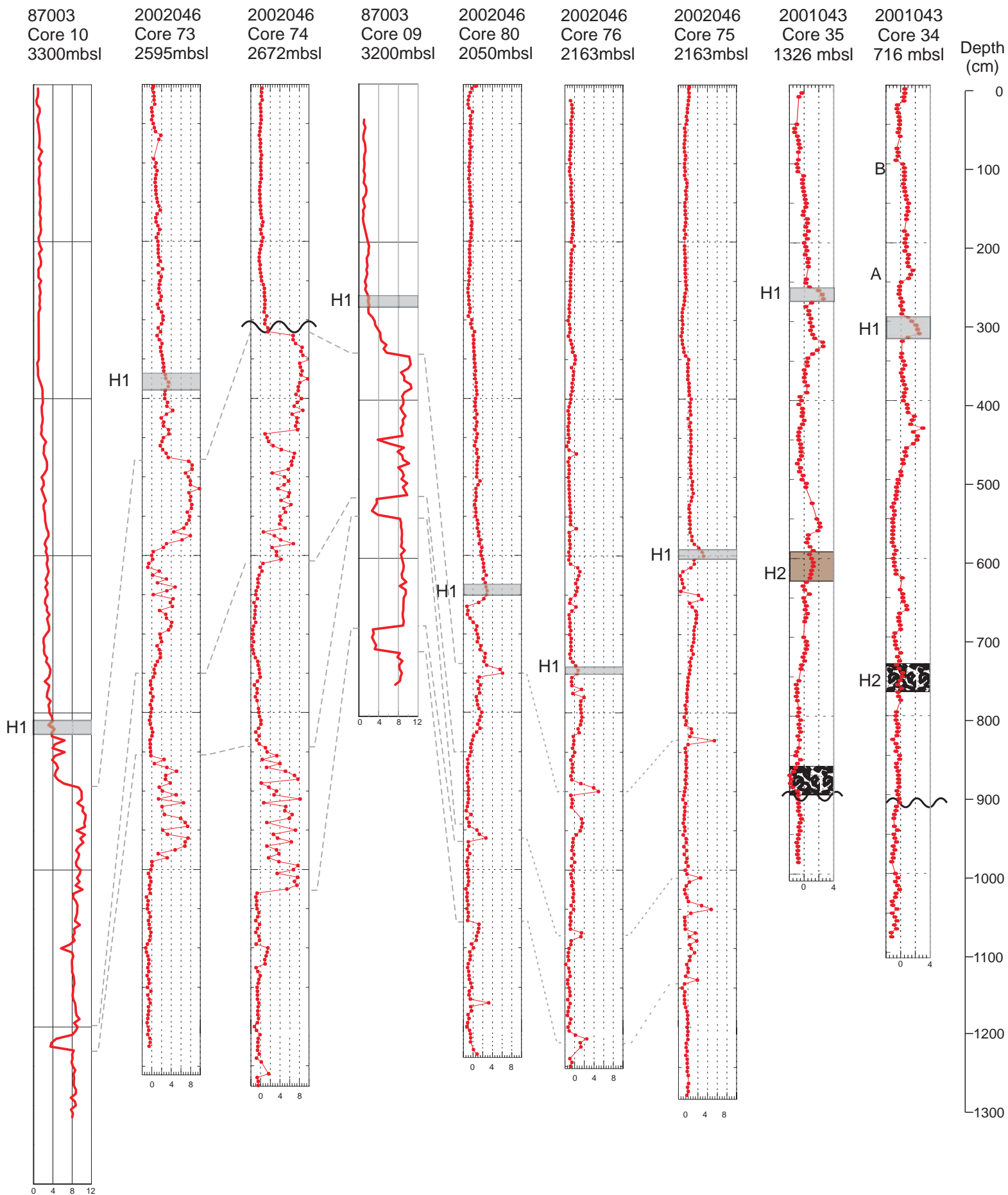


**Figure 13:** Correlation of  $a^*$  colour trace in cores from continental rise.

Slope Cores

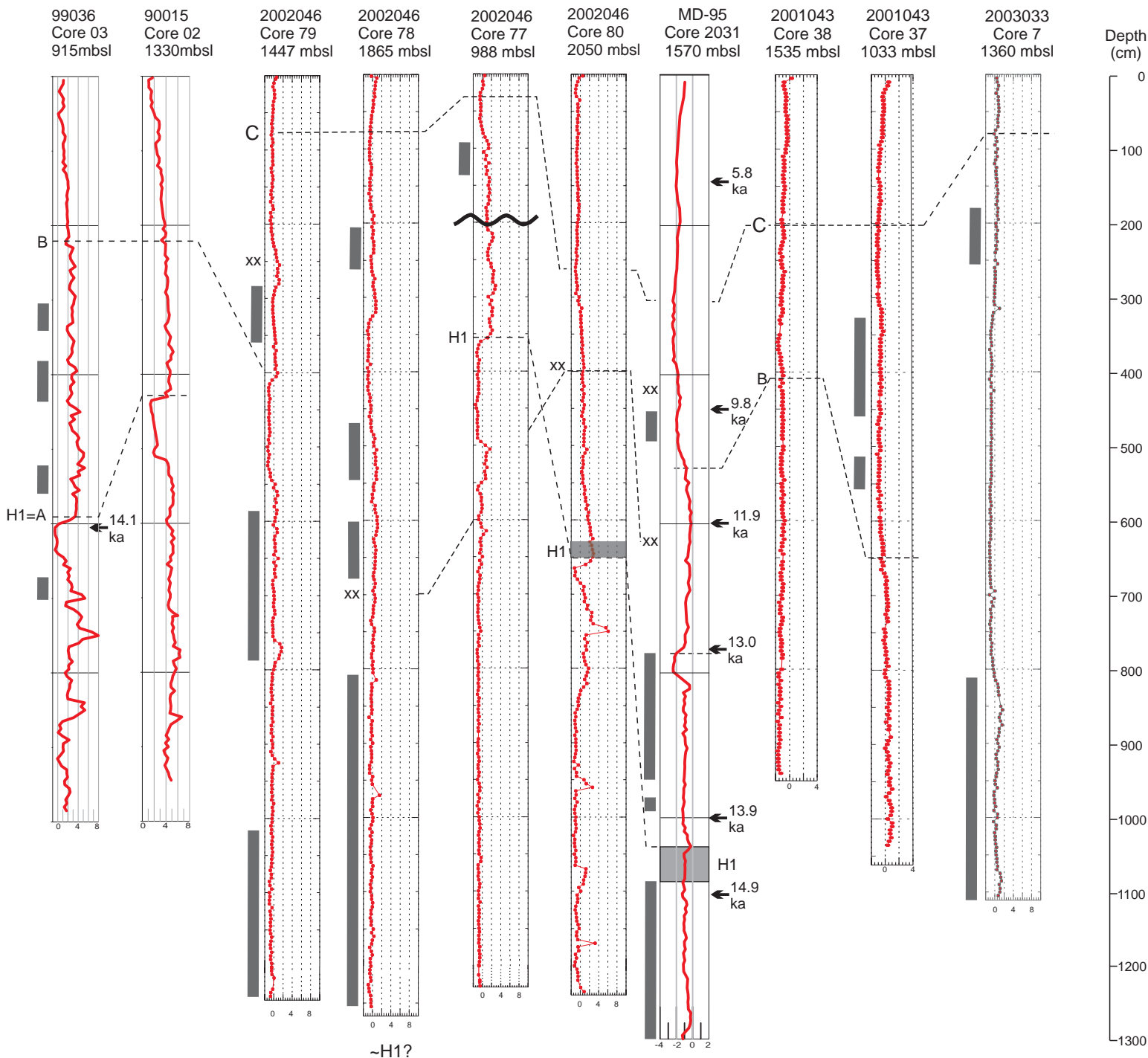
Canyon Cores

Northwest

Southeast

Southeast

Northwest



xx carbonate mud clasts  
 █ intervals with sand beds

← 5.8 ka age (reservoir corrected) in C-14 years BP

**Figure 14:** Correlation of a\* colour trace in cores from the continental slope between the Narwhal F-99 area (Piper et al. 2005) and the study area.



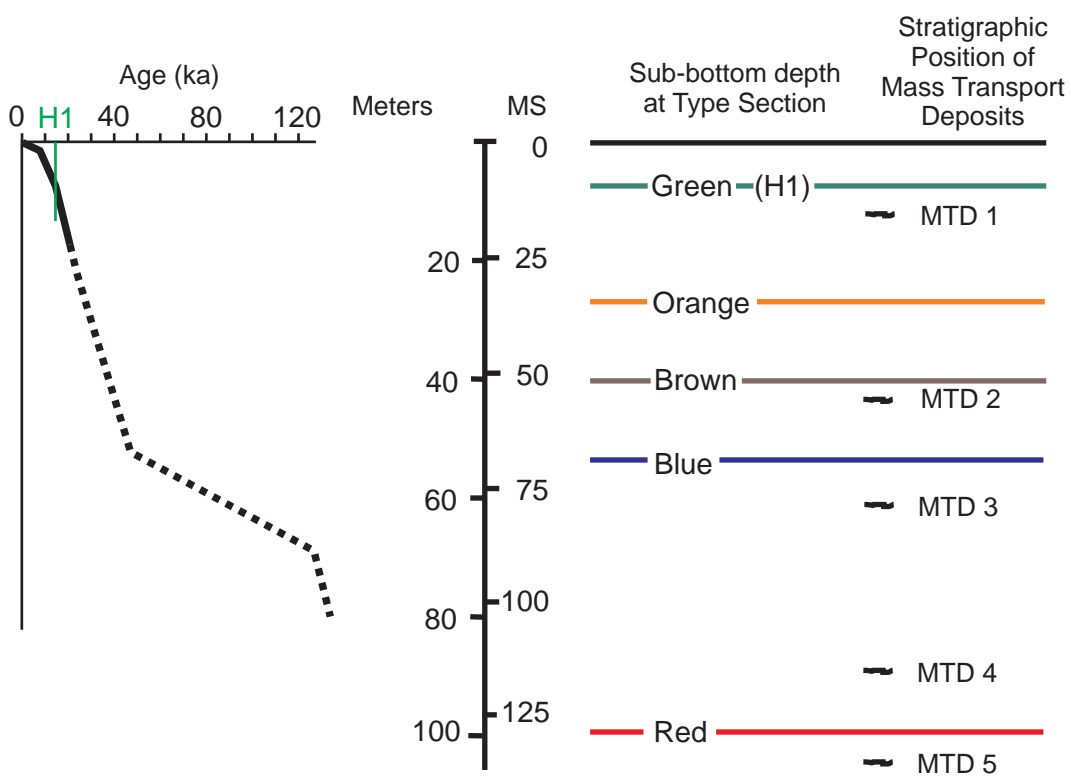


**Figure 15.** Plots showing sedimentation rate and tentative age model for the stratigraphic succession. For explanation, see text.

## **Sparker profiles illustrating faults**

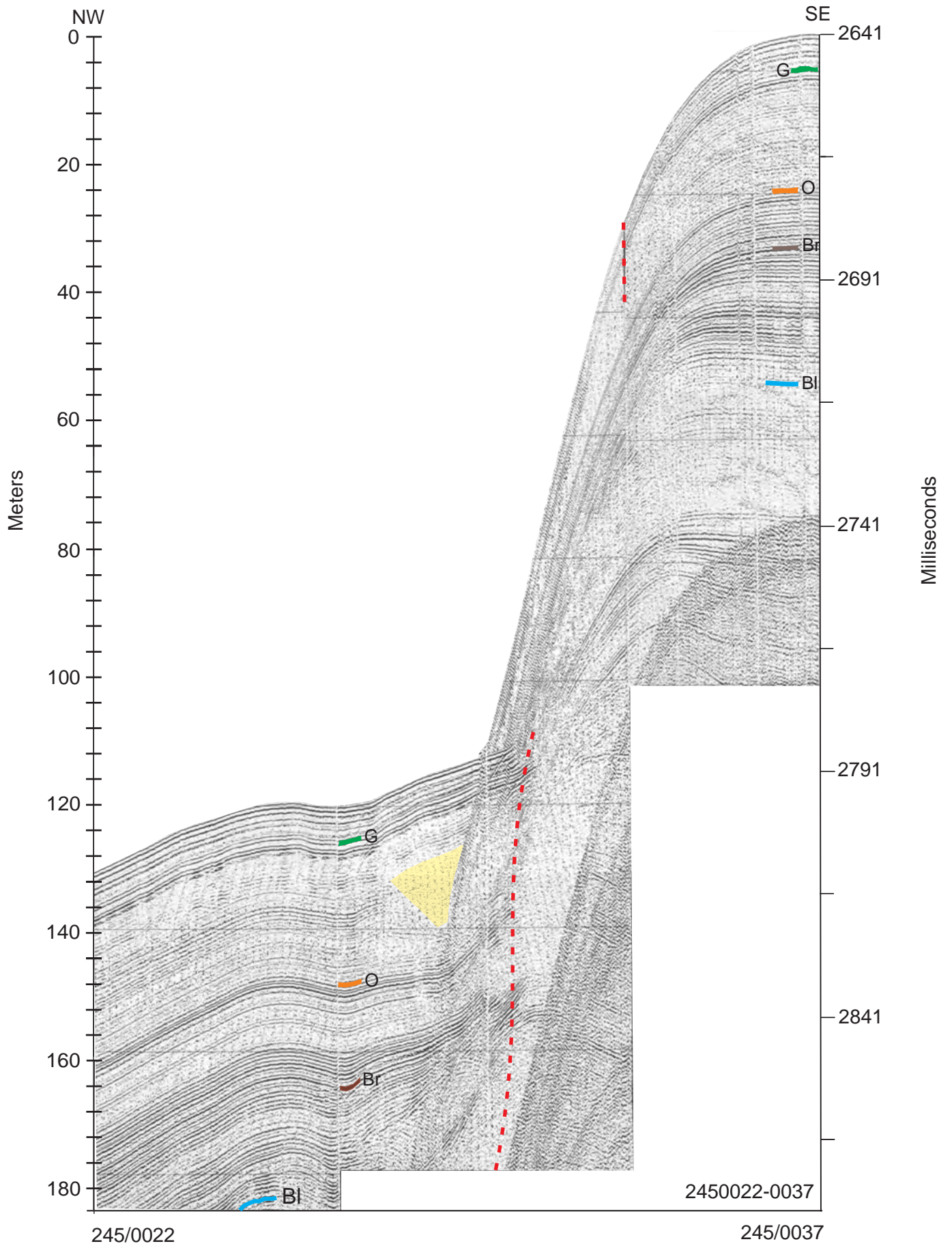
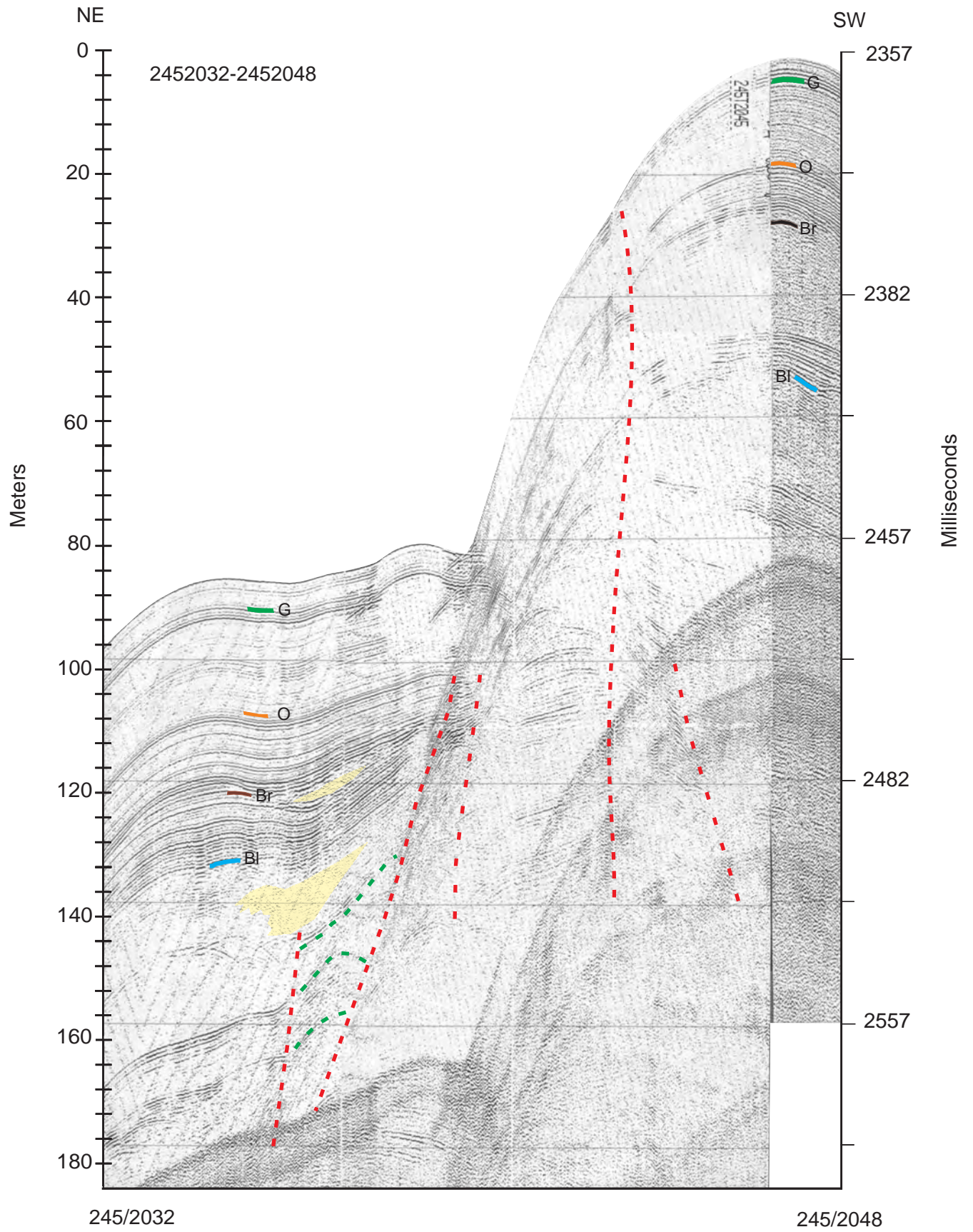
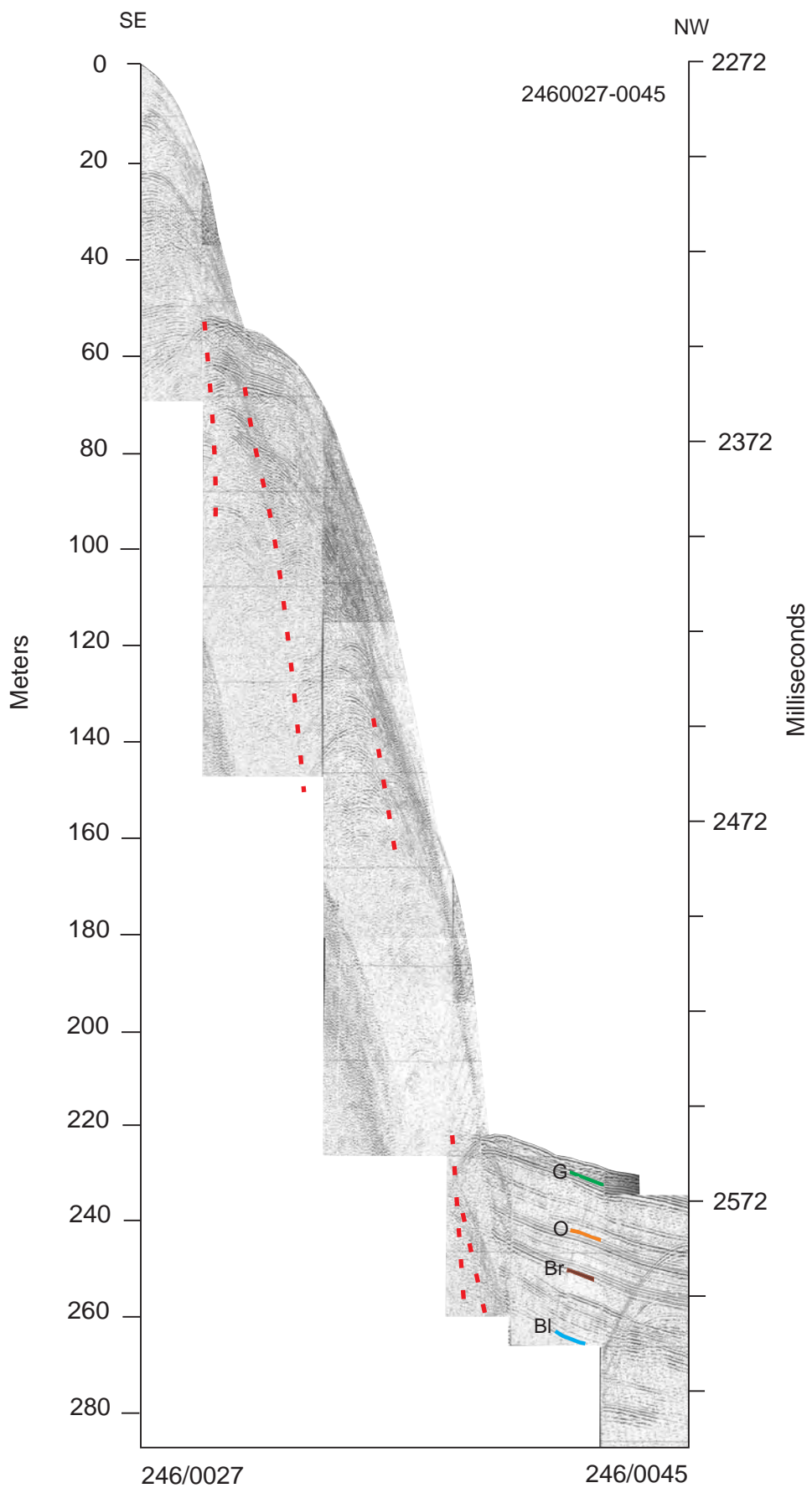


Figure A1





**Figure A3**

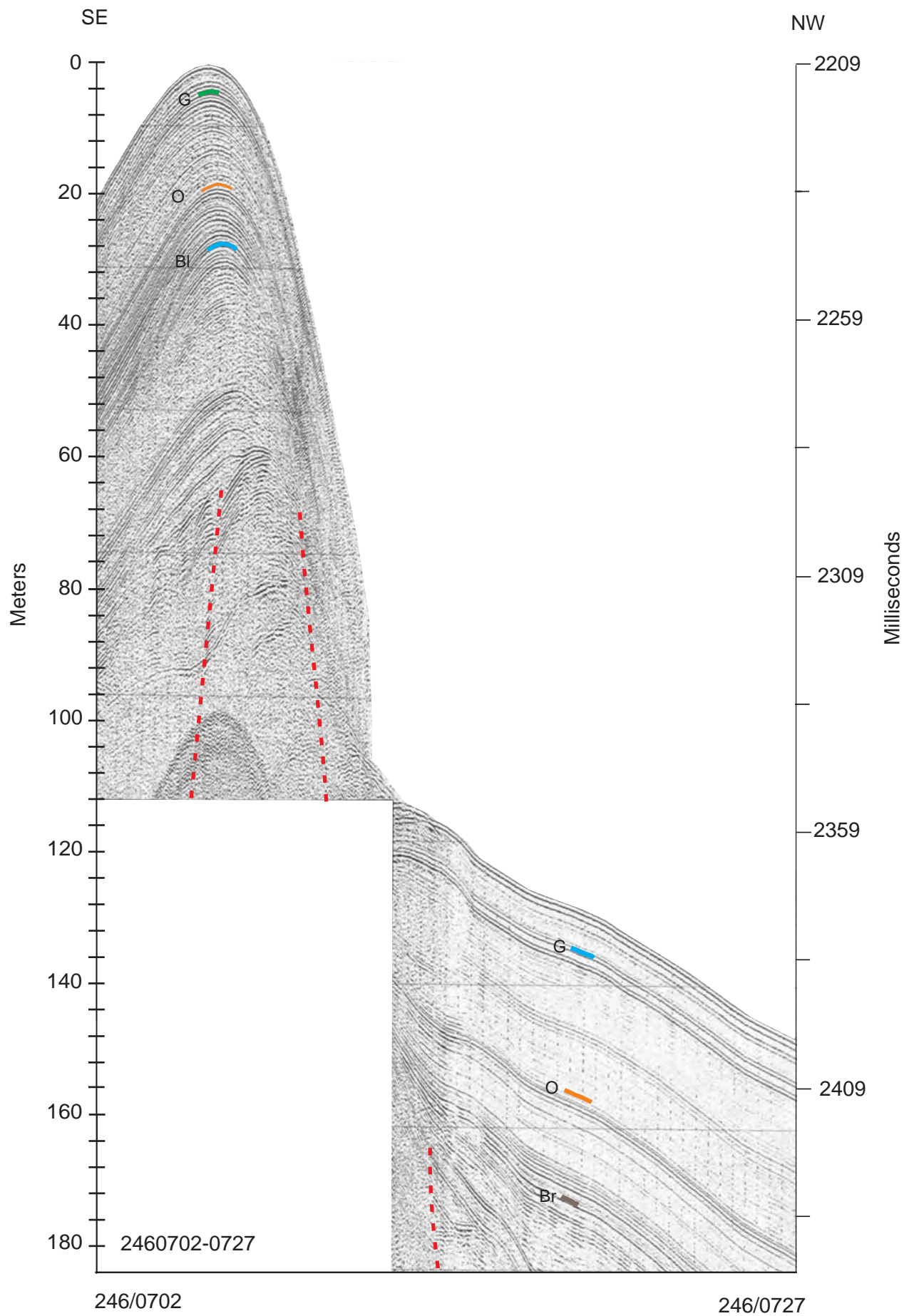
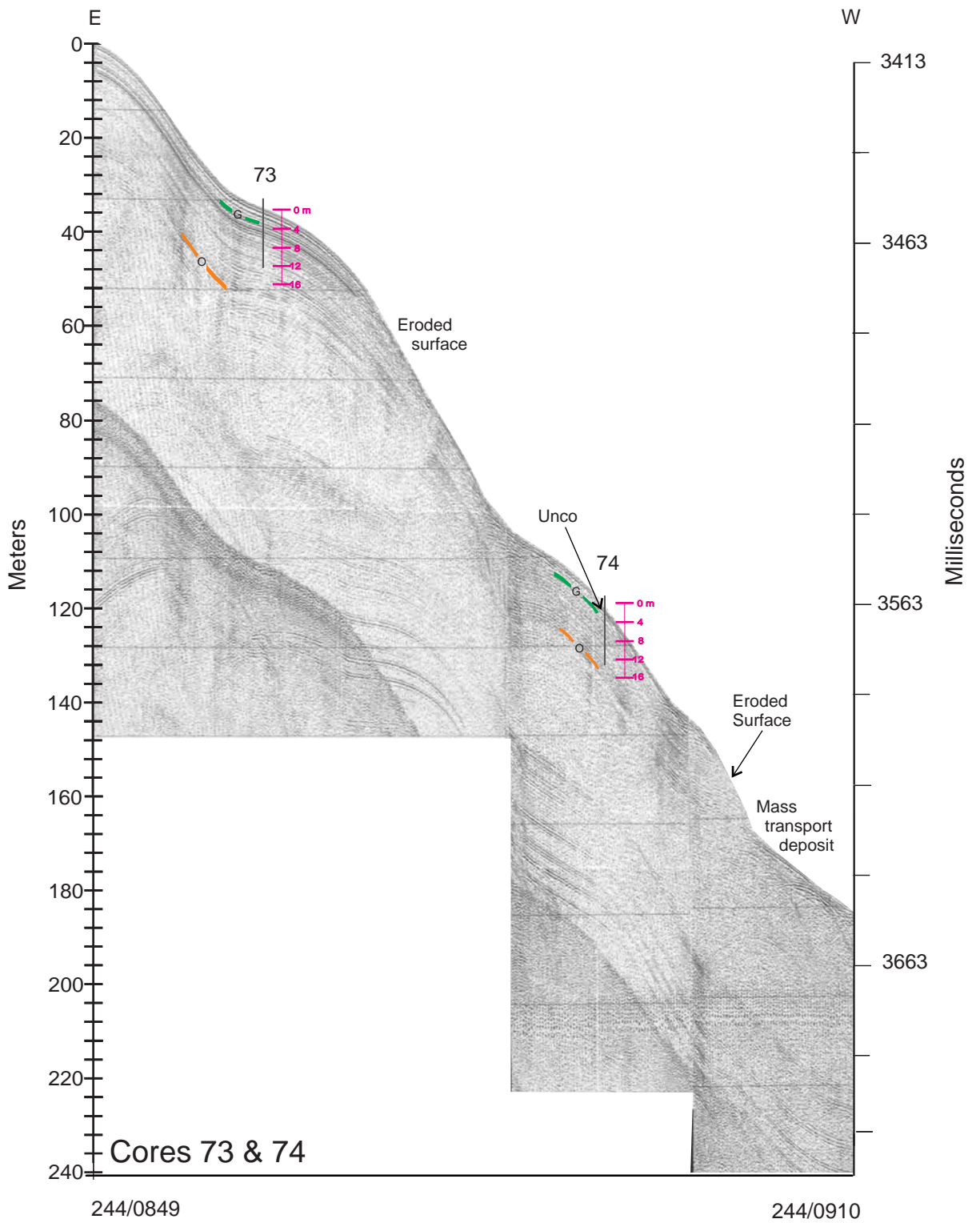


Figure A4

## **Sparker profiles showing core locations**



**Figure B1**



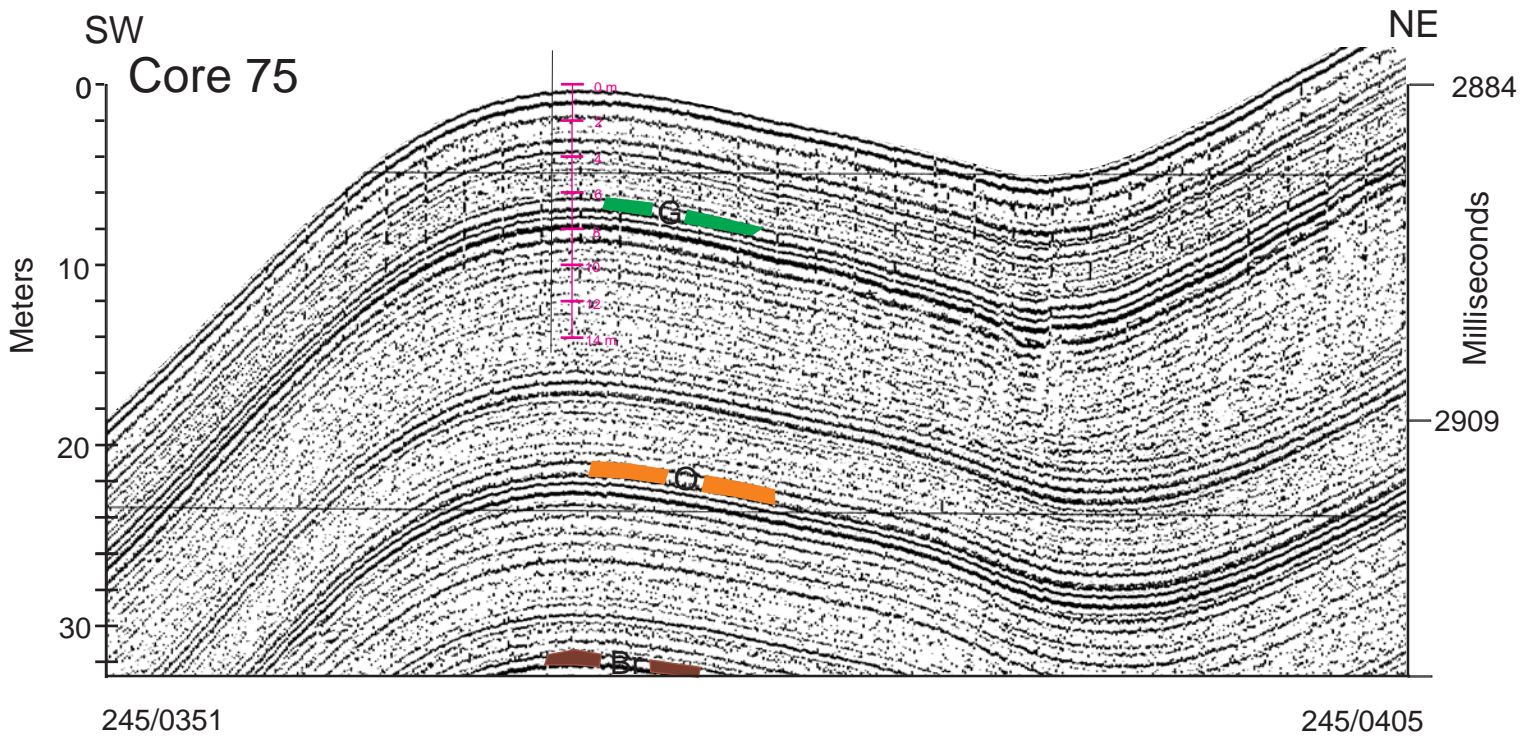


**Figure B2**

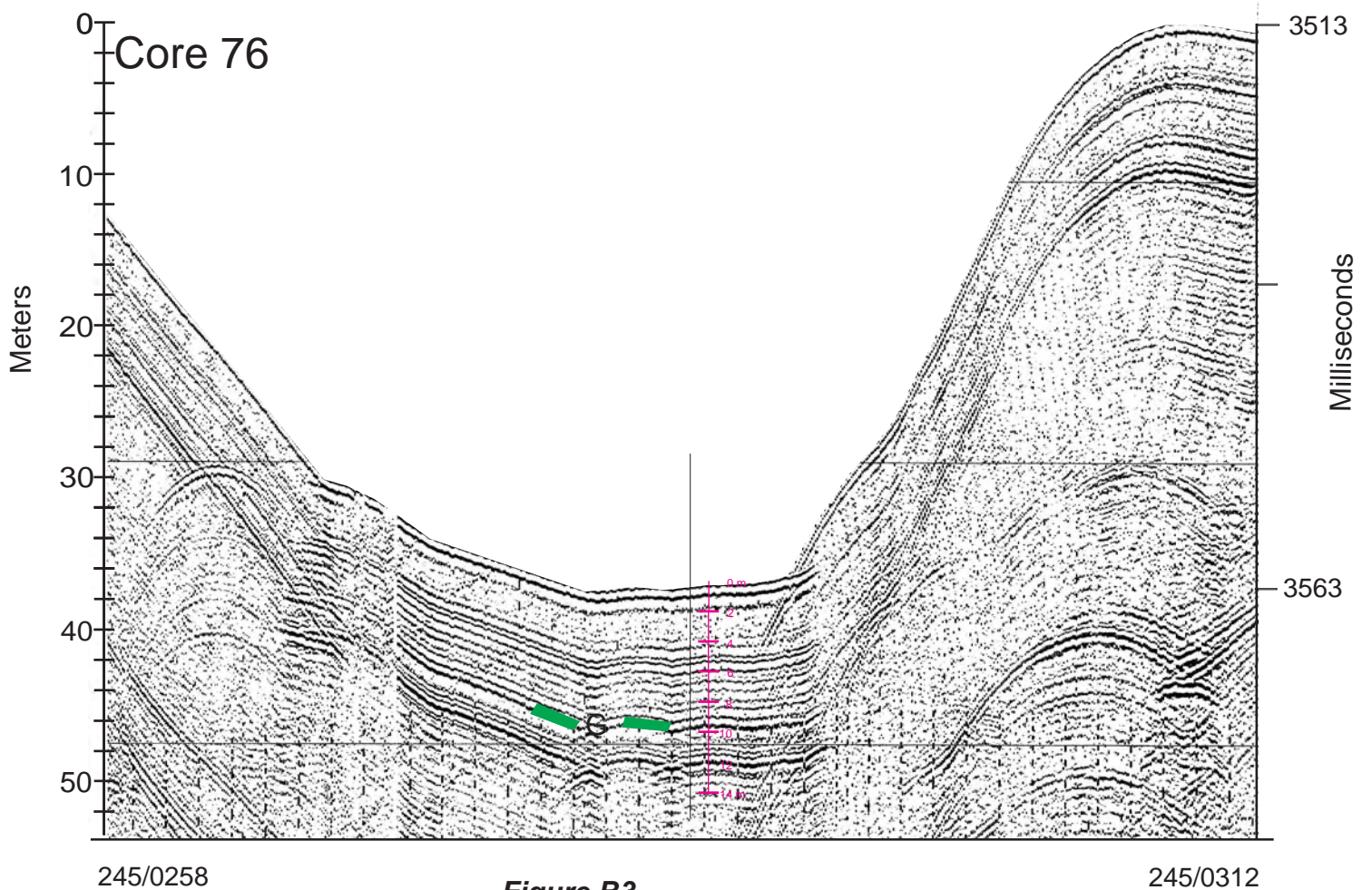


**Figure B3**

# Core 77

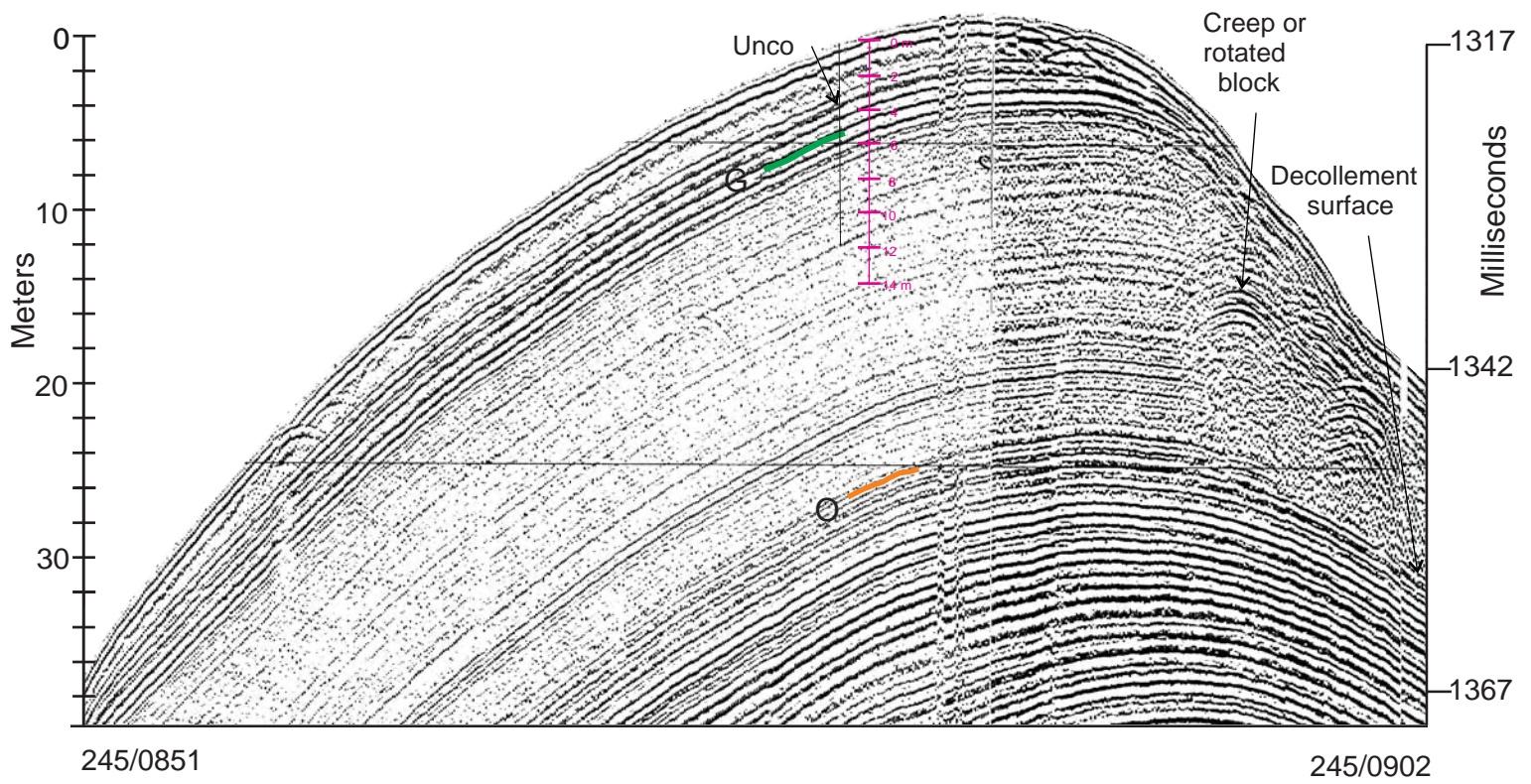


**Figure B4**

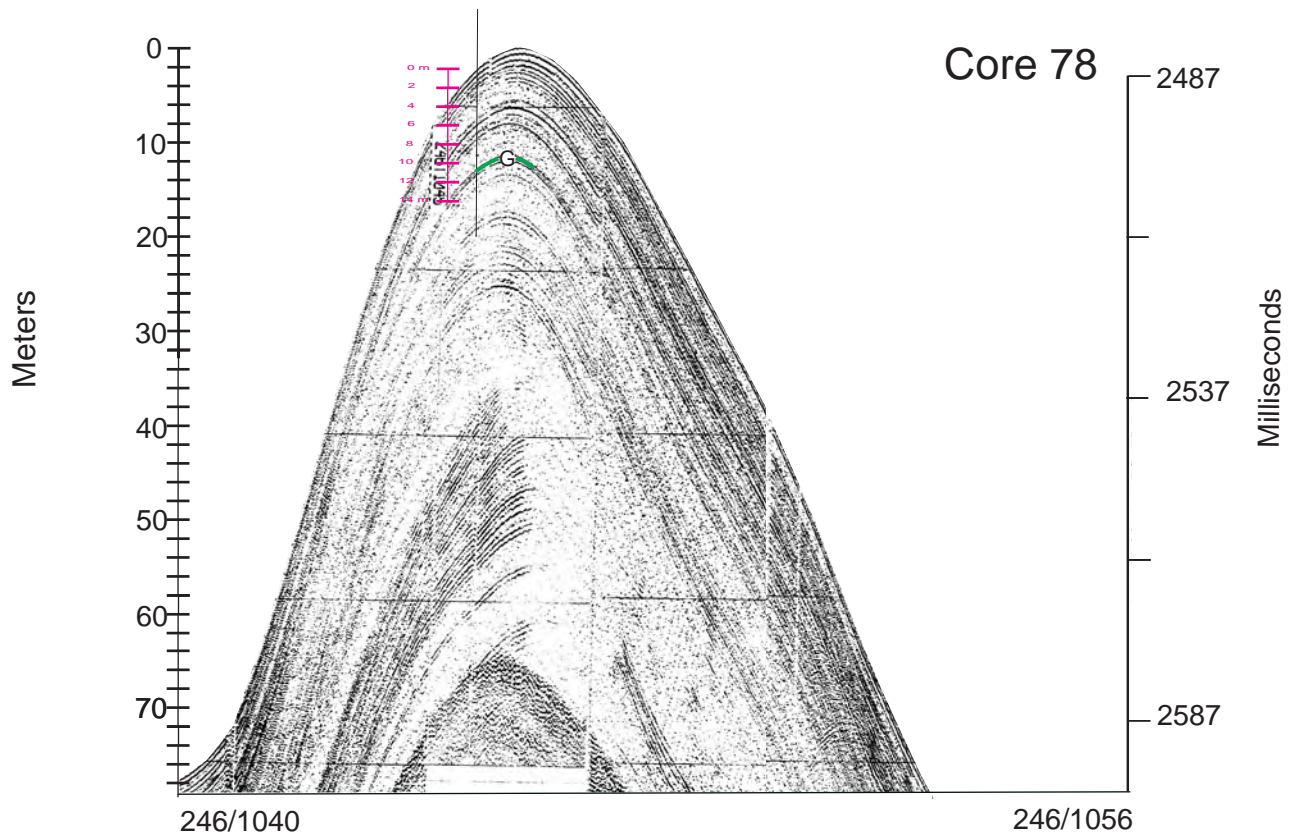


**Figure B5**

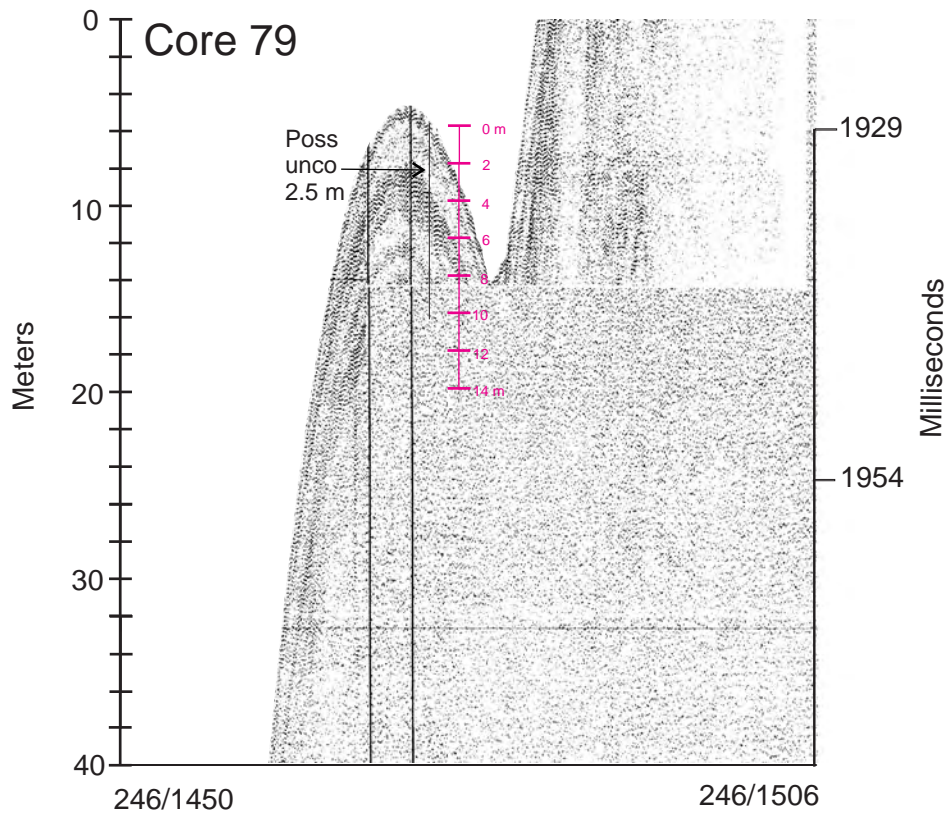


**Figure B6**

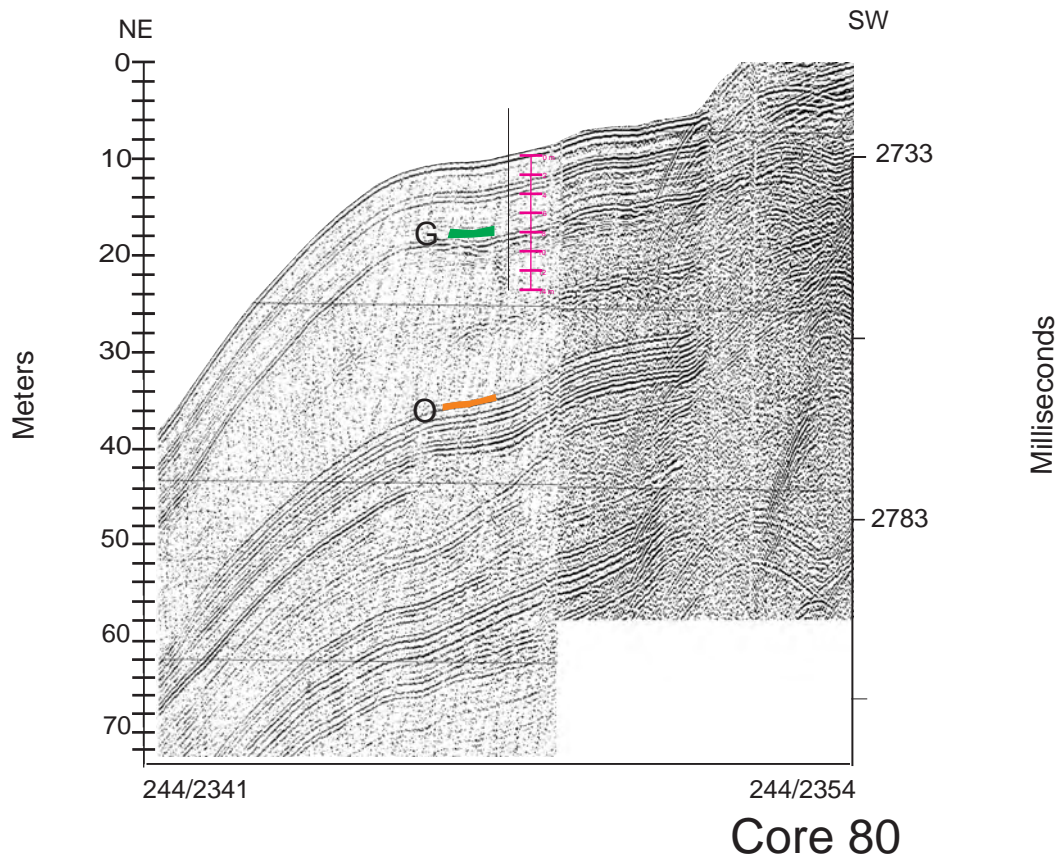


**Figure B7**

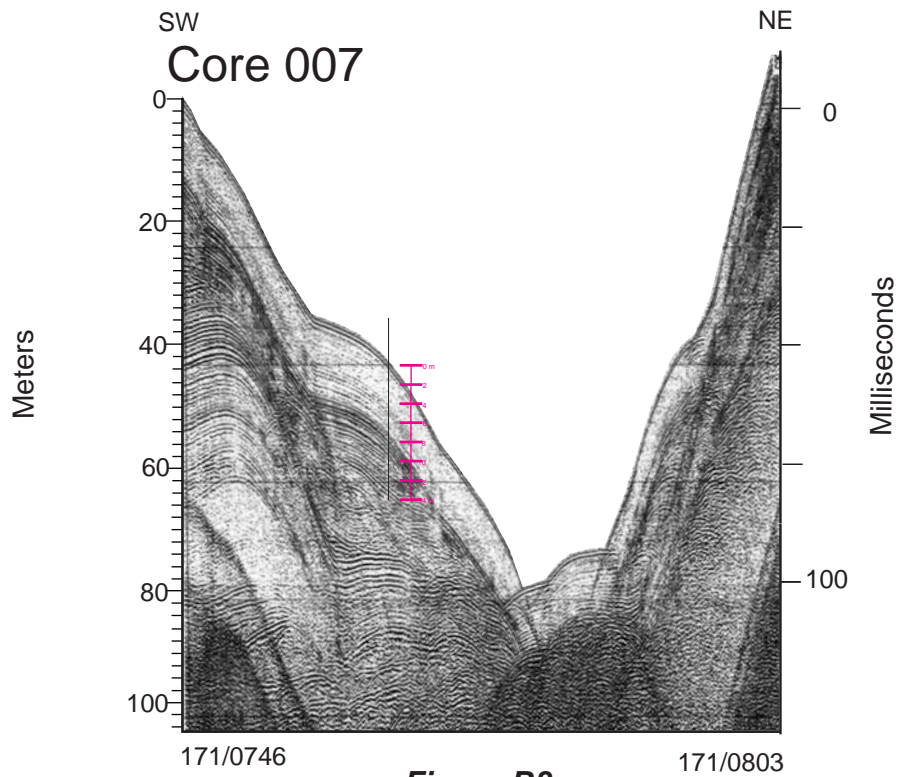


**Figure B8**

## **Sparker profiles illustrating mass-transport deposits**

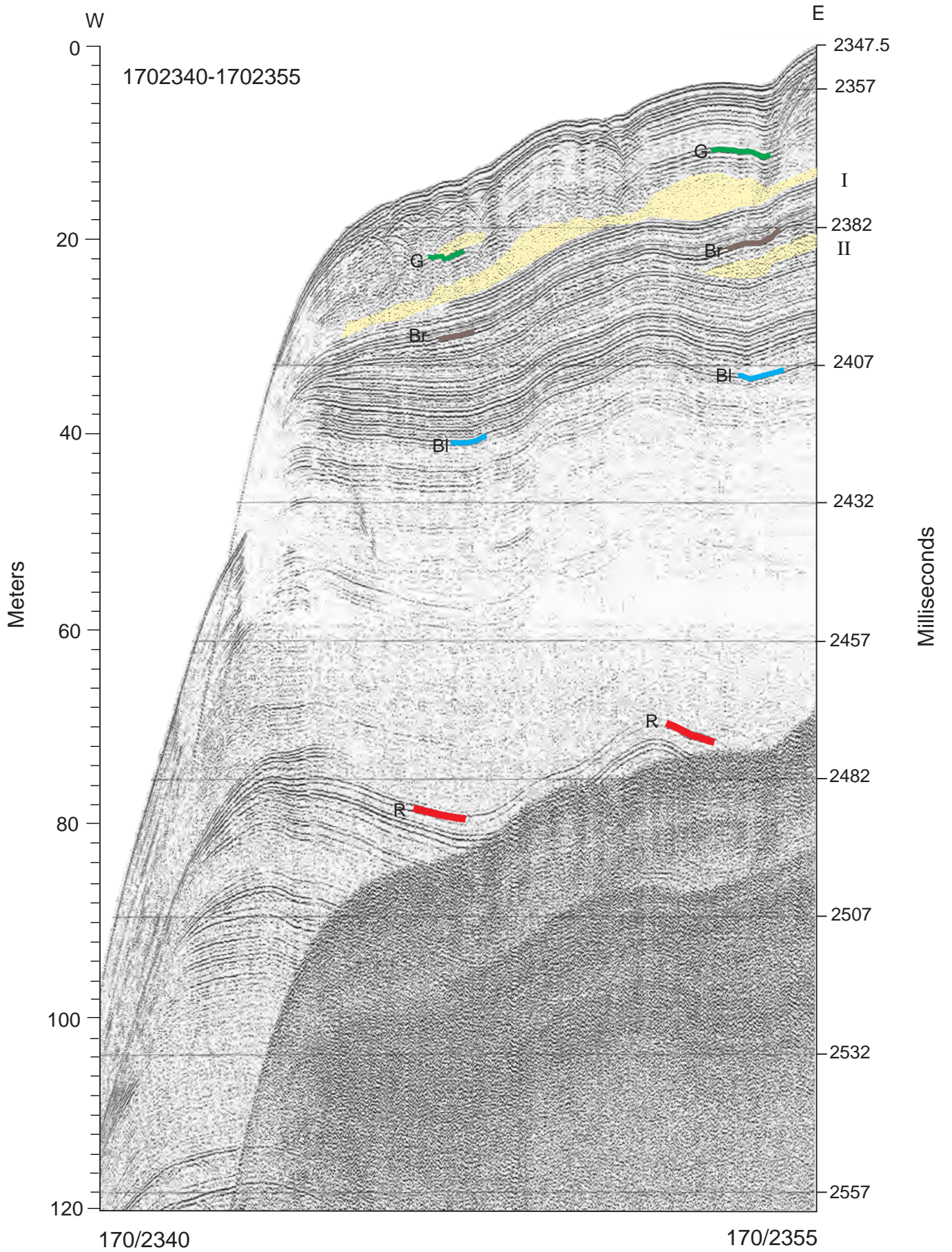
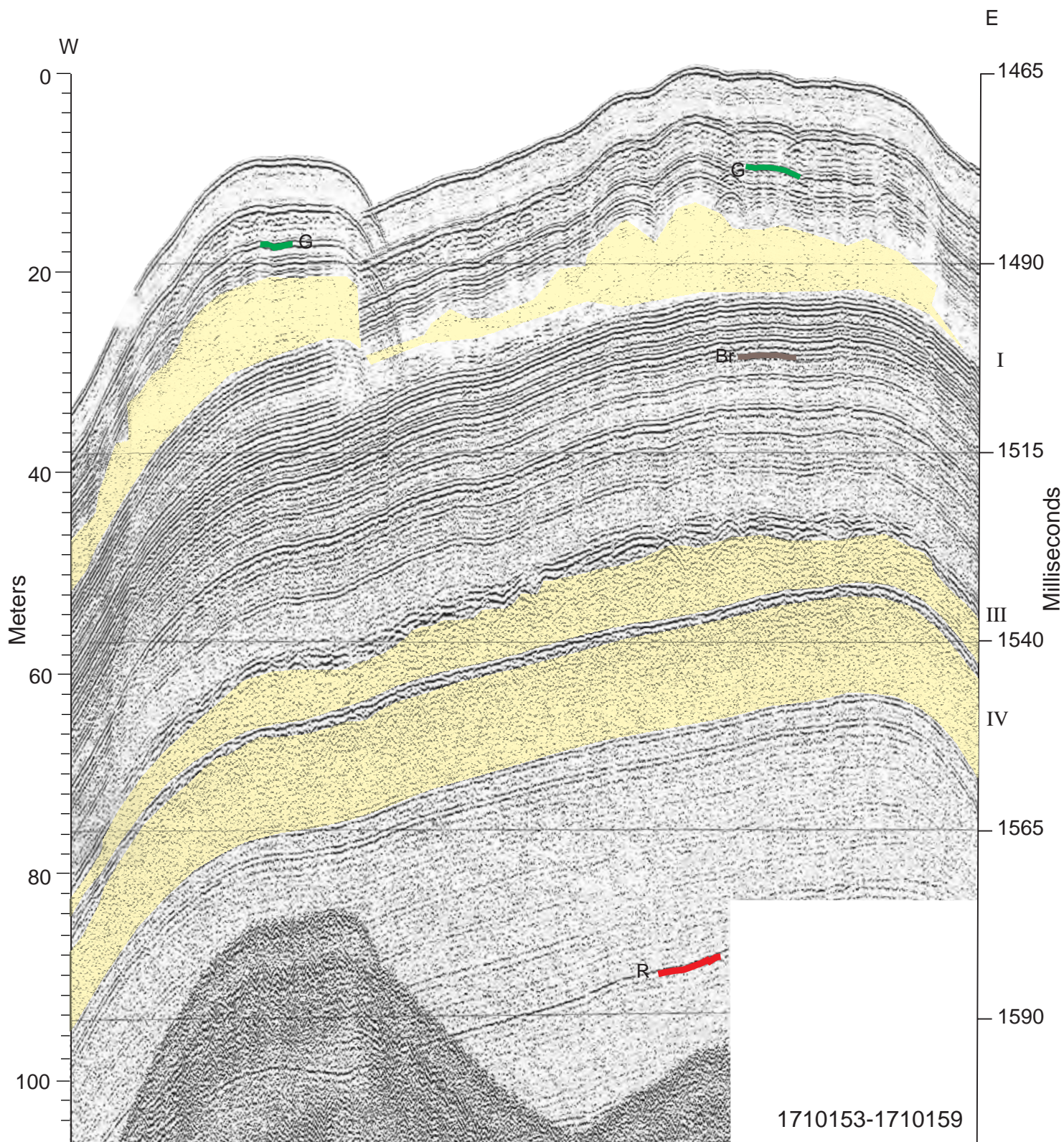


**Figure C1**



171/0153

Figure C2

171/0159

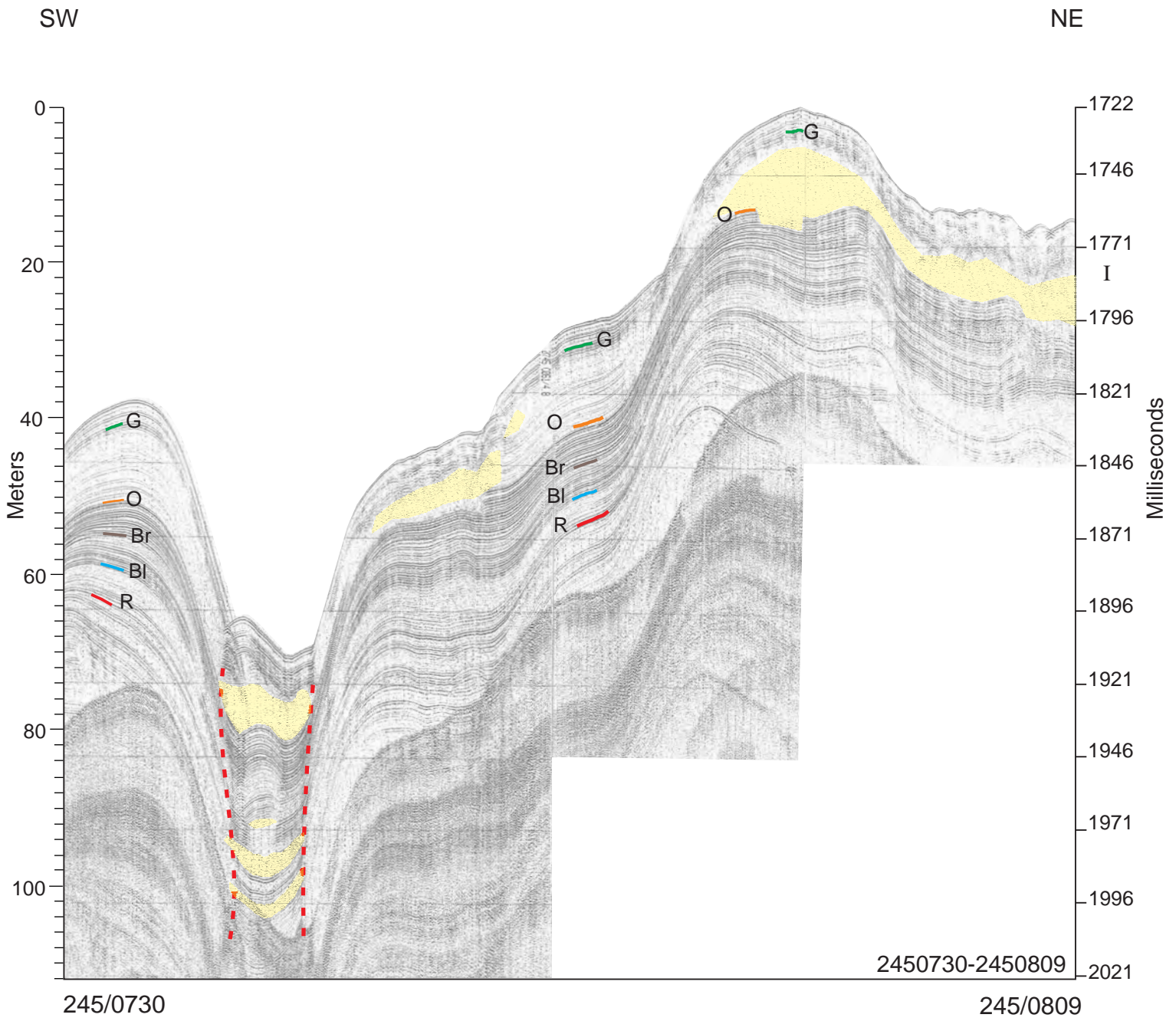
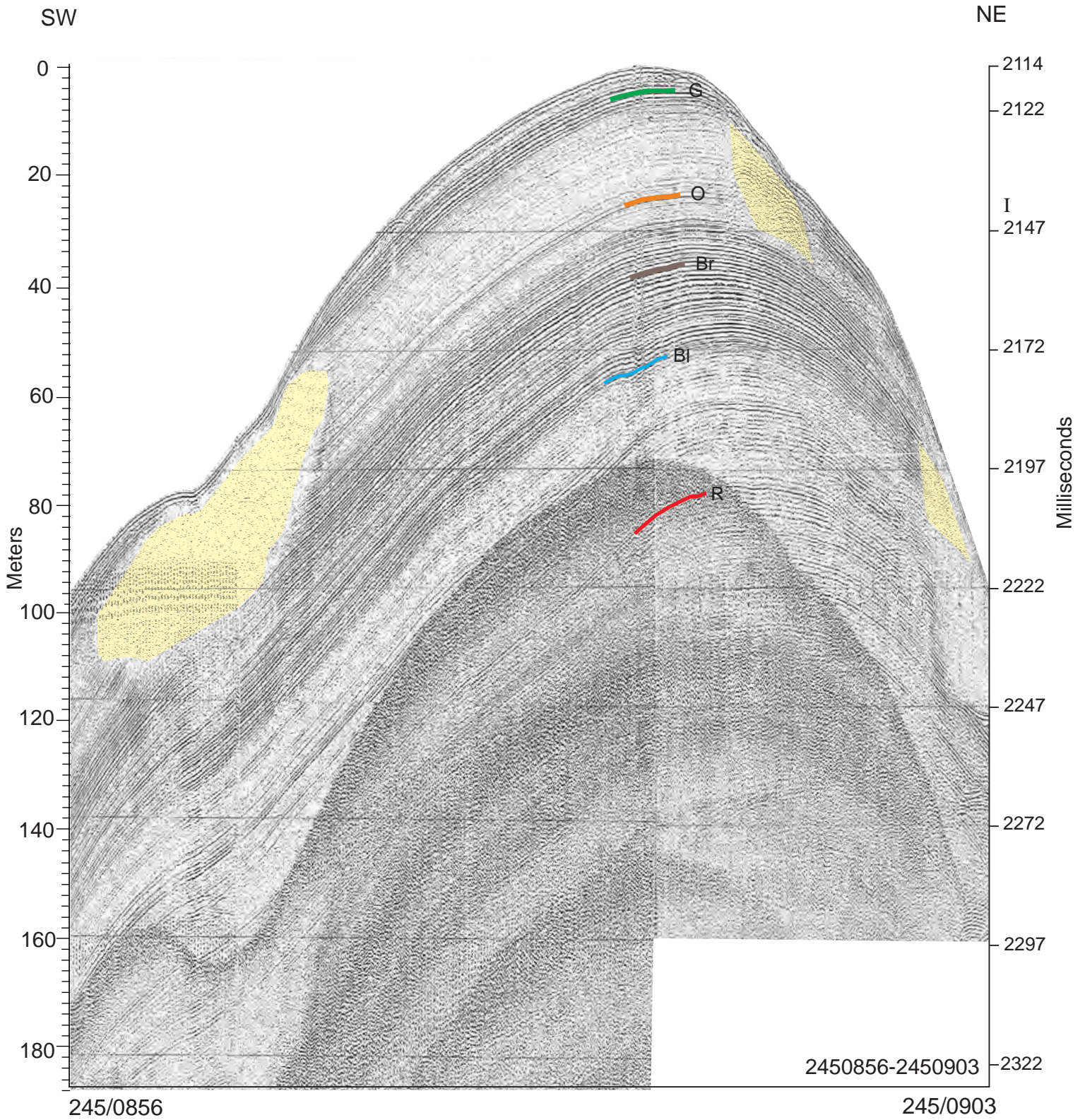
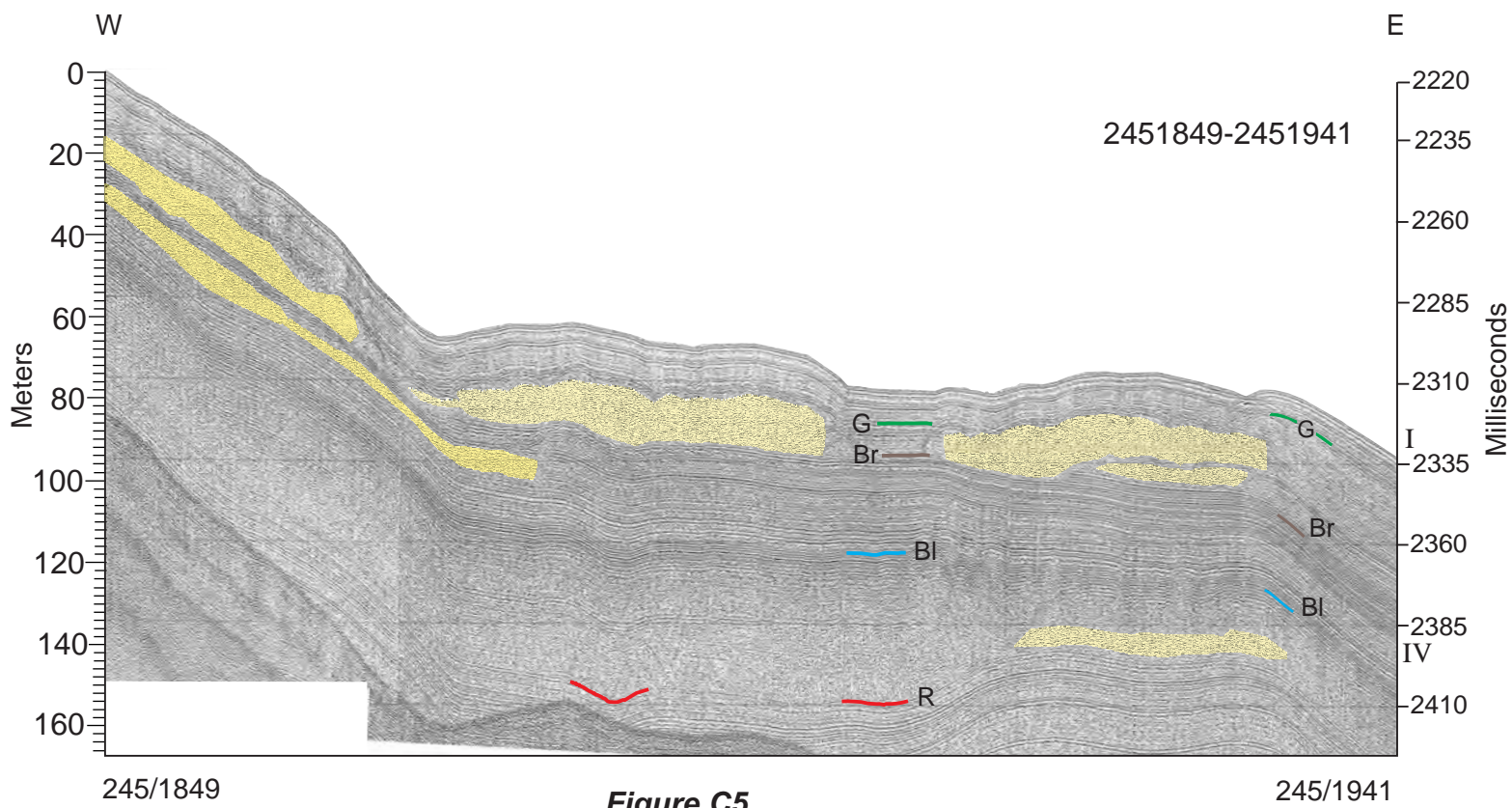


Figure C3





**Figure C4**



**Figure C5**

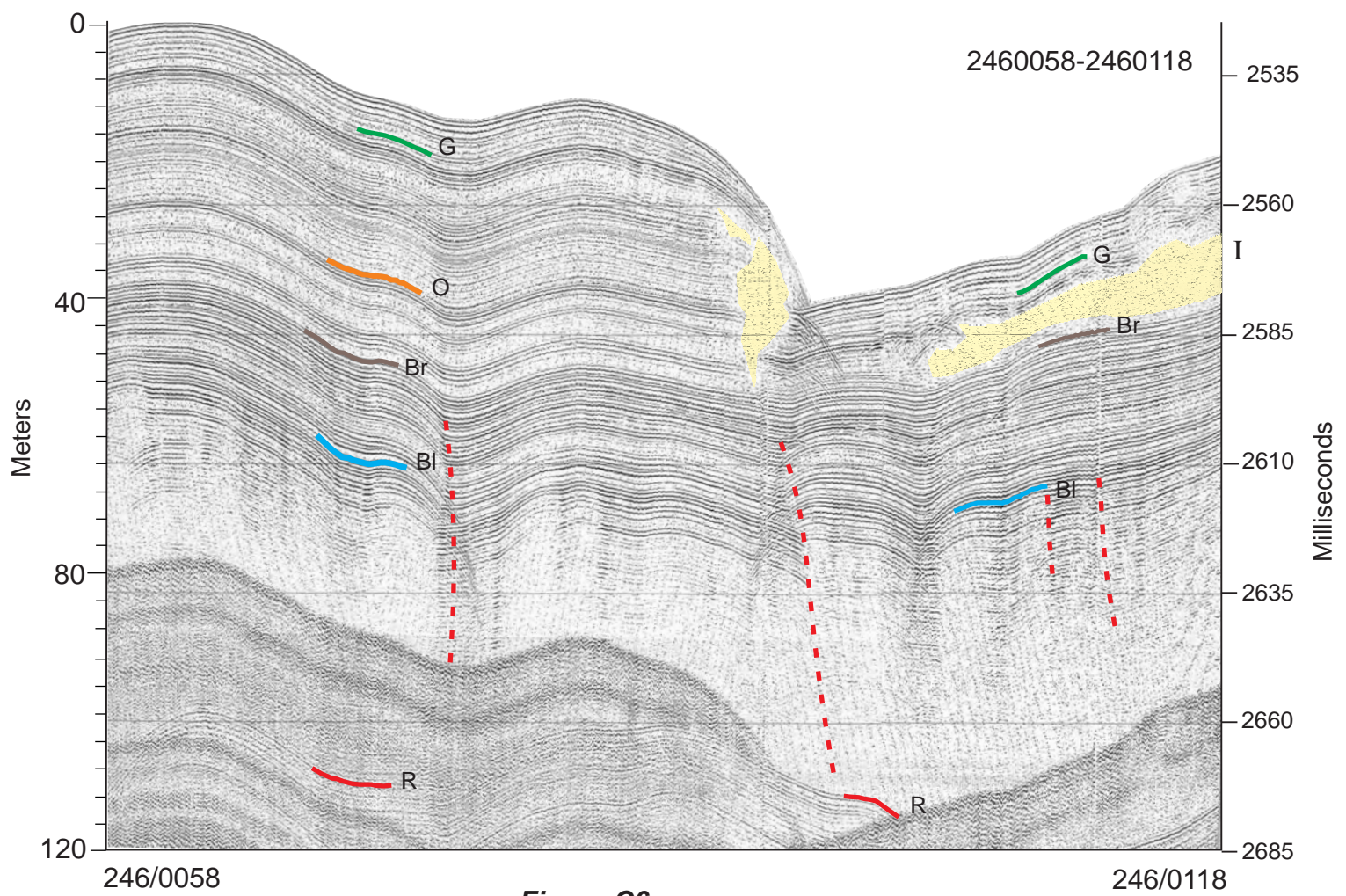


**Figure C6**

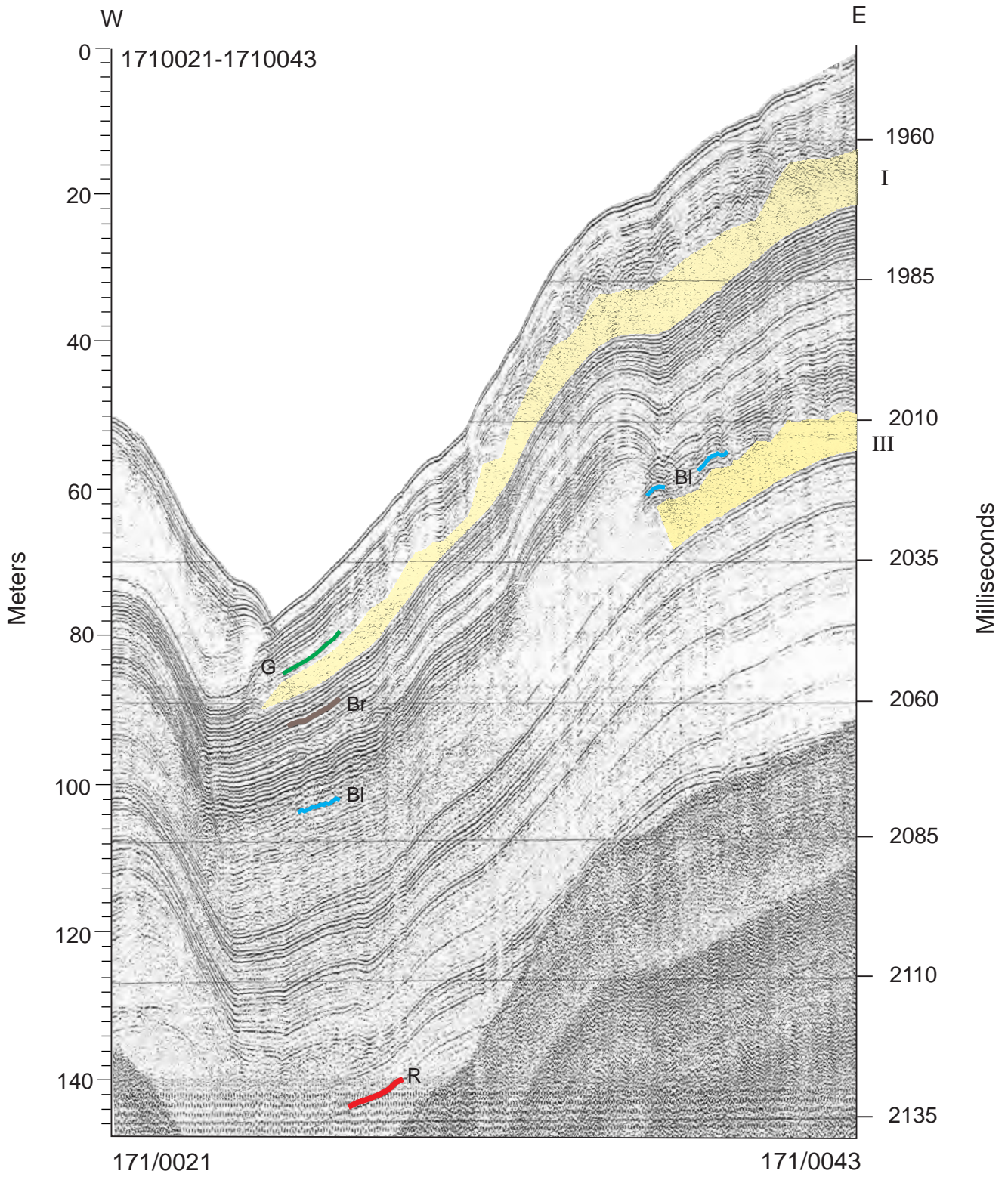
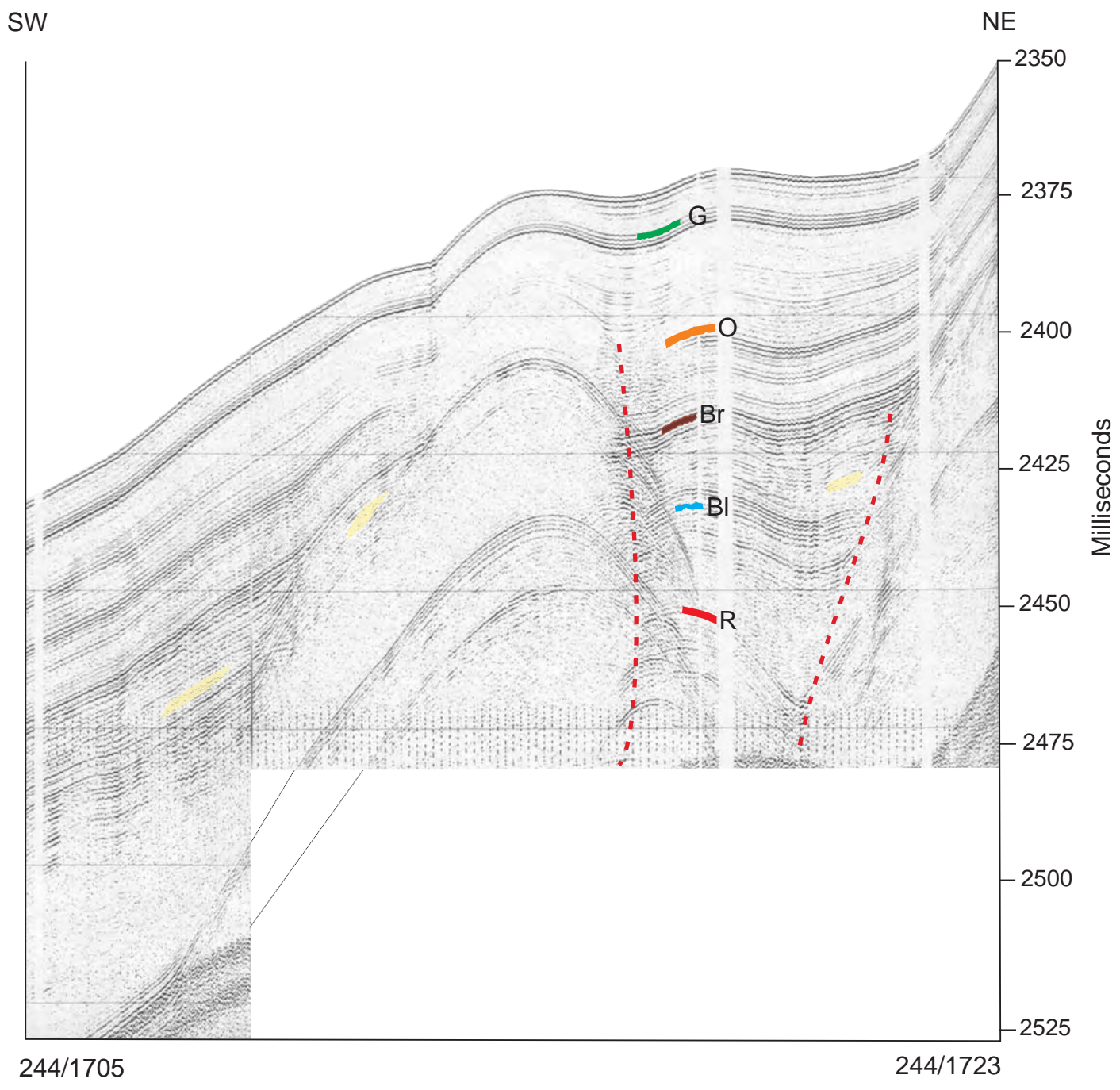
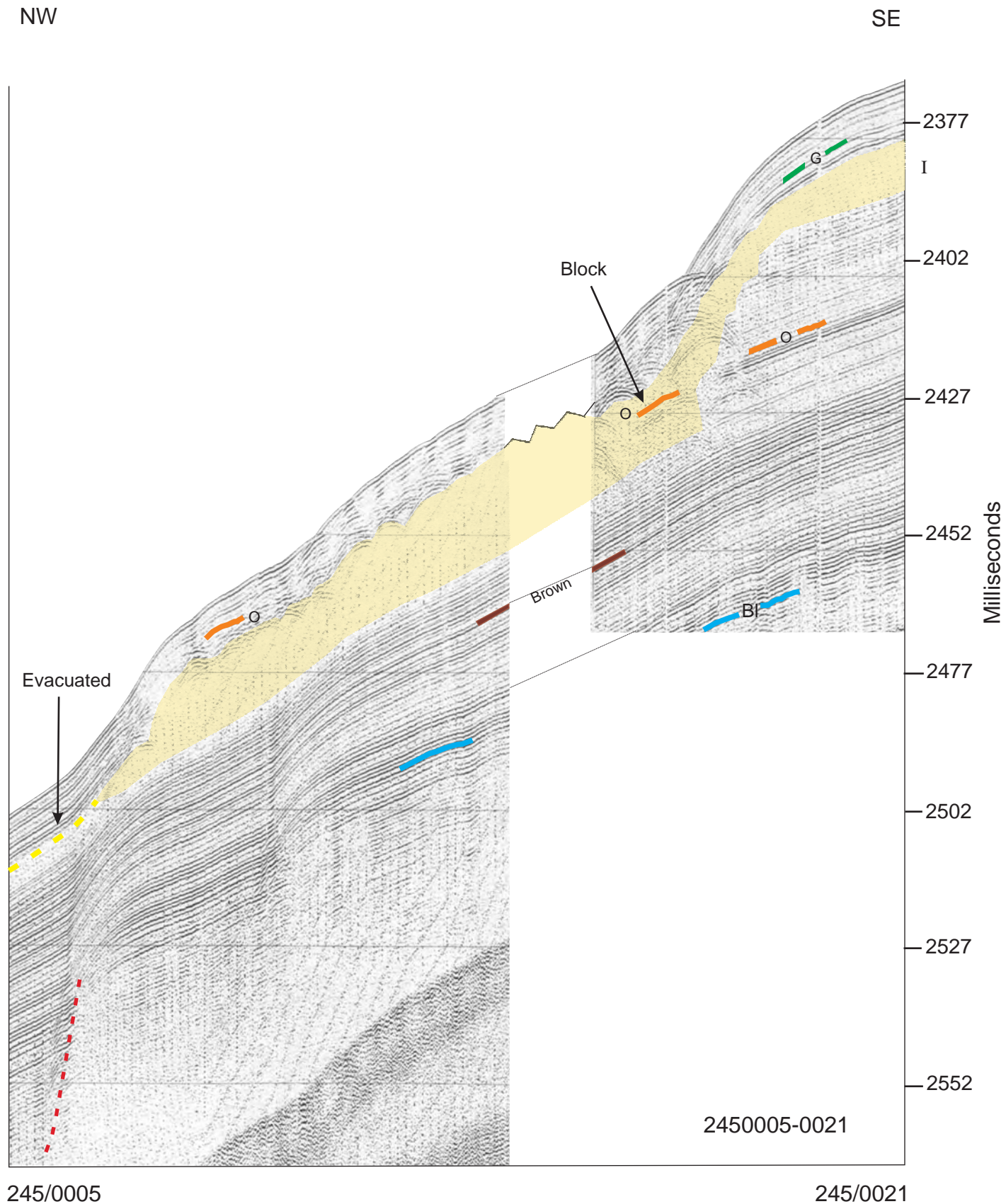


Figure C7



**Figure C8**



**Figure C9**

SE

NW

2450516-0533

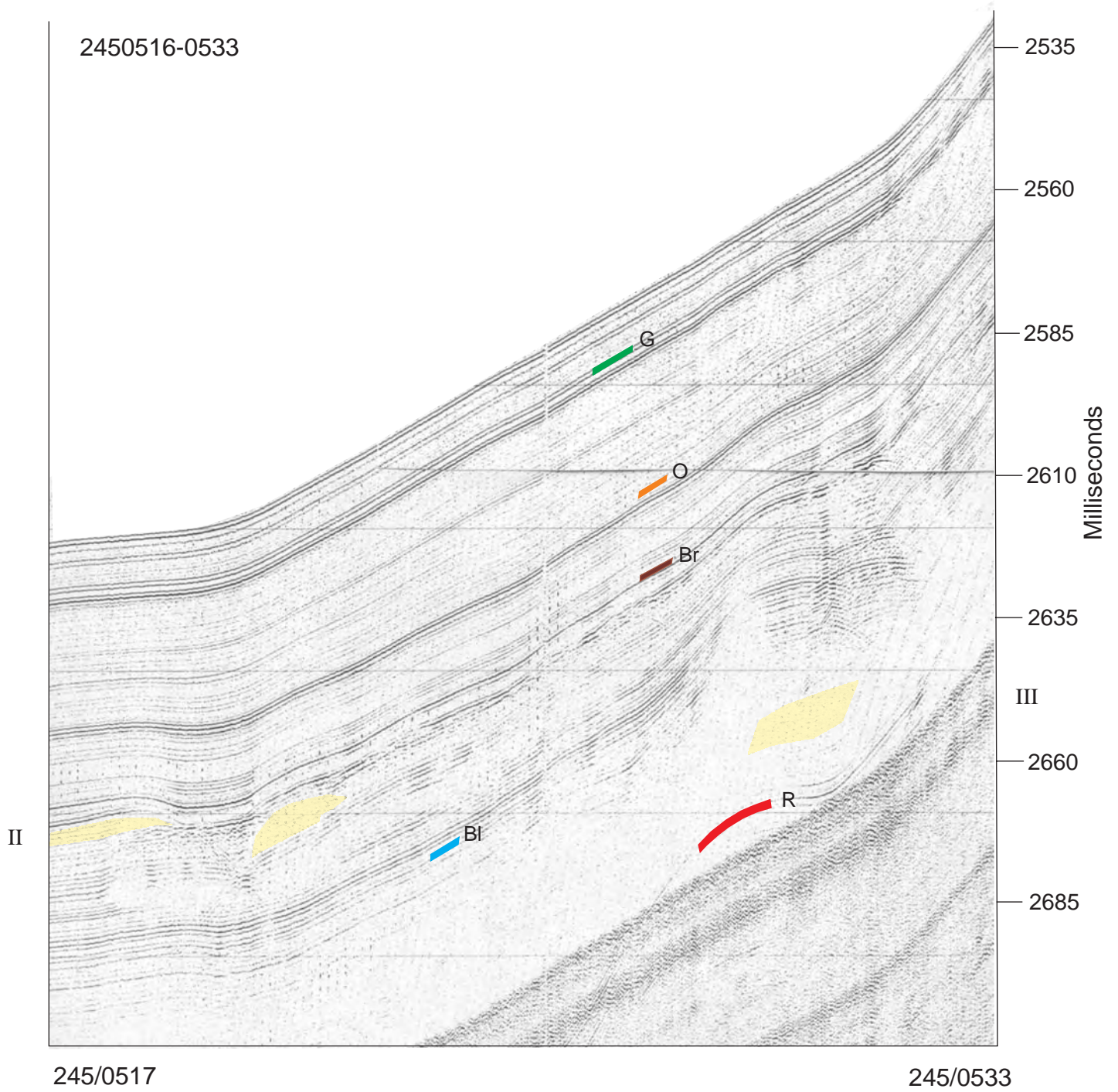
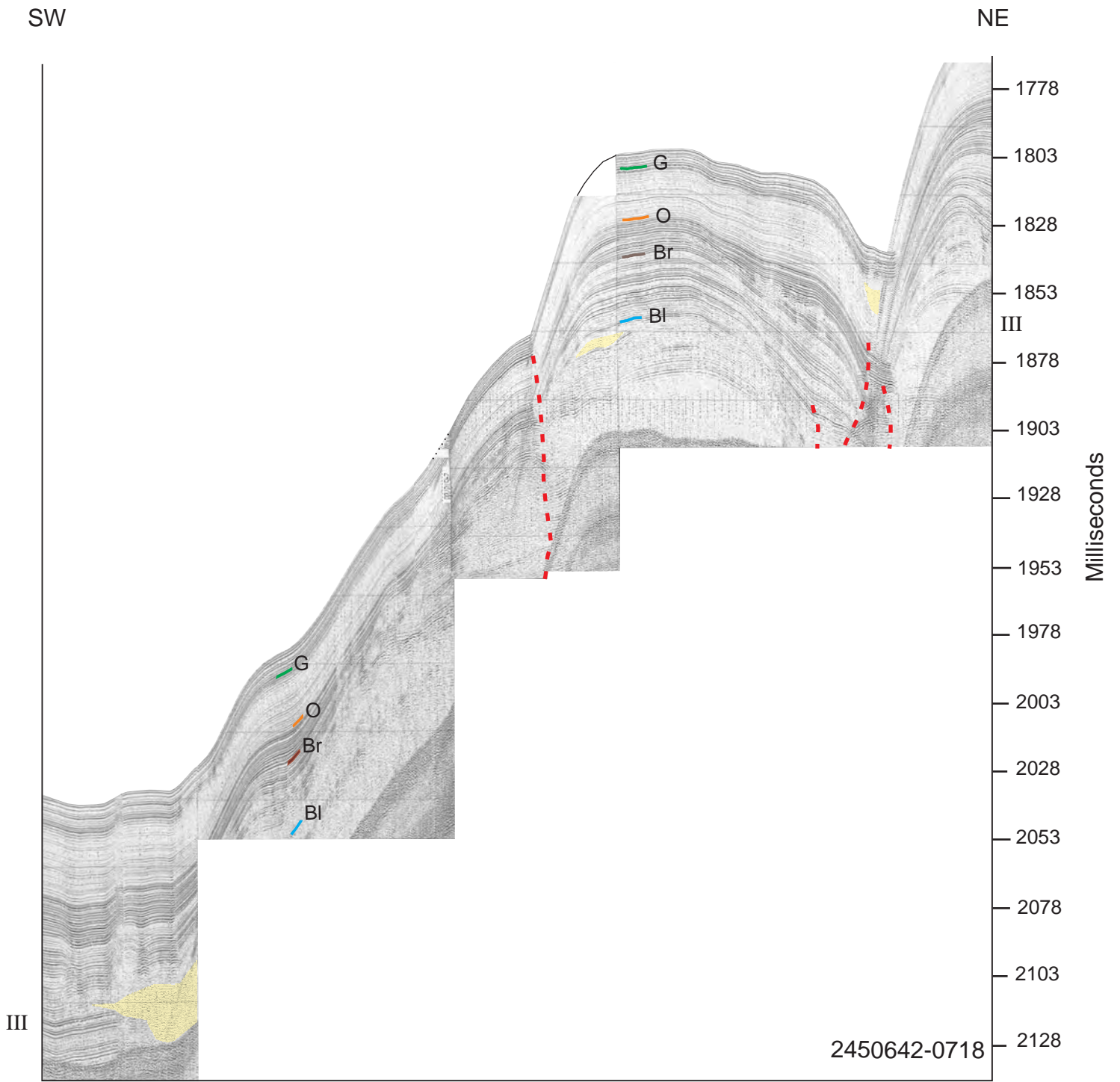


Figure C10



245/0642

245/0717

**Figure C11**

W

E

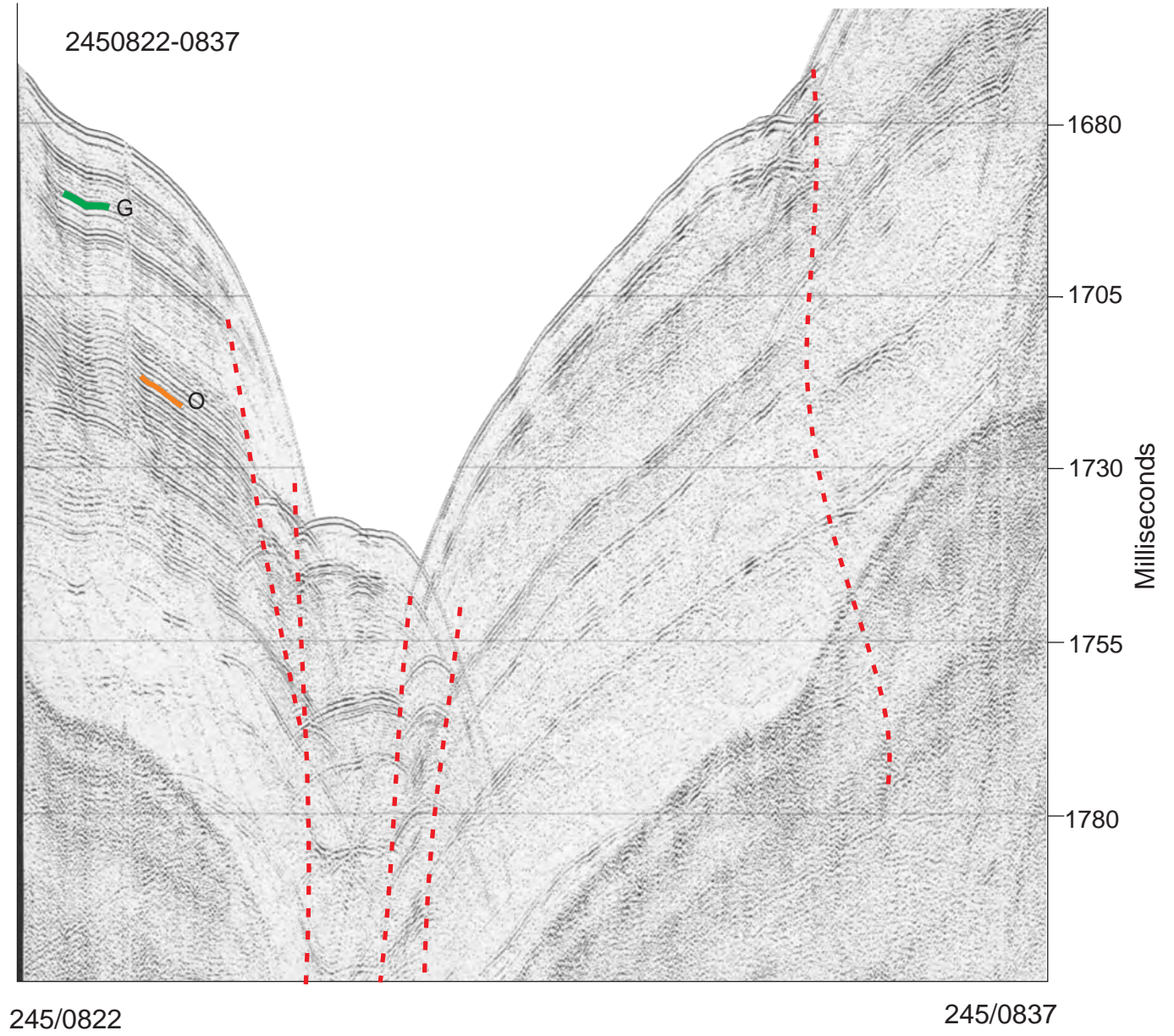
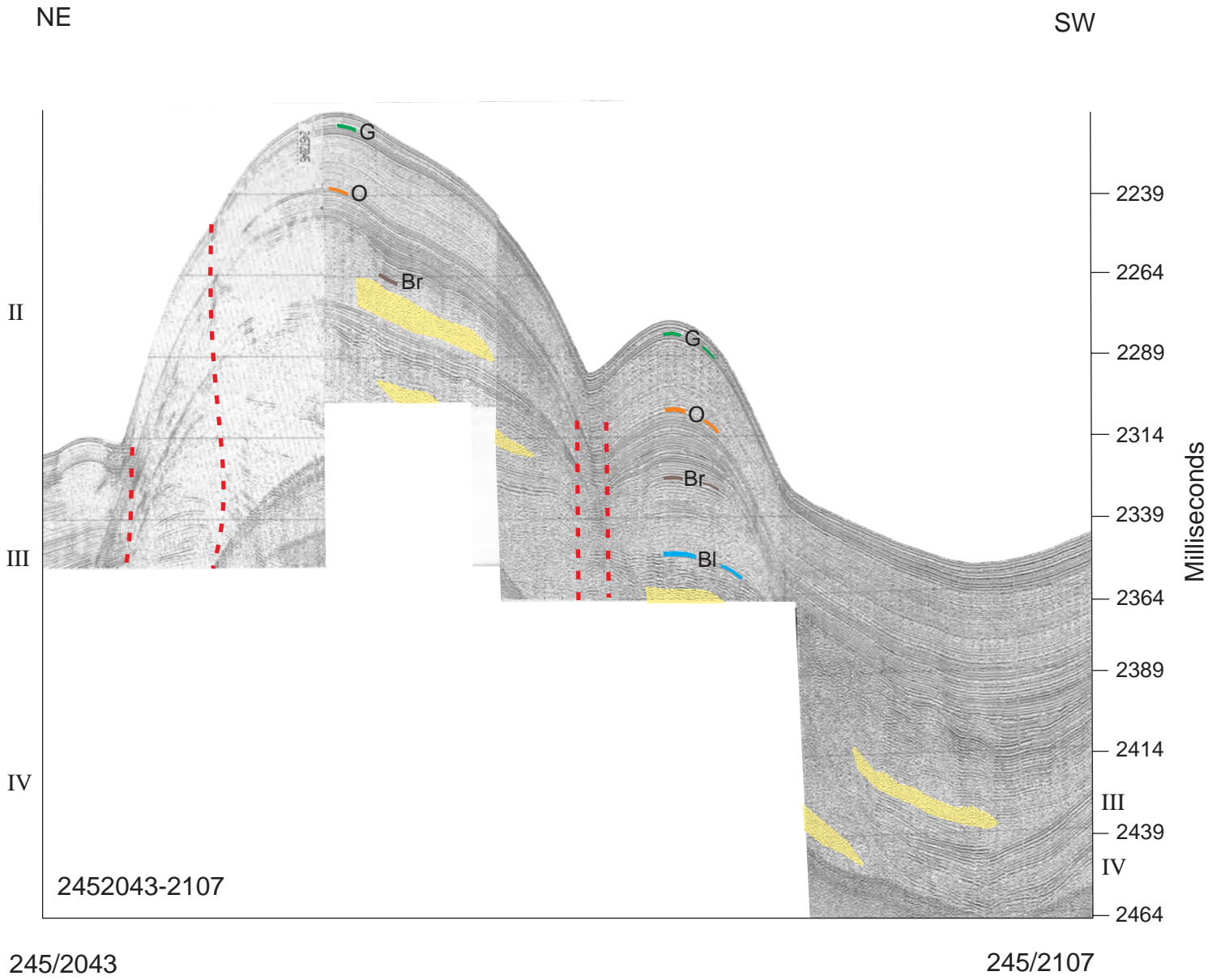
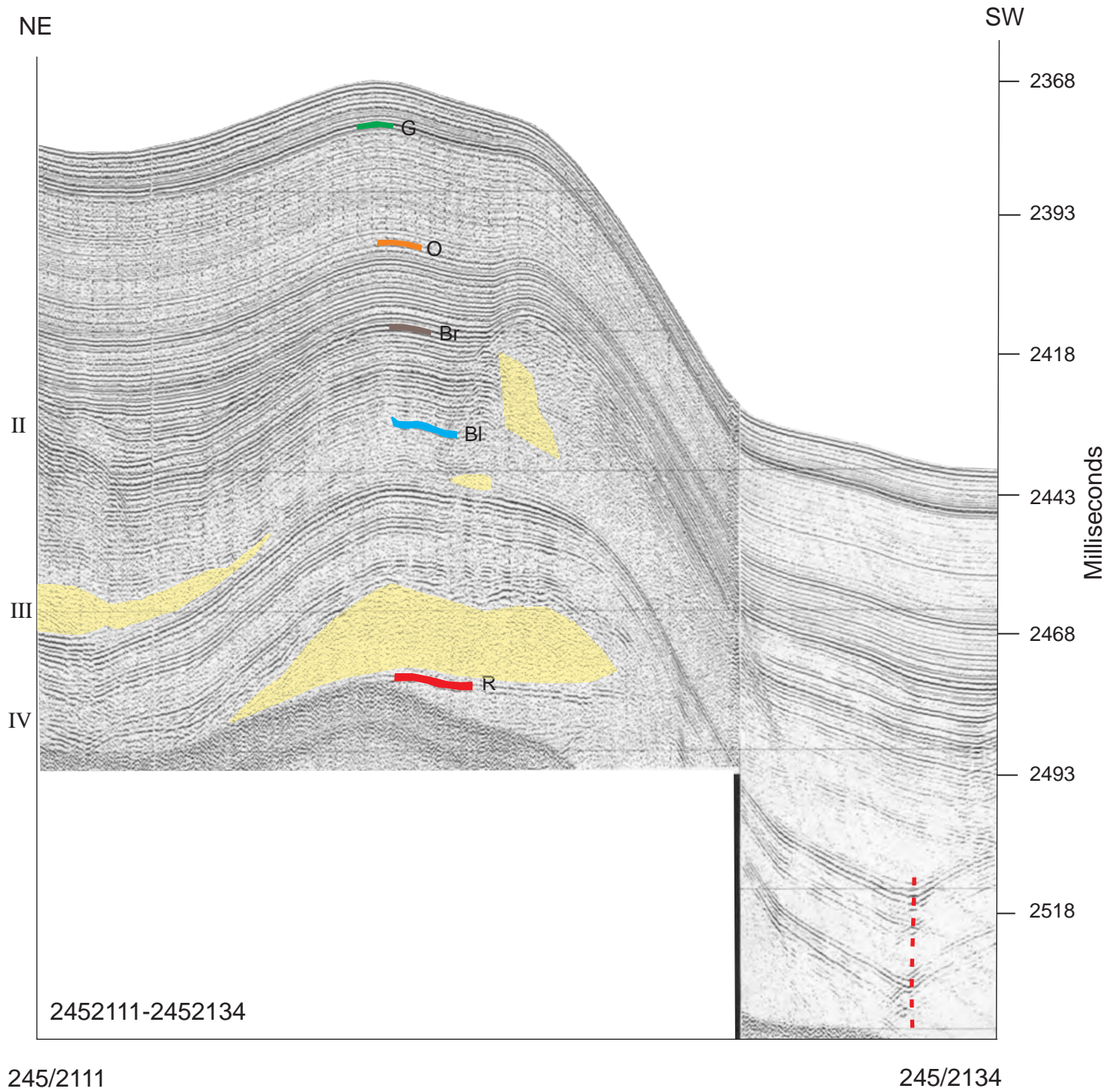


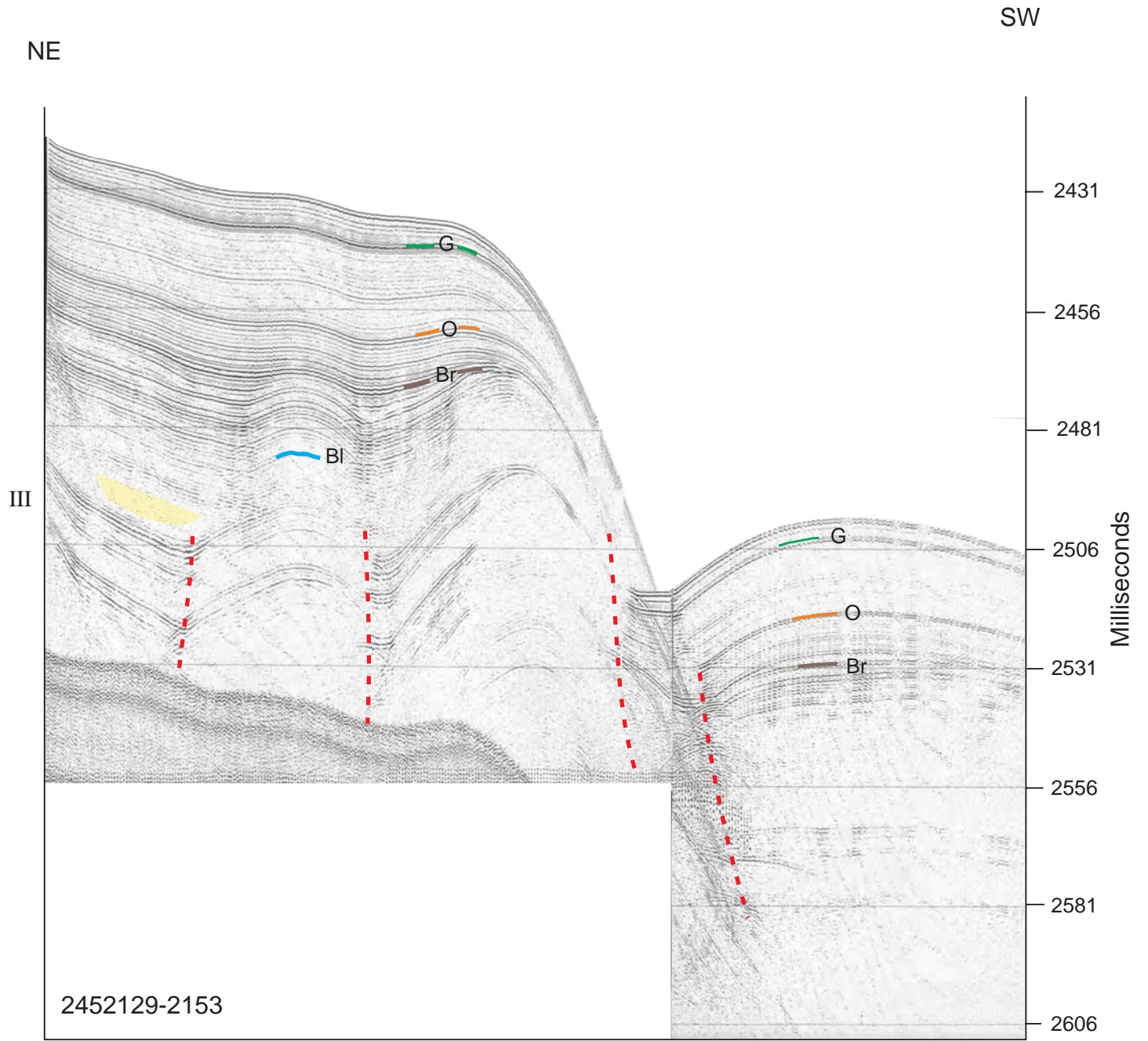
Figure C12





**Figure C13**





245/2129

**Figure C15**

245/2153

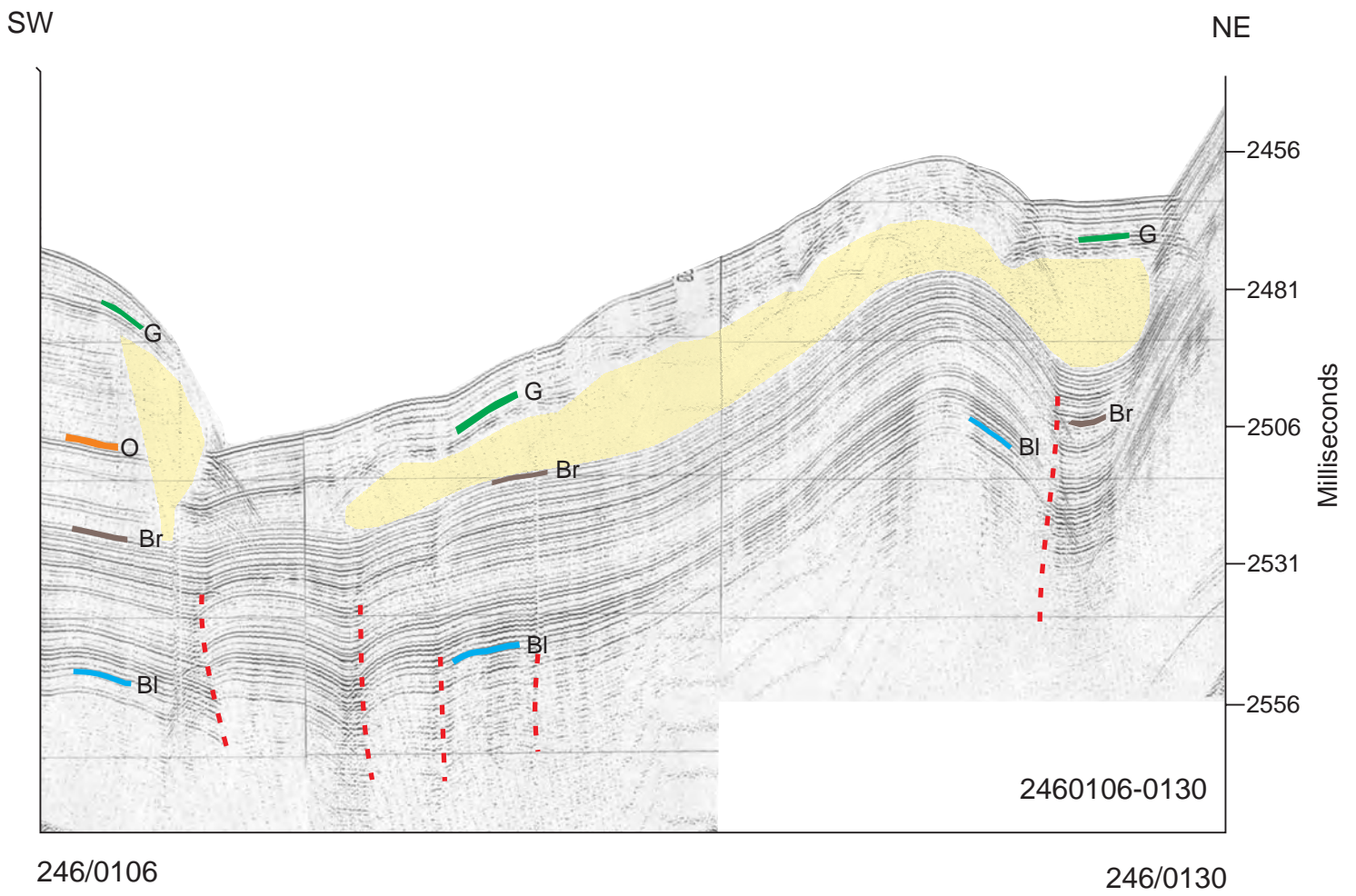


**Figure C16**

NW

SE | NE

SW

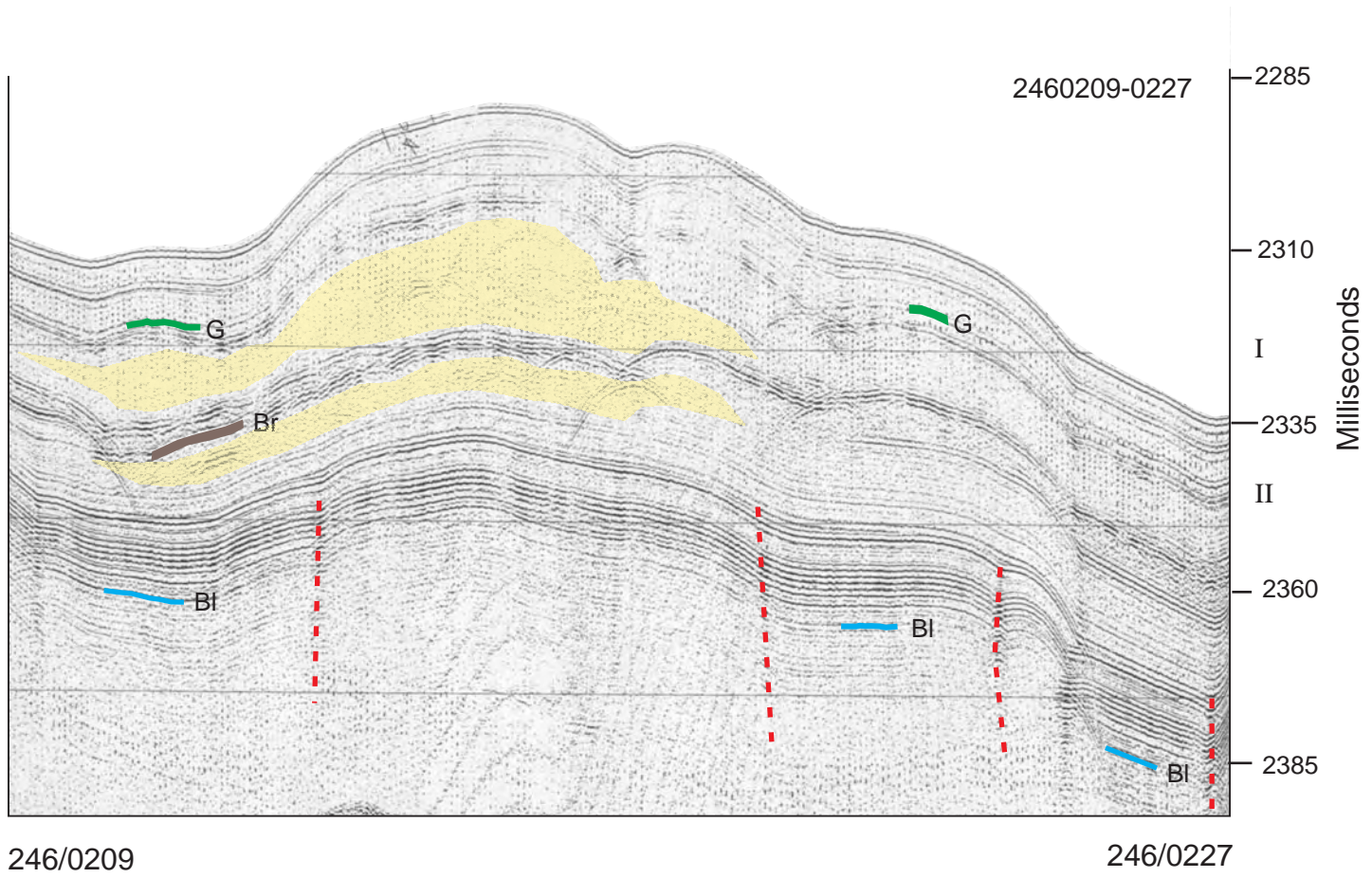
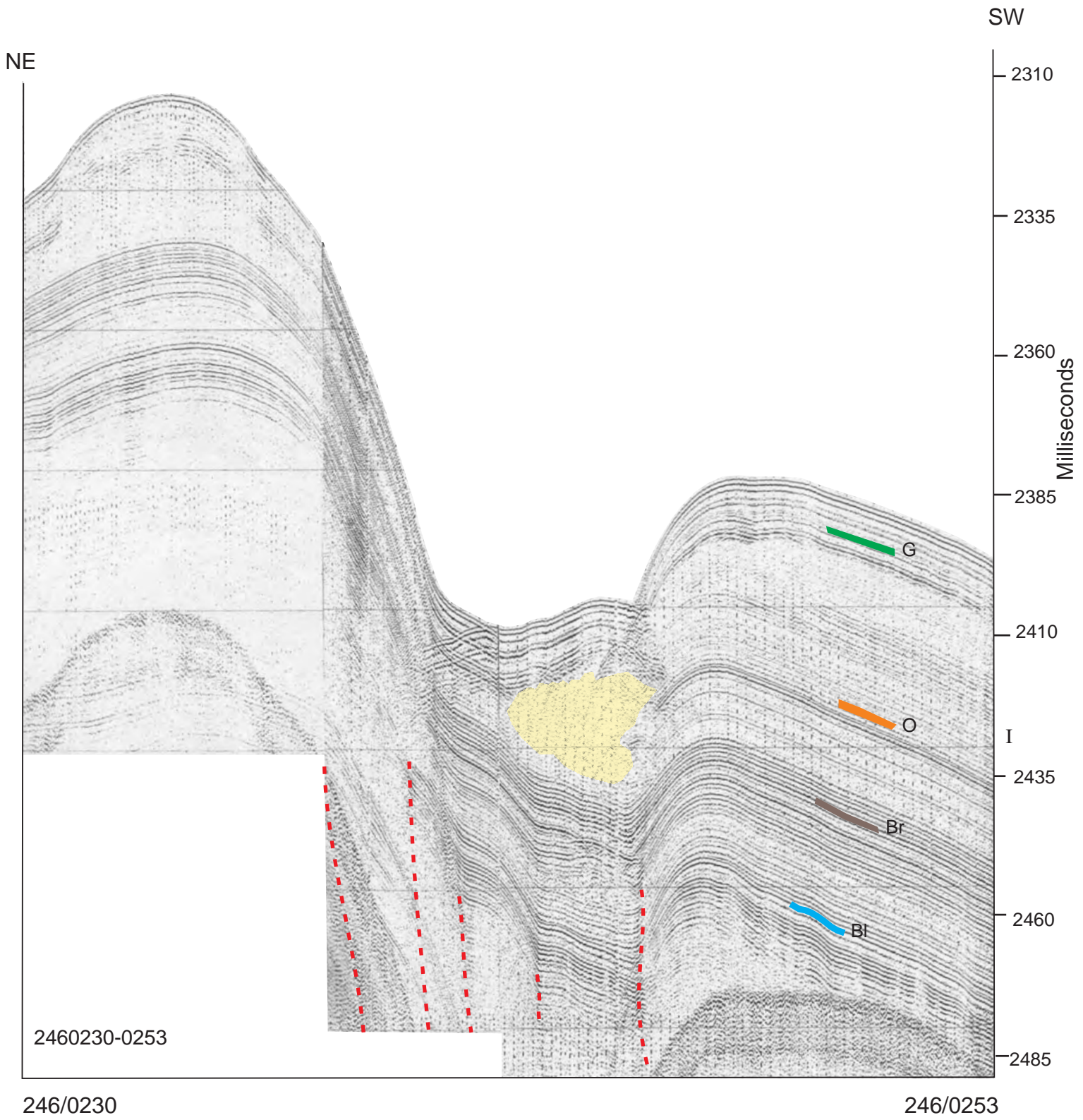
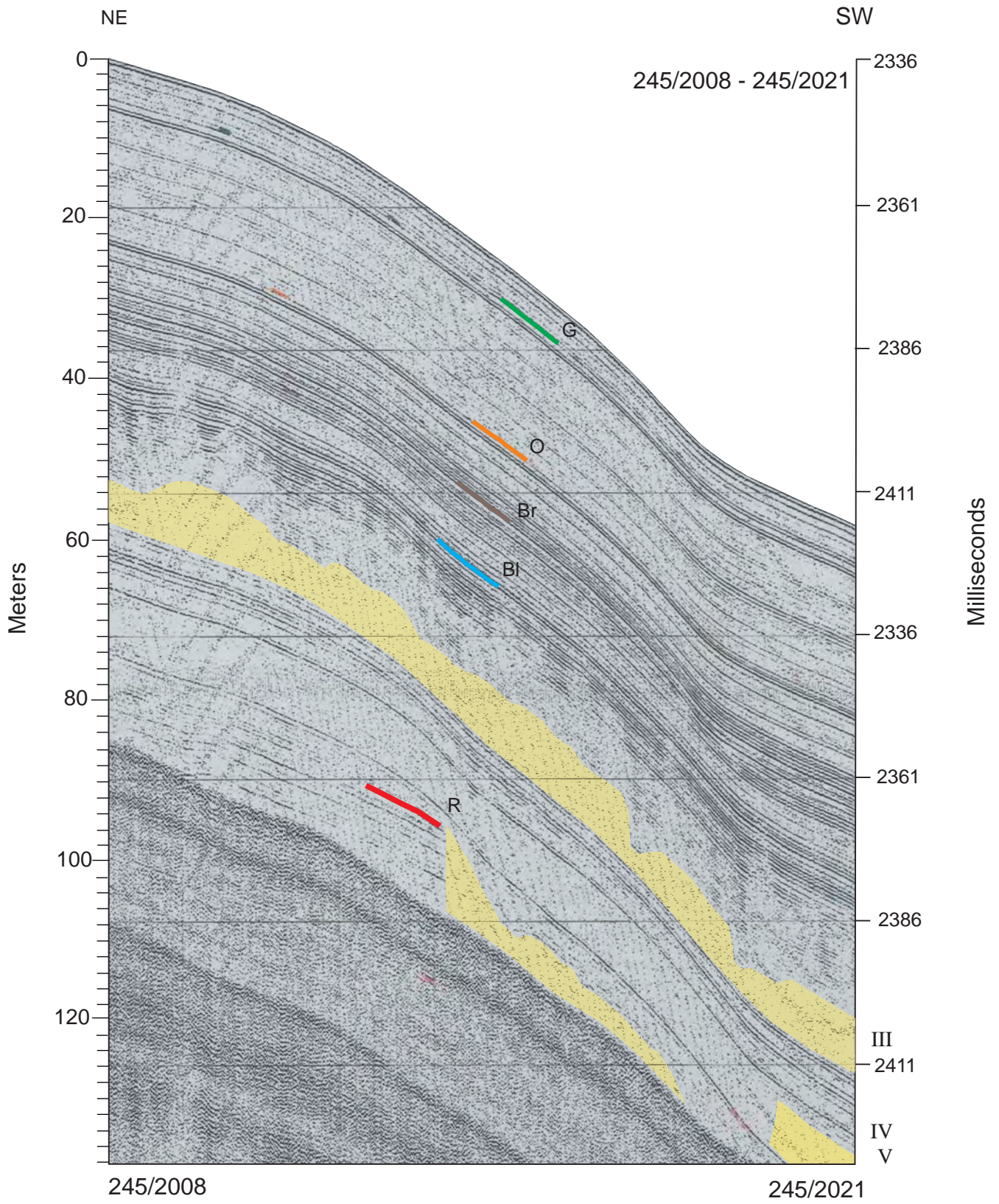


Figure C17



**Figure C18**



**Figure C19**

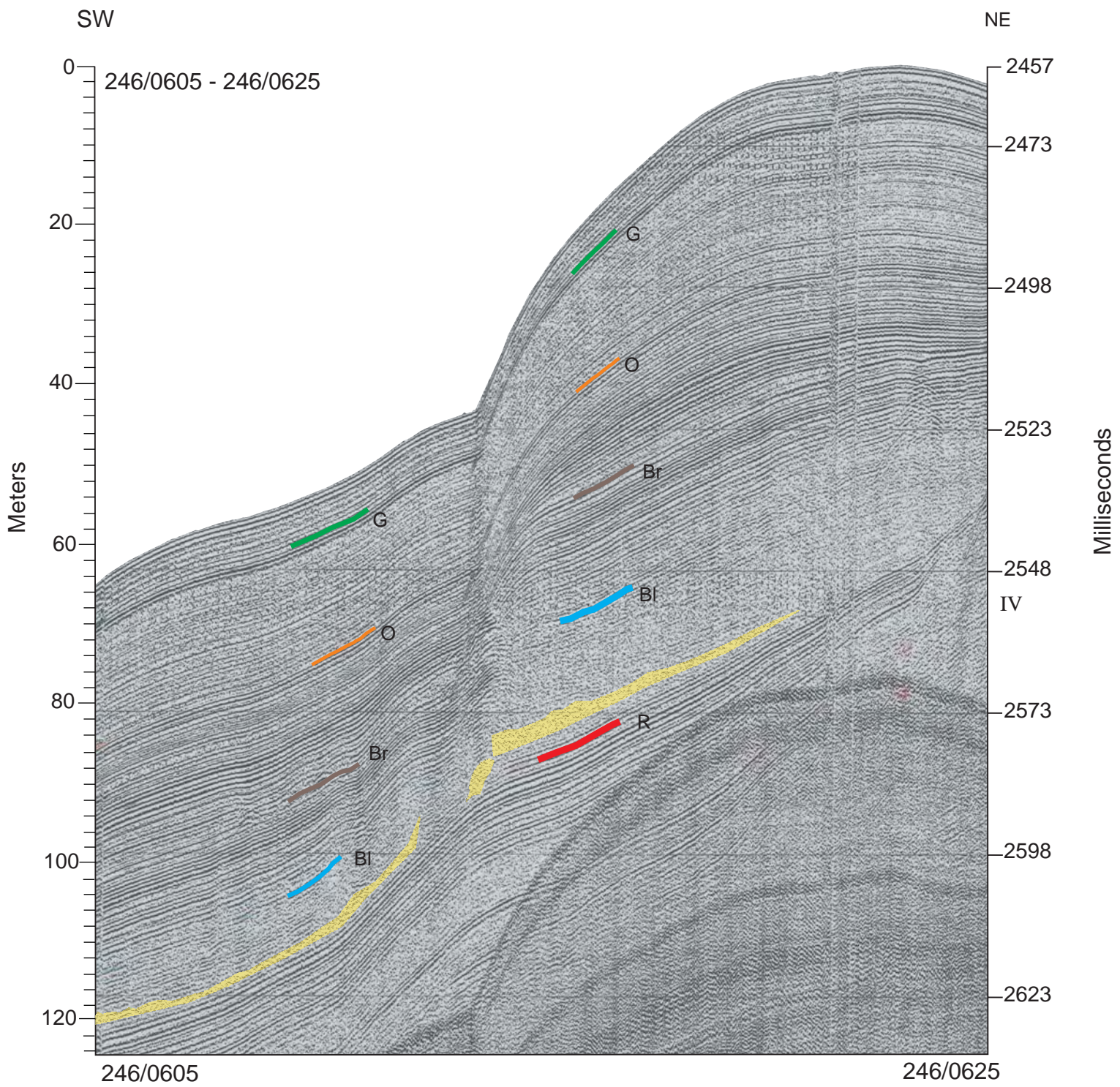
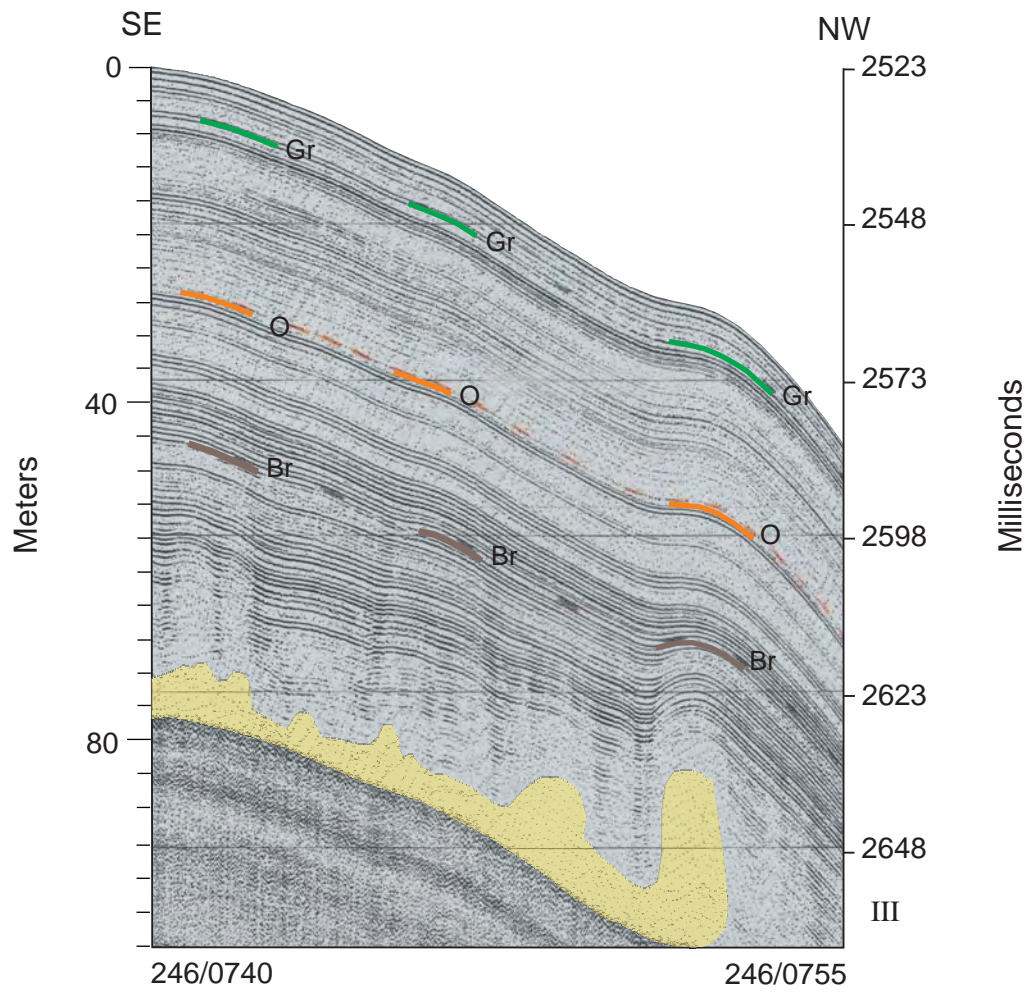
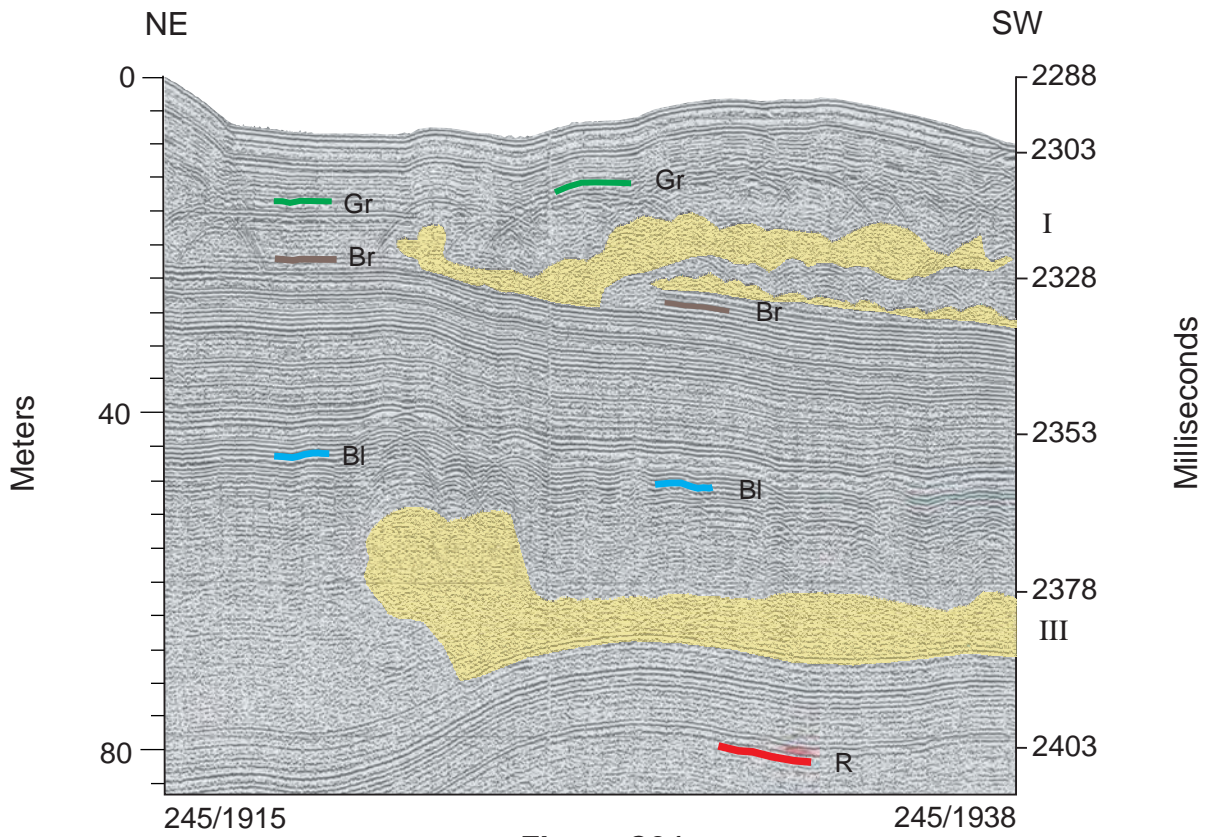


Figure C20















## **Appendix 4: Core logs**

## Core Summary Legend

### Symbol Legend

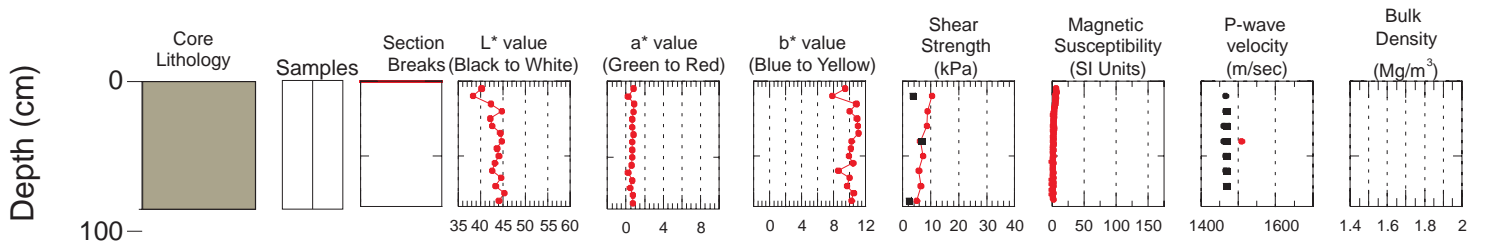
Erosional Contact	
Lamination/Thin Beds	
Core Disturbance	
Radiocarbon Date	
Grain Size Subsample	
Bulk Density Subsample	
Atterberg Limit Subsample	
Gas Subsample	
Geomechanical Subsample	
Shell Hash	

### Colour Legend

Foram Ooze	
Olive Grey Mud (Ogm)	
Olive Grey Sandy Mud (Ogm1)	
Olive Grey Mud with Ice-Rafted Detritus (Ogm2)	
Brick Red Mud (Brm)	
Red Brown Mud (Rbm)	
Red Brown Sandy Mud (Rbm1)	
Red Brown Mud with Ice-Rafted Detritus (Rbm2)	
Brown Mud (Bm)	
Brown Sandy Mud (Bm1)	
Brown Mud with Ice-Rafted Detritus (Bm2)	
Grey Mud (Gm)	
Grey Sandy Mud (Gm1)	
Grey Mud with Ice-Rafted Detritus (Gm2)	
Tan Mud	
Sand or Gravel	
Debris Flow	
Mudclast Conglomerate	
Diamicton	
Folded Mud Block	

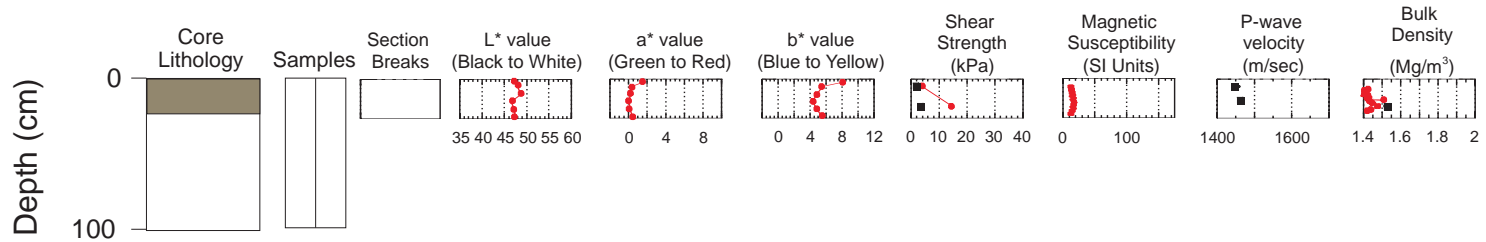
# Hudson 2003033 Trigger Weight Core 007

TD 84cm 44°54.1162 N 54°33.5938 W Water depth 1360 m



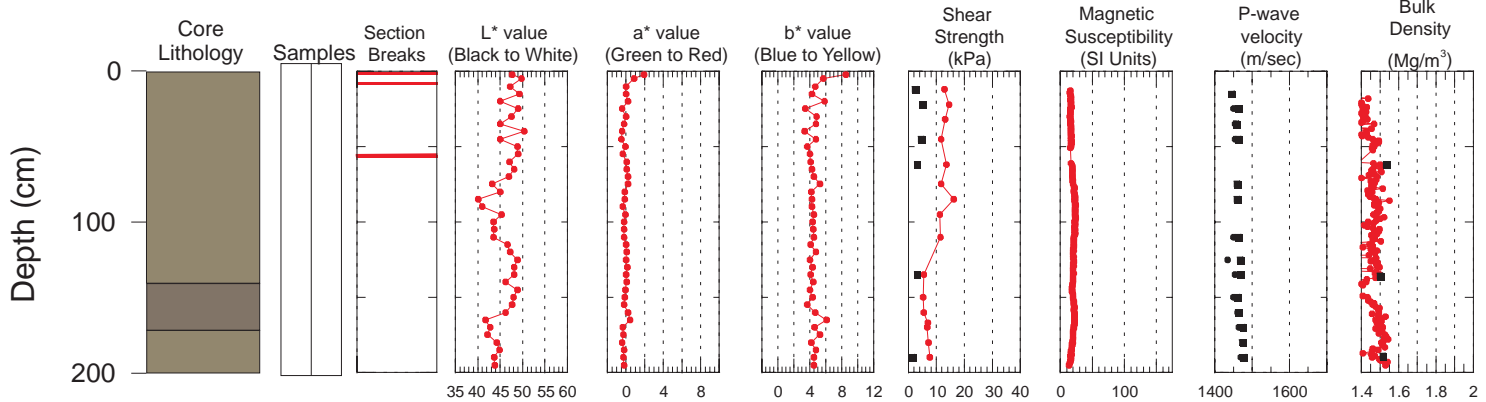
# Hudson 2002046 Trigger Weight Core 073

TD 26cm 44°23.7757 N 55°25.1034 W Water depth 2595 m



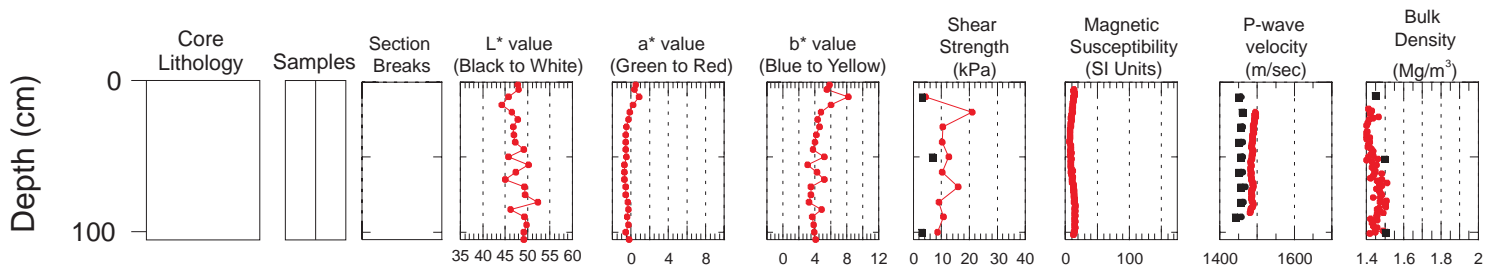
# Hudson 2002046 Trigger Weight Core 074

TD 200cm 44°23.5631 N 55°26.2372 W Water depth 2672 m



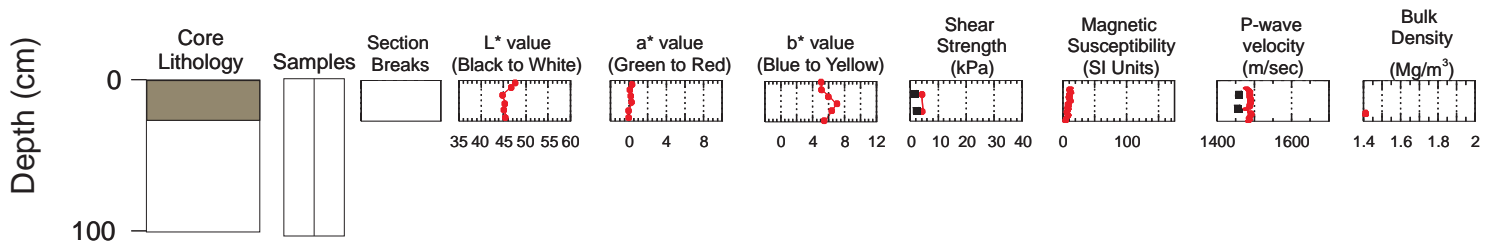
# Hudson 2002046 Trigger Weight Core 075

TD 105cm 44°25.4403 N 54°36.8288 W Water depth 2163 m



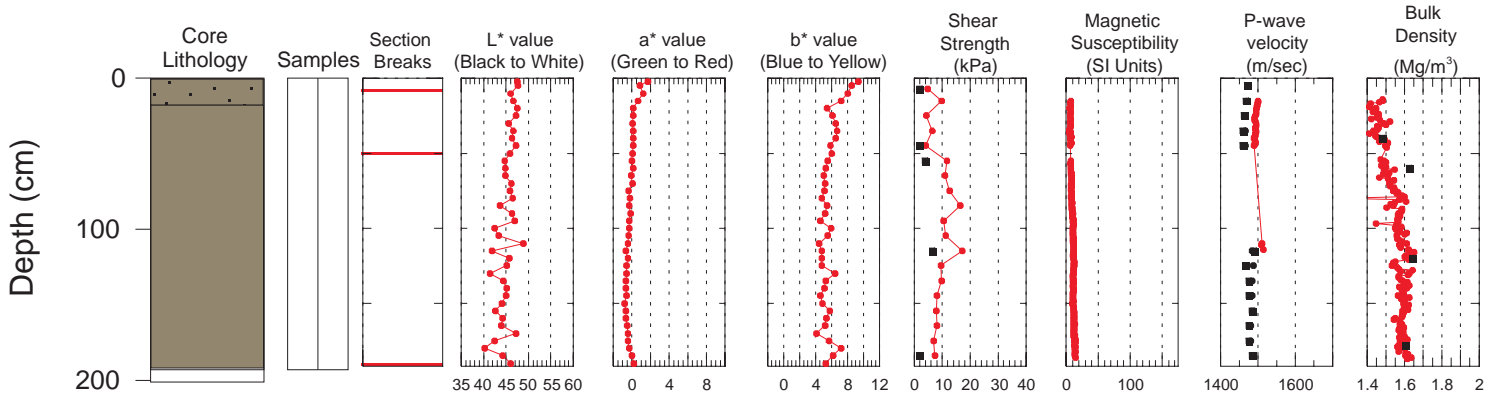
# Hudson 2002046 Trigger Weight Core 076

TD 27cm 44°27.4008 N 54°32.6588 W Water depth 2163 m



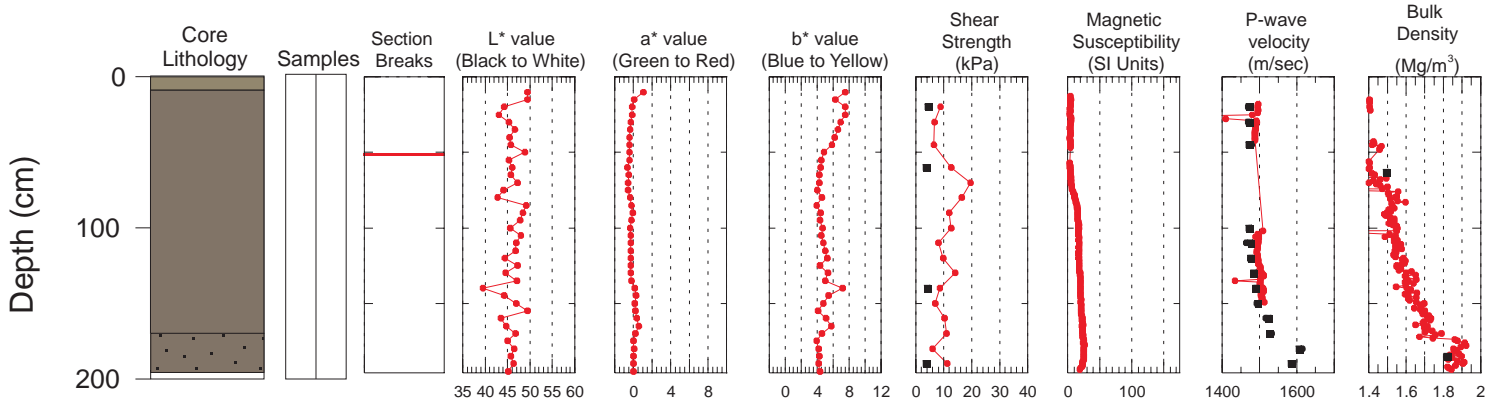
# Hudson 2002046 Trigger Weight Core 077

TD 192cm 44°41.8158 N 54°27.2066 W Water depth 988 m



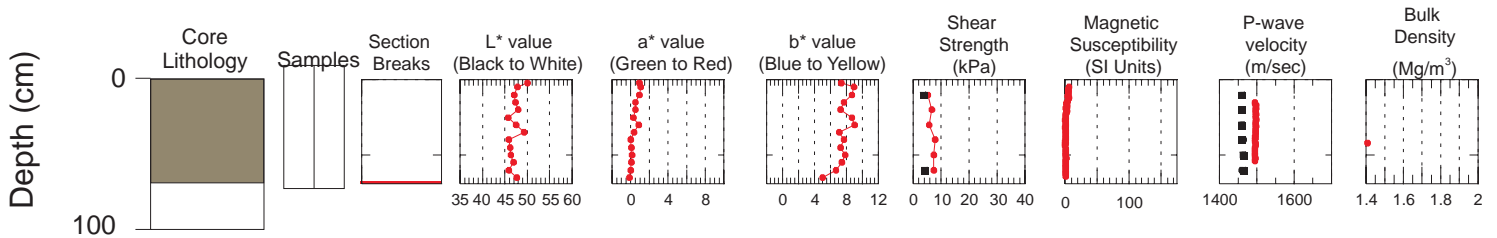
# Hudson 2002046 Trigger Weight Core 078

TD 196cm 44°48.5765 N 54°53.7667 W Water depth 1865 m



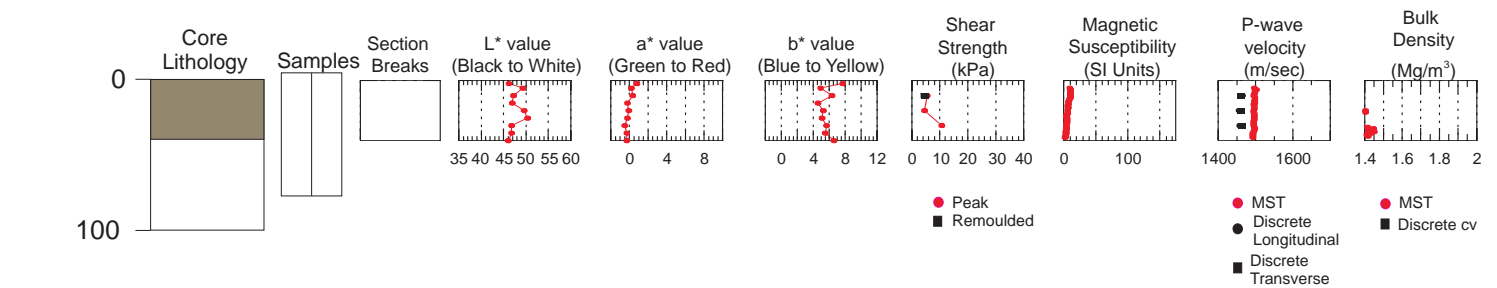
# Hudson 2002046 Trigger Weight Core 079

TD 69cm 44°51.1849 N 55°01.0709 W Water depth 1447 m



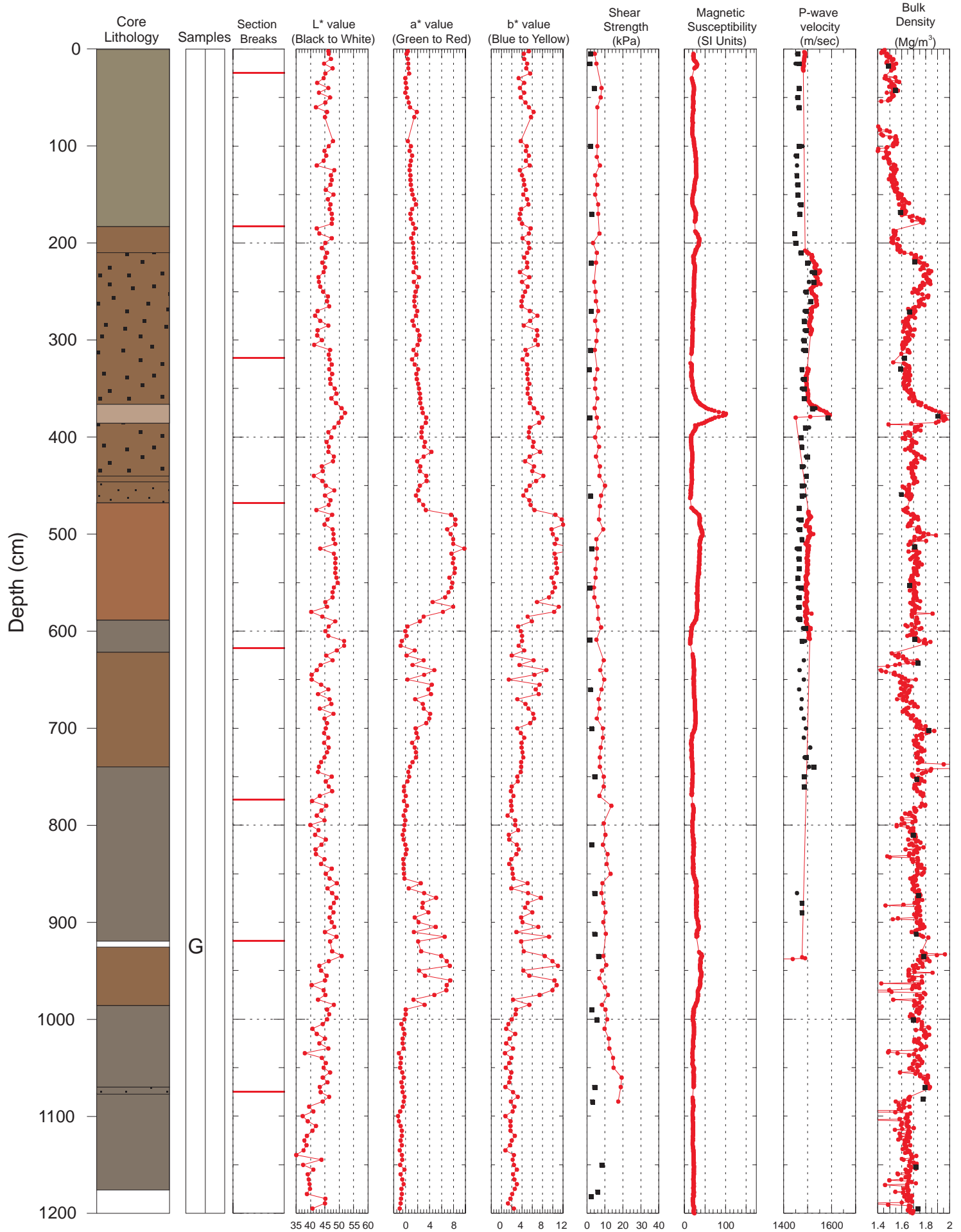
# Hudson 2002046 Trigger Weight Core 080

TD 40cm 44°39.6200 N 54°50.8974 W Water depth 2050 m



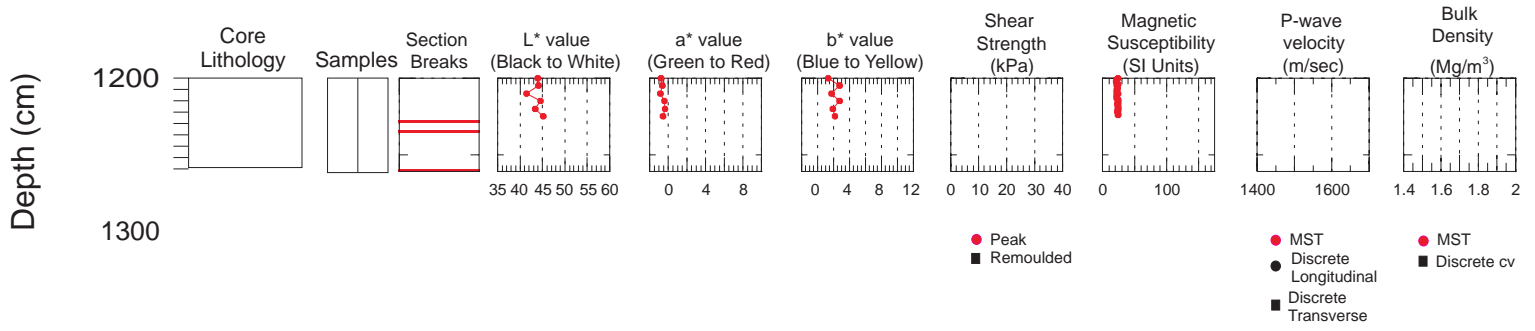
# Hudson 2002046 Piston Core 073

TD 1261cm 44°23.7757 N 55°25.1034 W Water depth 2595 m



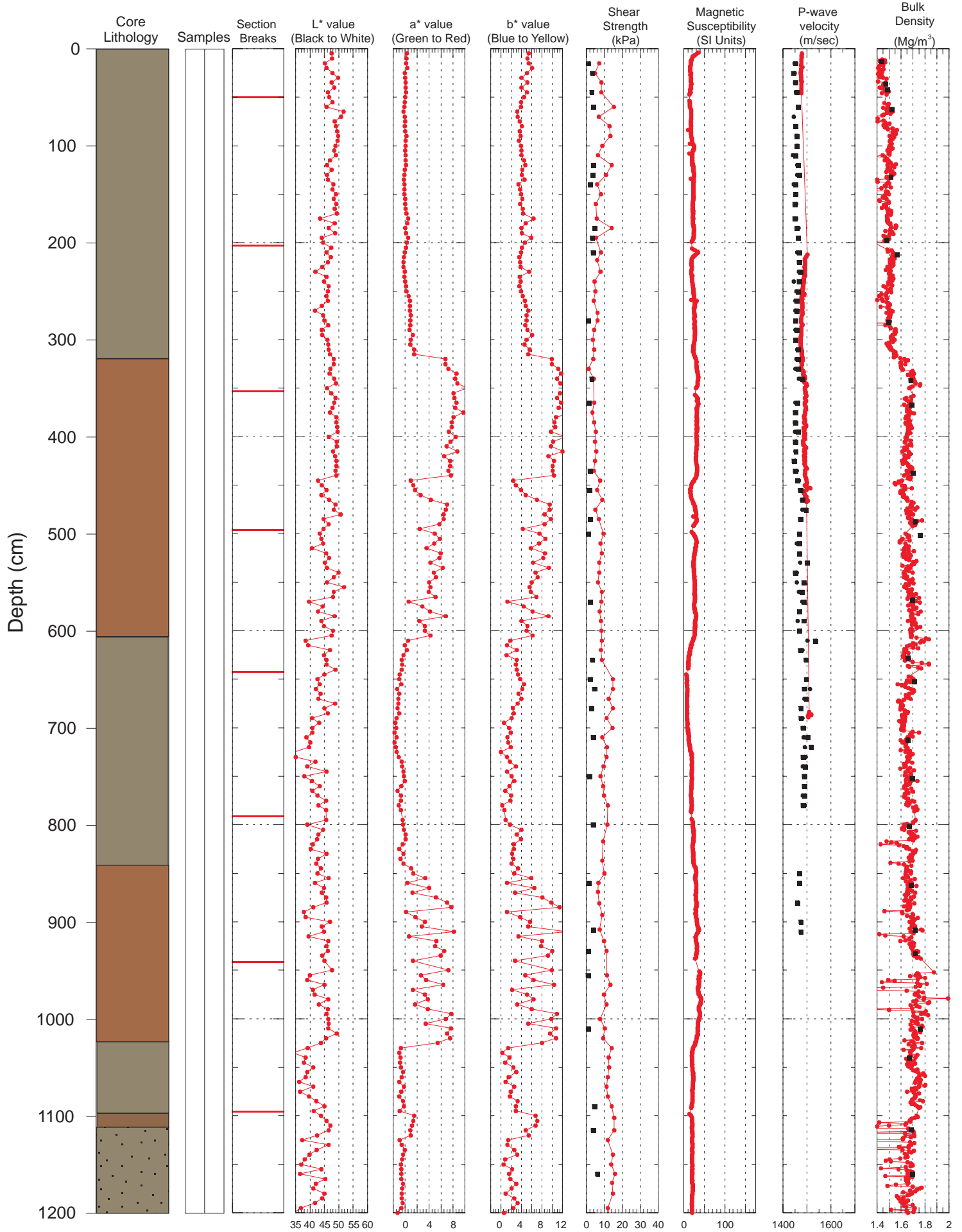
# Hudson 2002046 Piston Core 073

TD 1261cm 44°23.7757 N 55°25.1034 W Water depth 2595 m



# Hudson 2002046 Piston Core 074

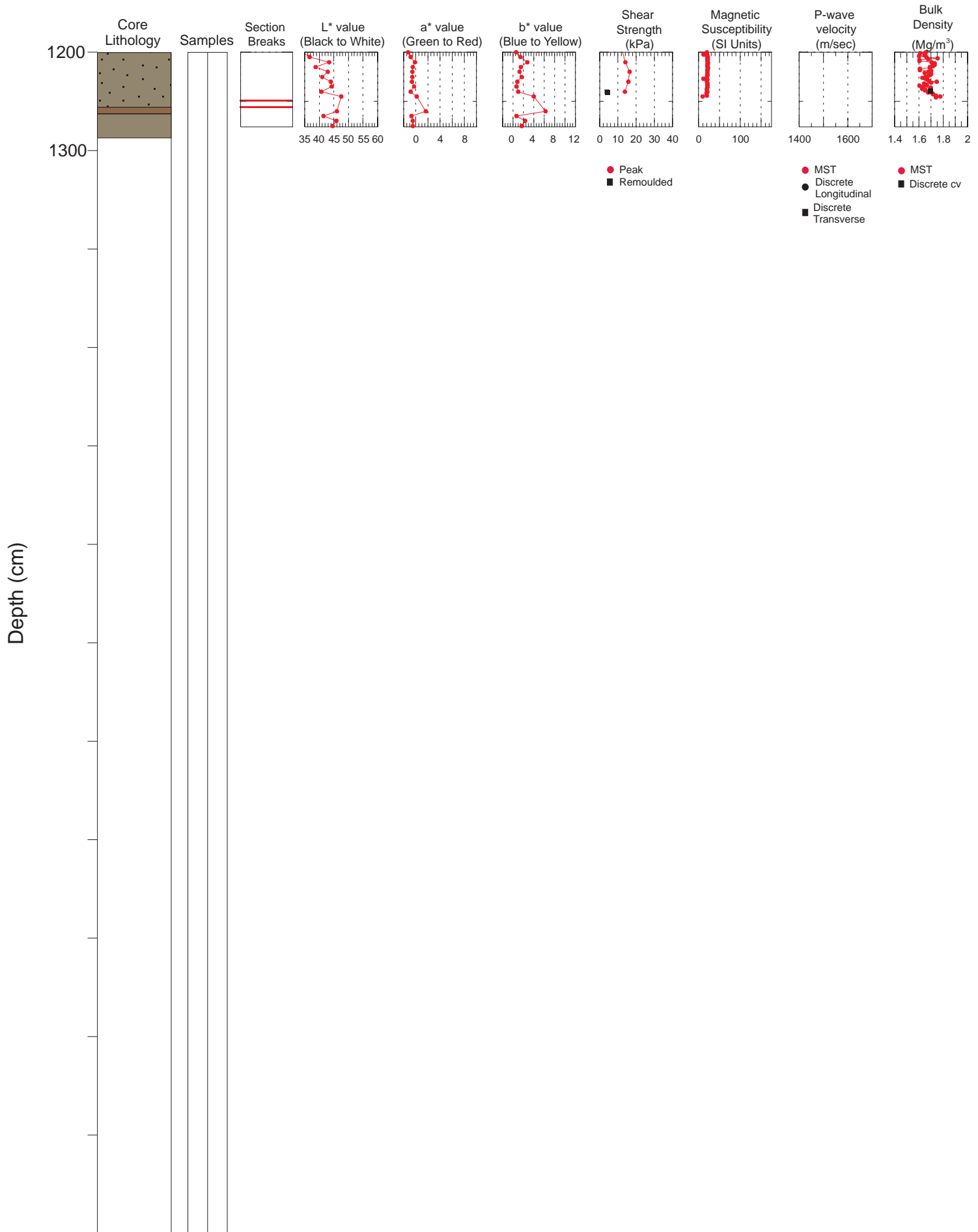
TD 1276cm 44°23.5631 N 55°26.2372 W Water depth 2672 m





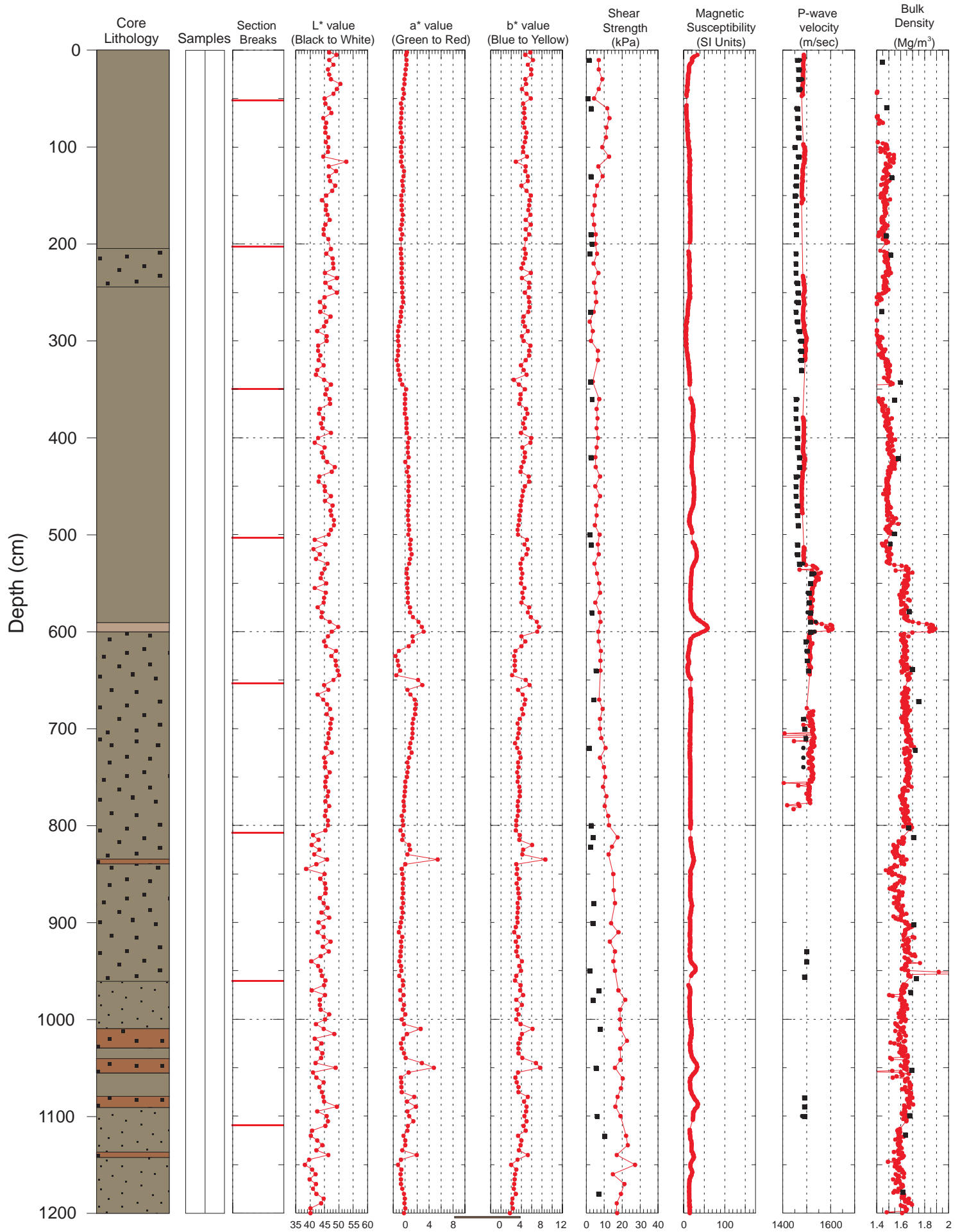
# Hudson 2002046 Piston Core 074

TD 1276cm 44°23.5631 N 55°26.2372 W Water depth 2672 m



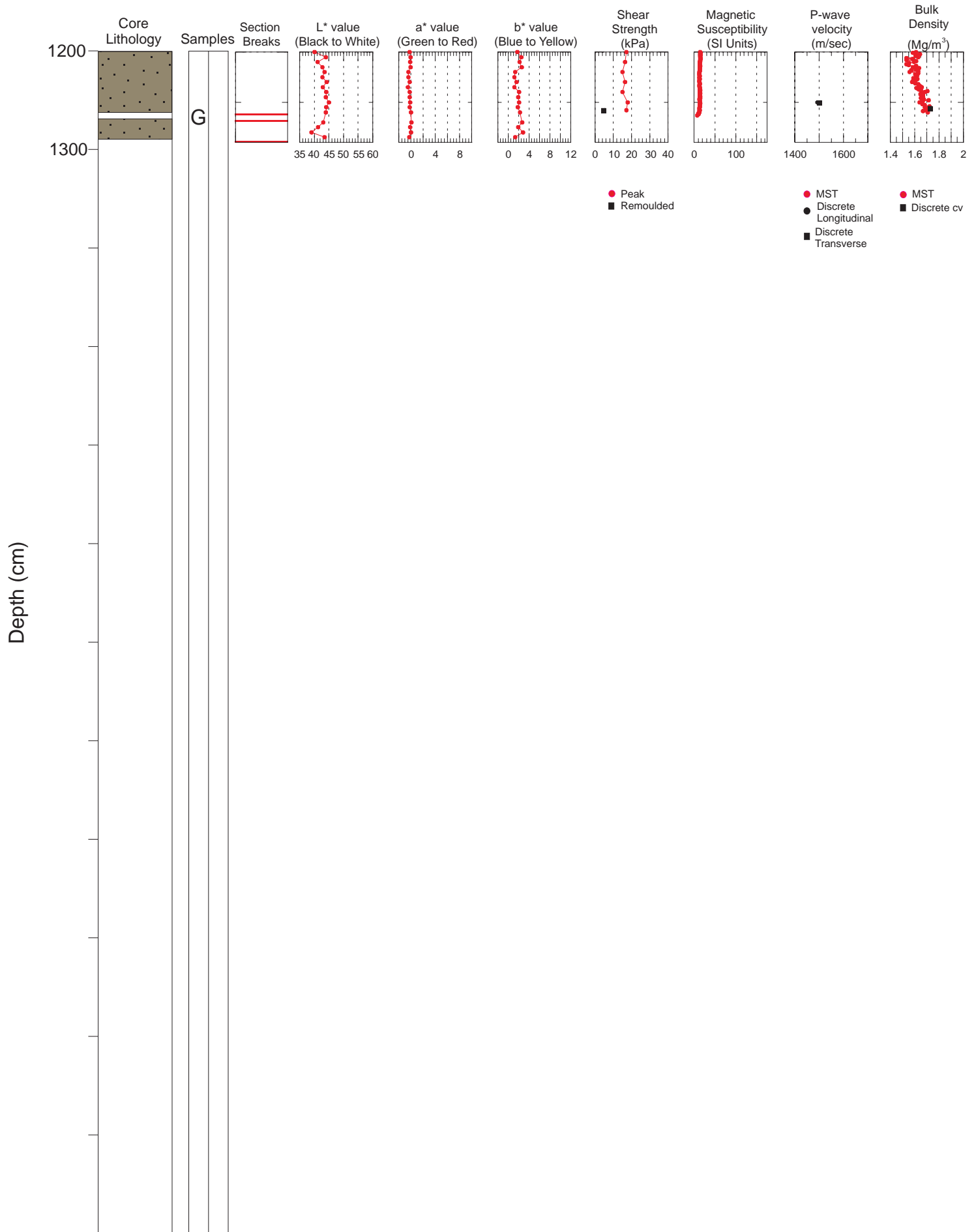
# Hudson 2002046 Piston Core 075

TD 1290cm 44°25.4403 N 54°36.8288 W Water depth 2163 m



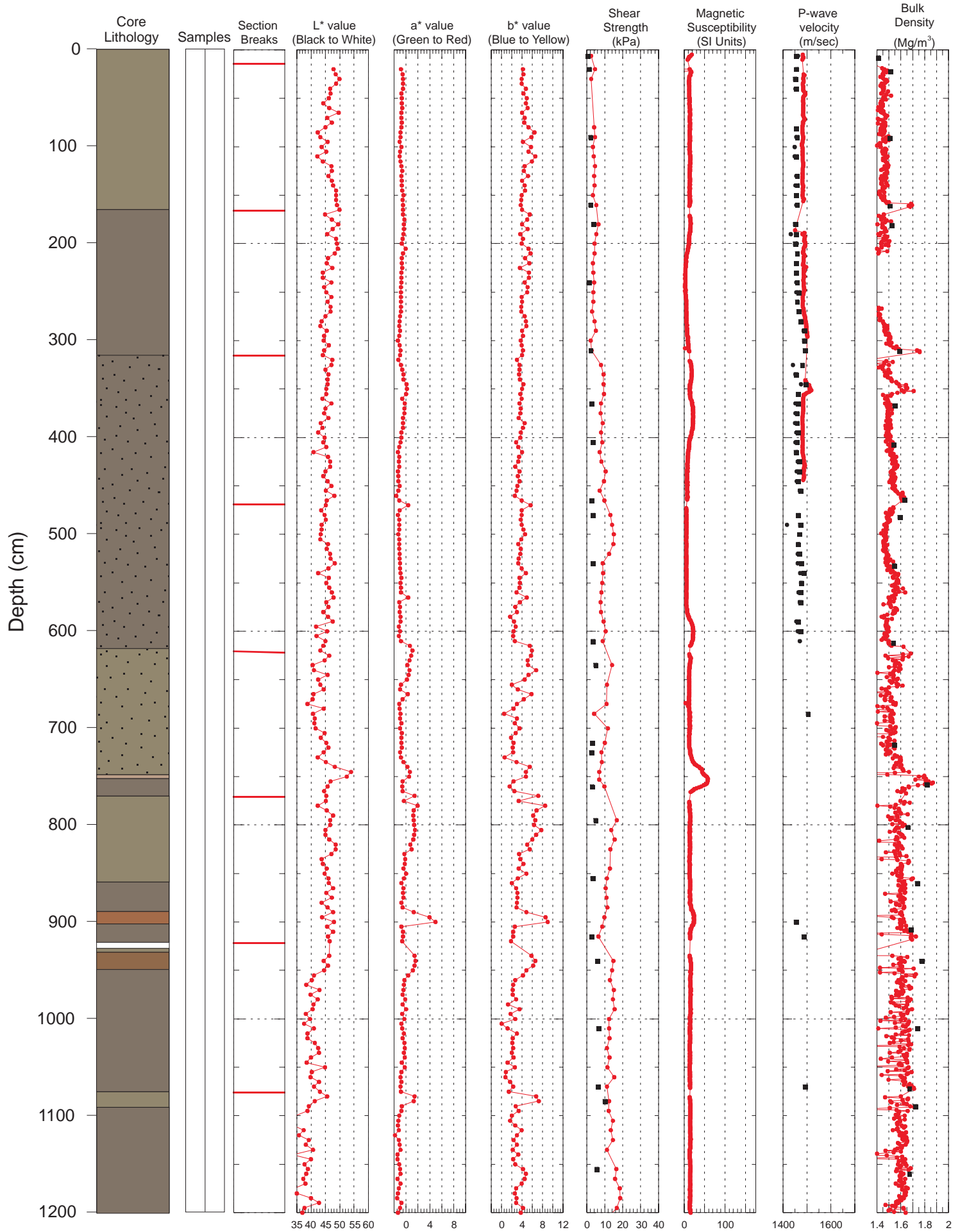
# Hudson 2002046 Piston Core 075

TD 1290cm 44°25.4403 N 54°36.8288 W Water depth 2163 m



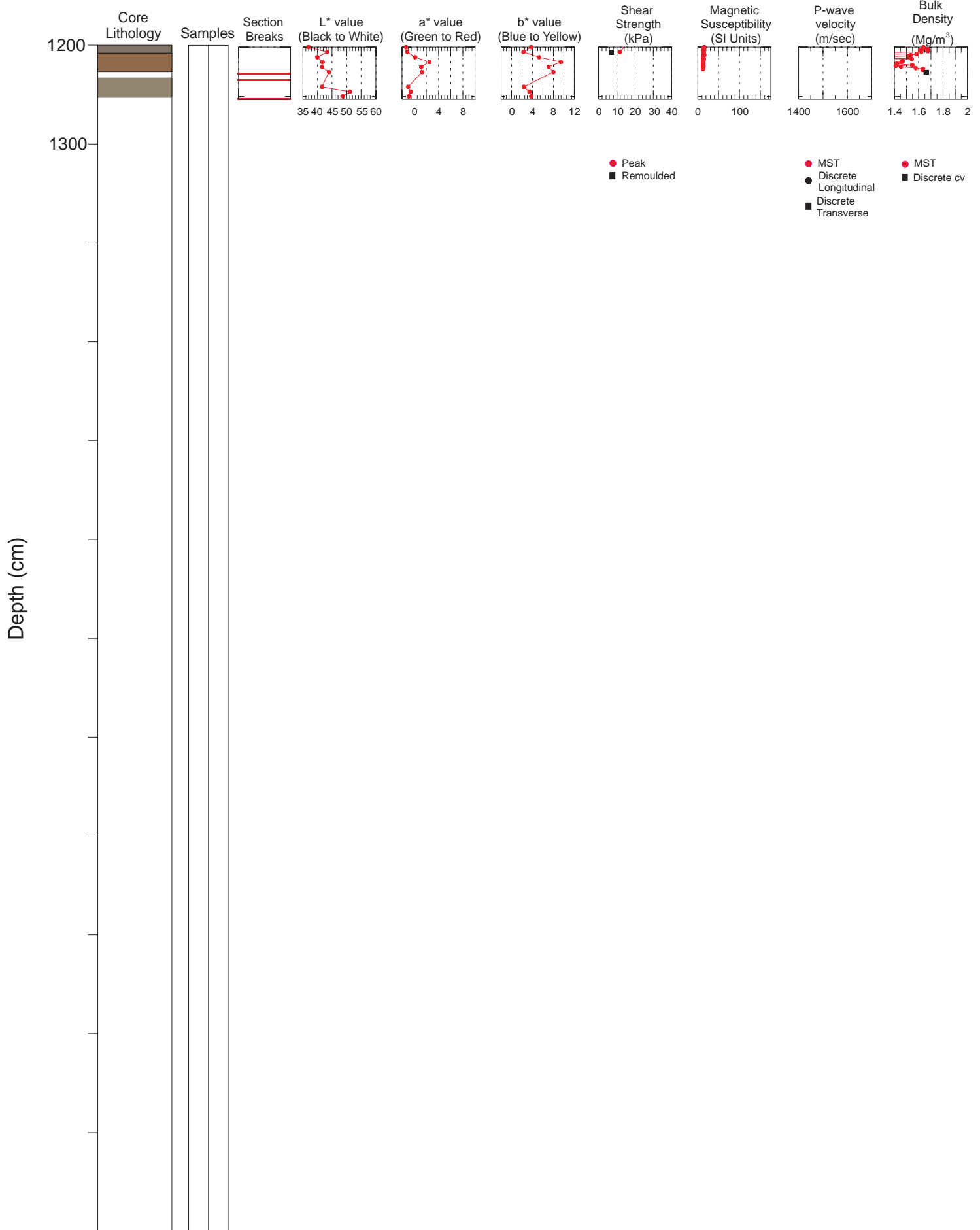
# Hudson 2002046 Piston Core 076

TD 1253cm 44°27.4008 N 54°32.6588 W Water depth 2163 m



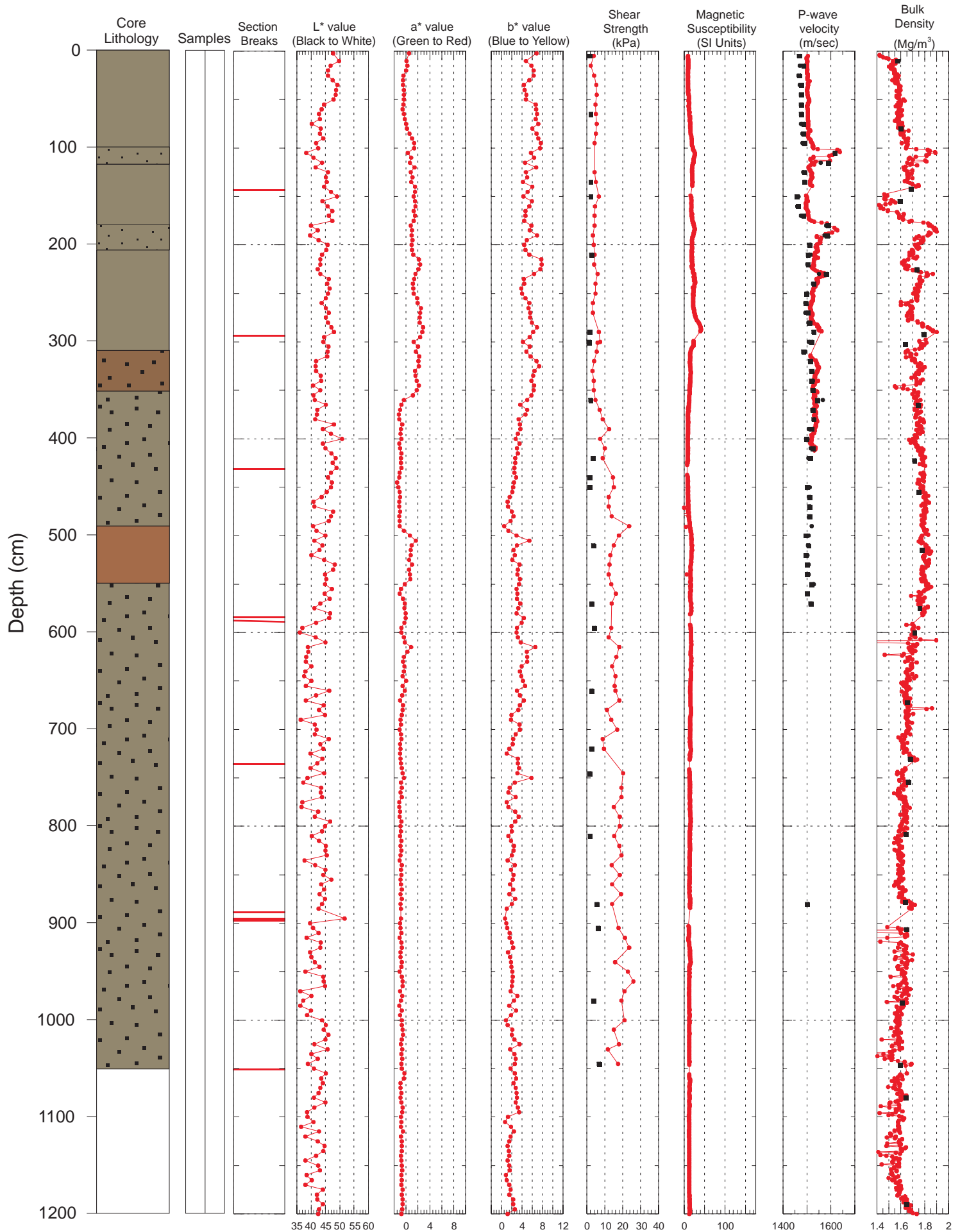
# Hudson 2002046 Piston Core 076

TD 1253cm 44°27.4008 N 54°32.6588 W Water depth 2163 m



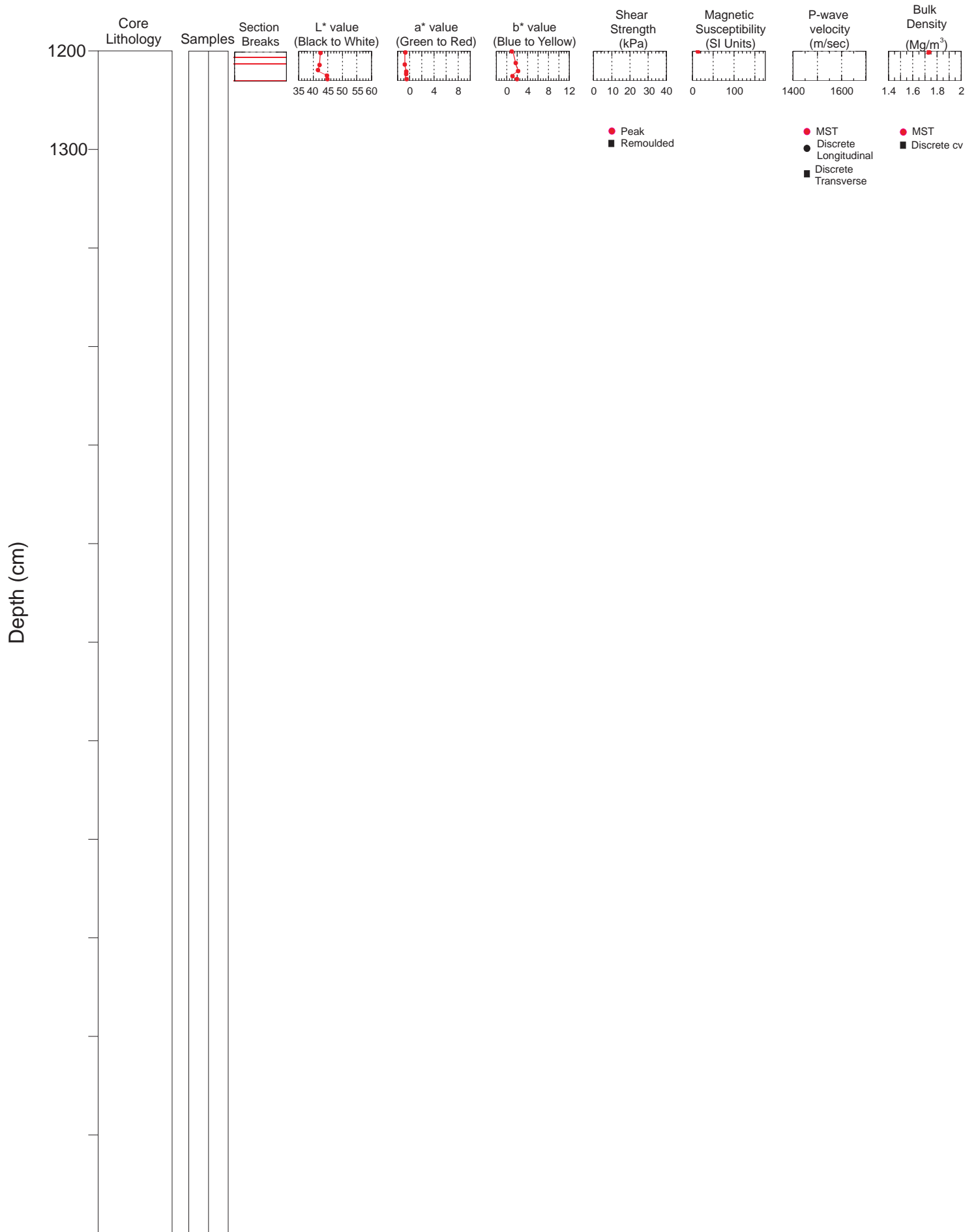
# Hudson 2002046 Piston Core 077

TD 1230cm 44°41.8158 N 54°27.2066 W Water depth 988 m



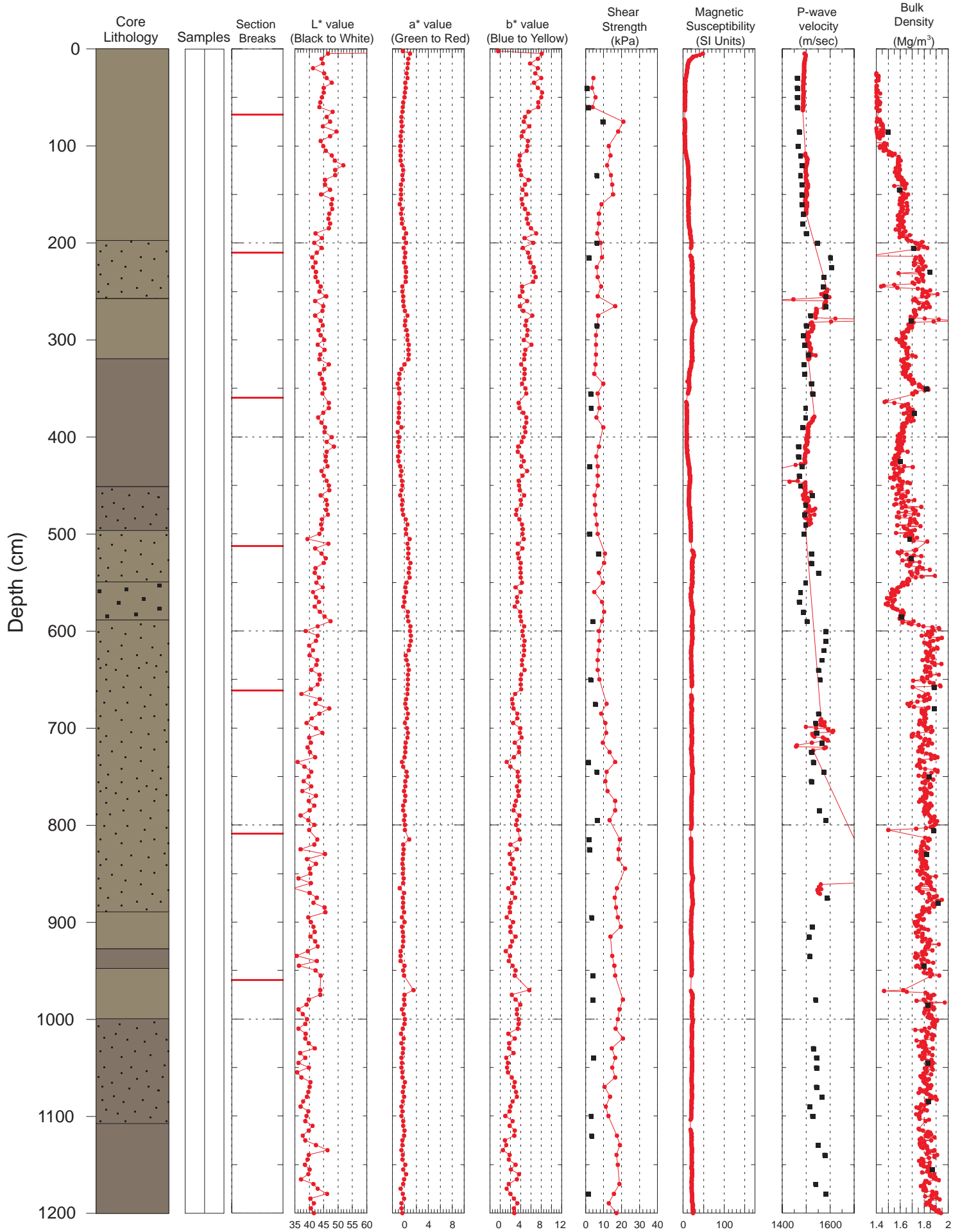
# Hudson 2002046 Piston Core 077

TD 1230cm 44°41.8158 N 54°27.2066 W Water depth 988 m



# Hudson 2002046 Piston Core 078

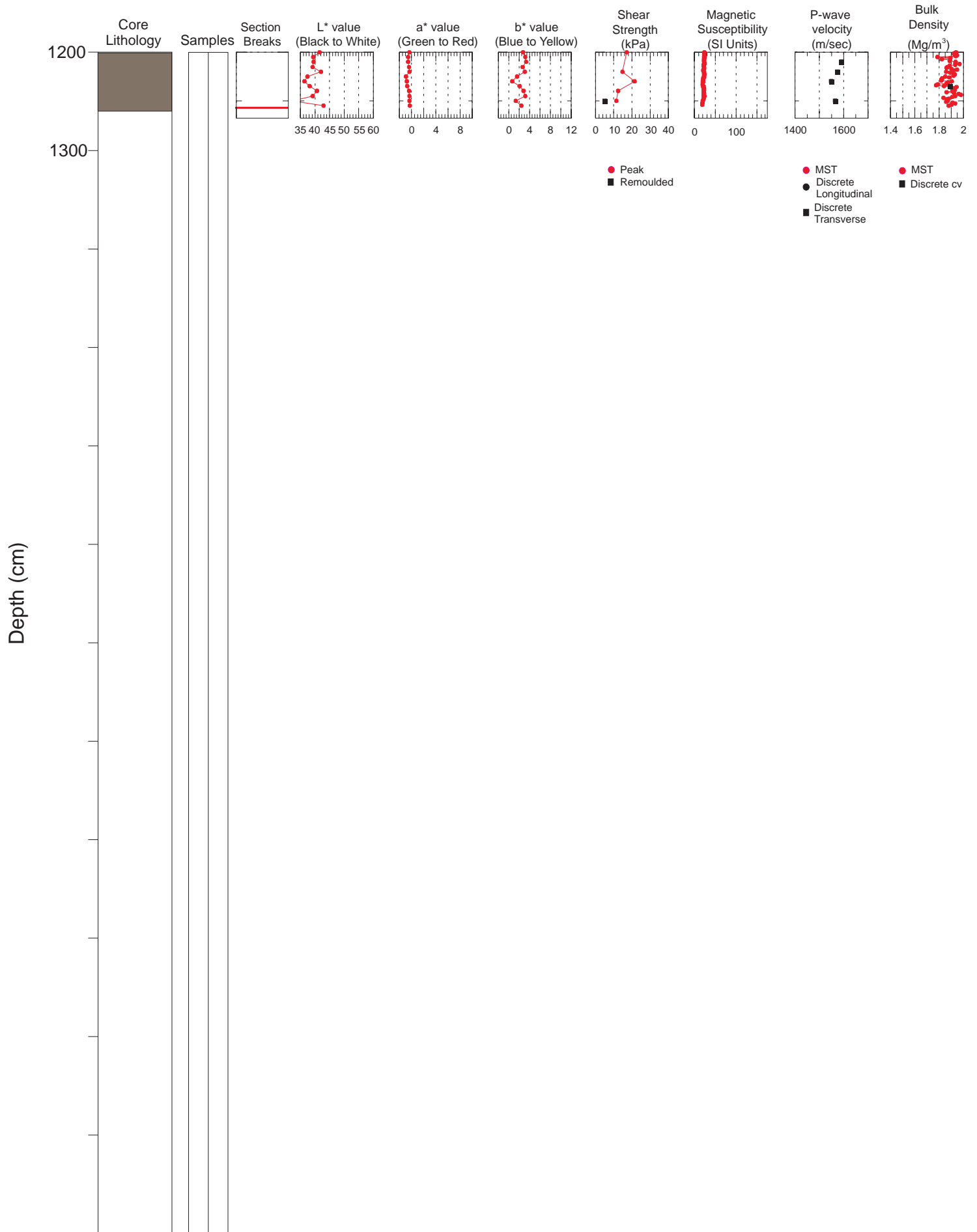
TD 1268cm 44°48.5765 N 54°53.7667 W Water depth 1865 m





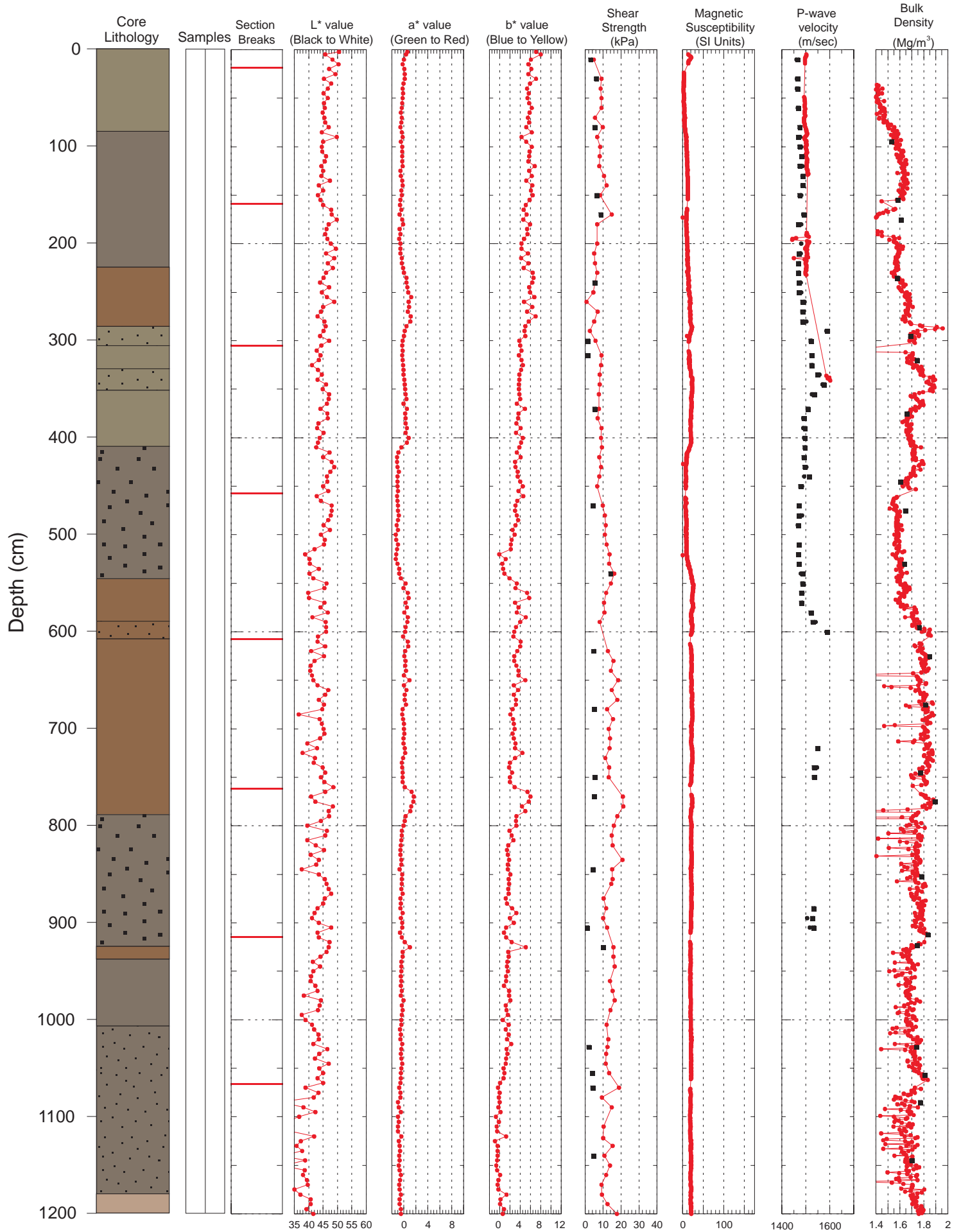
# Hudson 2002046 Piston Core 078

TD 1268cm 44°48.5765 N 54°53.7667 W Water depth 1865 m



# Hudson 2002046 Piston Core 079

TD 1245cm 44°51.1849 N 55°01.0709 W Water depth 1447 m



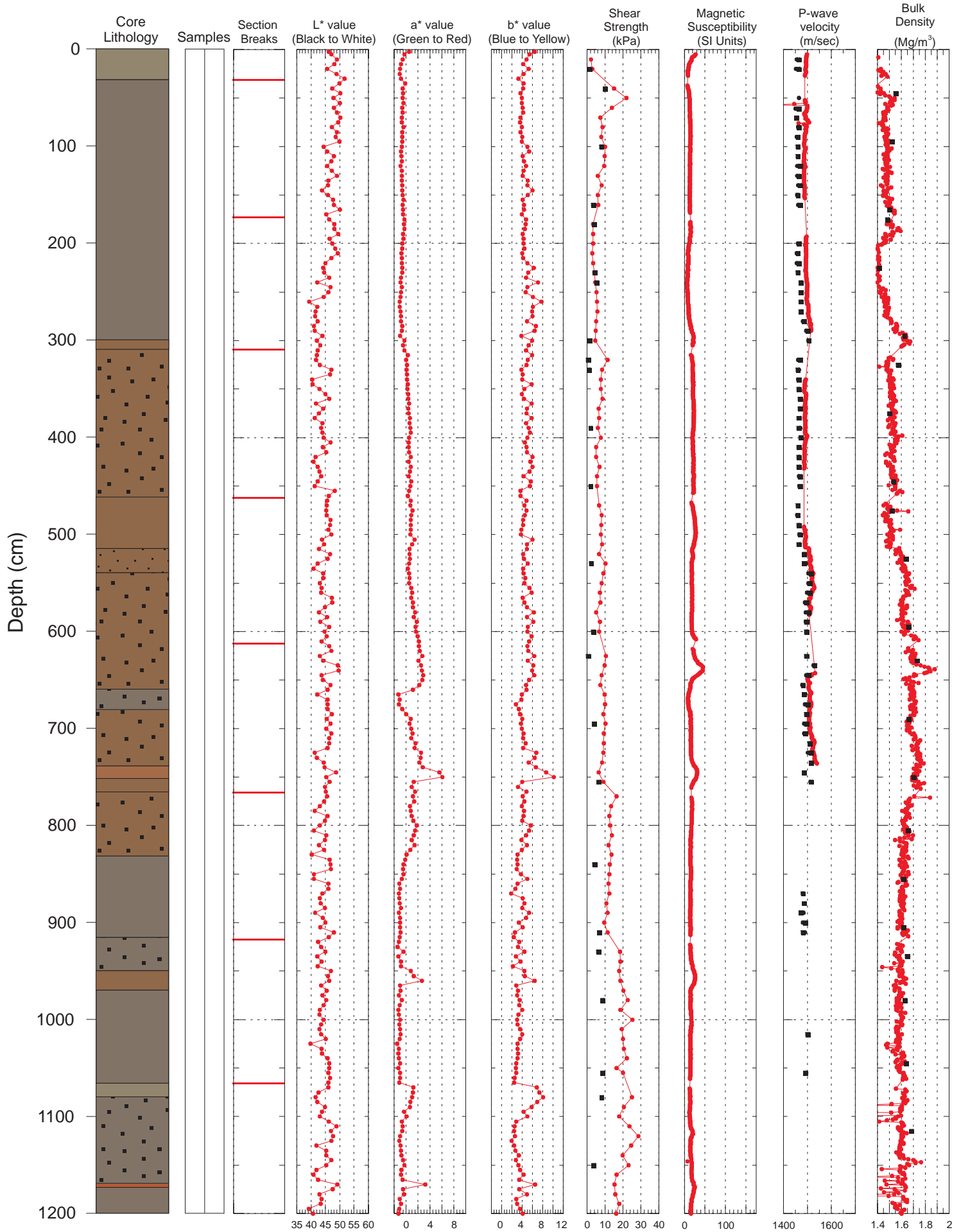
# Hudson 2002046 Piston Core 079

TD 1245cm 44°51.1849 N 55°01.0709 W Water depth 1447 m



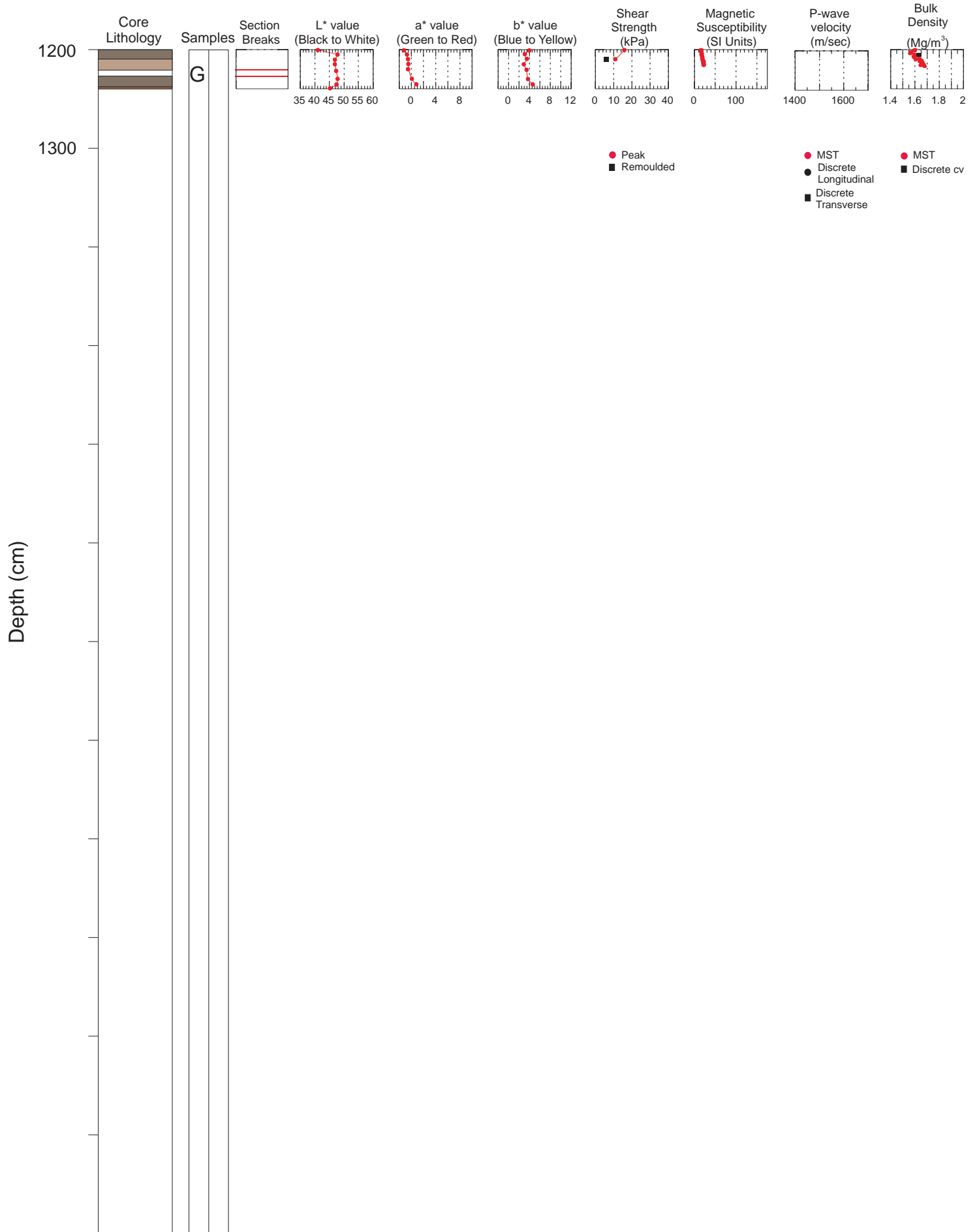
# Hudson 2002046 Piston Core 080

TD 1240cm 44°39.6200 N 54°50.8974 W Water depth 2050 m



# Hudson 2002046 Piston Core 080

TD 1240cm 44°39.6200 N 54°50.8974 W Water depth 2050 m



# Hudson 2003033 Piston Core 007

TD 1111cm 44°54.1162 N 54°33.5938 W Water depth 1360 m

